ANL/ES-40
Volume 2

ANL/ES-40
Volume 2

ENVIRONMENTAL STATUS OF THE LAKE MICHIGAN REGION

VOLUME 2. PHYSICAL LIMNOLOGY OF LAKE MICHIGAN

PART 1. PHYSICAL CHARACTERISTICS OF LAKE MICHIGAN AND ITS RESPONSES TO APPLIED FORCES

CLIFFORD H. MORTIMER

PART 2. DIFFUSION AND DISPERSION

GABRIEL T. CSANADY

U of C-AUA-USERDA

ARGONNE NATIONAL LABORATORY, ARGONNE, ILLINOIS

Prepared for the U. S. ENERGY RESEARCH
AND DEVELOPMENT ADMINISTRATION
under Contract W-31-109-Eng-38

Printed in the United States of America
Available from
National Technical Information Service
U. S. Department of Commerce
5285 Port Royal Road
Springfield, Virginia 22161
Price: Printed Copy $5.45; Microfiche $2.25

ANL/ES-40 Vol. 2
Environmental and
Earth Sciences
(UC-11)

ARGONNE NATIONAL LABORATORY
9700 South Cass Avenue
Argonne, Illinois 60439

ENVIRONMENTAL STATUS OF THE LAKE MICHIGAN REGION

Volume 2. Physical Limnology of Lake Michigan

Part 1. Physical Characteristics of Lake Michigan and Its Responses to Applied Forces

by

Clifford H. Mortimer*

Part 2. Diffusion and Dispersion

by

Gabriel T. Csanady**

Consultants to
Environmental Statement Project

June 1975

*Center for Great Lakes Studies, University of Wisconsin--Milwaukee
**Woods Hole Oceanographic Institution, Woods Hole, Massachusetts

CONTENTS

CONTENTS

FIGURES

PART 1

PART 2

TABLES

PART 1

PREFACE

Assessments of the environmental impacts of individual nuclear power plants sited on the shores of Lake Michigan have led to increased recognition of the need for regional considerations of the environmental impacts of various human activities, and a compendium of information on the environmental status of the region for use in assessing such impacts. In response to these needs, a report series describing the status of Lake Michigan and its watershed is in preparation. The series is entitled "Environmental Status of the Lake Michigan Region"; this report is part of that series.

The report series provides a reasonably comprehensive descriptive review and analysis of natural features and characteristics, as well as past, present, and proposed natural processes and human activities, that influence the environmental conditions of Lake Michigan, its watershed, and certain adjacent metropolitan areas. This series will constitute a regional reference document useful both to scientific investigators and to other persons involved in environmental protection, resource planning, and management. In these regards, the "Environmental Status of the Lake Michigan Region" will serve in part as an adjunct to reports of broader scope, such as the Great Lakes Basin Commission's Framework Study.

Other Volumes Published to Date in this Series

Vol. 7. *Earthquake History and Measurement with Application to the Lake Michigan Drainage Basin.* Richard B. Keener. NTIS-$4.00. 19 pp.

Vol. 9. *Soils of the Lake Michigan Drainage Basin--An Overview.* Forest Stearns, Francis D. Hole, and Jeffrey Klopatek. NTIS-$4.00. 22 pp.

Vol. 10. *Vegetation of the Lake Michigan Drainage Basin.* Forest Stearns and Nicholas Kobriger. NTIS-$5.45. 113 pp.

Vol. 15. *Mammals of the Lake Michigan Drainage Basin.* Charles A. Long. NTIS-$5.45. 109 pp.

ENVIRONMENTAL STATUS OF THE LAKE MICHIGAN REGION

VOL. 2. PHYSICAL LIMNOLOGY OF LAKE MICHIGAN

PART 1. PHYSICAL CHARACTERISTICS OF LAKE MICHIGAN AND ITS RESPONSES TO APPLIED FORCES

by

Clifford H. Mortimer

Abstract

This part of Volume 2 on the unique physical characteristics of Lake Michigan briefly treats basin geomorphology, water budget, light penetration, and the heat budget terms. More extensive examination is given to gravitational and frictional forces acting upon the water body, Coriolis force, and interactions between the vertical fluxes of wind-induced turbulence and heat-related buoyancy.

Representative responses of the Lake to applied wind forces are: (i) wind-driven currents and near-shore geostrophic (Coriolis-balanced) currents, generally unidirectional but subject to frequent direction changes and reversals, and (ii) periodic currents generated by waves, principally long internal and surface waves in the form of seiches modified by the earth's rotation, constituting the free modes of oscillation of the basin.

After winter circulation, the annual temperature cycle begins with the thermal bar phase of spring warming, followed by stratification in summer and fall. After stratification, wind stress and Coriolis force combine to produce frequent and extensive upwellings. These forces generate geostrophic currents near shore and internal waves of several kinds, including those of near-inertial period (15 to 17 hr), producing rotating currents conspicuous in offshore waters. Near shore, the previously mentioned unidirectional (including Kelvin wave) responses predominate.

INTRODUCTION

One of the many ways in which Lake Michigan serves man, in common with other large lakes and coastal seas, is to provide a sink for disposal of waste materials and, increasingly in recent years, heat. Since a large portion of domestic and other wastes will continue to be waterborne in the foreseeable future, such use of Lake Michigan is inevitable and indeed proper, as long as the mechanisms of self-purification are not overloaded and other legitimate uses are not impaired. Of course, the central difficulty lies in defining impairment, damage, and possible trade-offs among users. Such judgments, increasingly shared by the public, must be based on the best available knowledge of the physical, chemical, and biological effects of waste introduction and the ultimate fate of the material and heat so introduced. The difficulties which professionals and the public have in making balanced assessments arise from a lack of quantitative knowledge of some of the interactions critical to the system. However, practical decisions cannot await the outcome of research: environmental impact statements must be written; judgments must be made, often in the adversarial atmosphere of a court of law. In the long run the monitoring, enforcement, and financing of environmental decisions require public support based on knowledge, to ensure a balanced, wise-use policy.

An understanding of the influences and ultimate fates of introduced wastes is only possible against a background knowledge of the transformations of mechanical and thermal energy taking place within time and space scales ranging from seasonal cycles and whole-basin motions on the one hand, to short-term local events within a few hundred feet of an effluent on the other. The purpose of this essay is to outline those aspects of the physical limnology of Lake Michigan particularly relevant to waste disposal, in terms understandable by the intelligent layman, here seen as a public decision maker, a professional in a nonphysical discipline, or as a member of the general public who wants to know what information is available and what is not. To present the essentials briefly is difficult, not only because the critical gaps in knowledge must be identified, but also because it would be dodging the issue to avoid the complex concepts of the eddy spectrum in turbulent diffusion, the influence of the earth's rotation, and the intimate interactions of the downward fluxes of mechanical and thermal energy through the air-water interface into the layers below. Indeed, to fulfill the task properly would require a textbook of physical limnology not yet written; but even to prepare an outline without strong emphasis on the nature of turbulence and turbulent flow in stratified fluids would be like trying to play "Hamlet" without the Prince.

Therefore the mechanisms of diffusion and dispersal will receive separate treatment in a following essay by G. T. Csanady, who has played a leading role in the investigation of this aspect of Great Lakes hydrodynamics. In the present essay we shall be concerned with: the form and characteristics of the basin; fluctuations in water quality; transmission of solar energy; heat budget components and seasonal changes in heat distribution; the principal forces acting upon the water body; interactions of turbulence and stratification; and characteristic patterns of motion. The list of references is restricted to sources specific to Lake Michigan, to authorities for general statements, and to a few papers for general reading.

BASIN FORM, REGIONAL DIVERSITY, HYDROLOGY

This section will not deal with the form of the basin in detail; we shall confine ourselves here to some brief comments on topography (depth chart, Fig. 1) and diversity of shorelines and bottom. The principal dimensions and hydrologic characteristics of the basin, including Green Bay, are listed in Table 1. The two principal embayments, both in the northern half of the Lake Michigan basin, are Grand Traverse Bay (a relatively deep body of water on the east side) and Green Bay (a relatively shallow bay on the west). Green Bay, 118 mi (190 km) long and about 23 mi (37 km) wide, has been the focus of investigations because of its size, relative separation from the main basin, and documented deteriorating water quality.

Most of the Basin bedrock is covered with glacial deposits. The northern part of the watershed is farmland and forest; urbanization is confined to the southern part; and in 1960 several million people lived in the drainage area, with consequent effects on watershed and lake, including severe local pollution (see U. S. Department of the Interior, 1968). In the northern half and in deeper waters the water quality is good.

DIVERSITY OF SHORELINES AND SEDIMENTS

In the northern half of the basin, which includes the deepest depression, maximum depth 923 ft (282 m), the bottom topography is relatively complex and a high proportion of the shoreline is rock. By contrast, in the southern half, which contains a second major depression of maximum depth 548 ft (167 m), the depth contours are smoother and large sections of the shoreline consist of sand dunes on the eastern side and of glacial debris (mixed clays, silts, sand, gravel and boulders) on the western side. Wave action on these western-central and southwestern shores, particularly from northeasterly storms with long fetch, has formed long stretches of low cliffs or bluffs, which are actively eroded during epochs of high lake levels. In this region there is also considerable heterogeneity in bottom material in the beach zone (defined below), where the bottom ranges from exposed clays through fine sands to coarser material and boulders. Some sorting has taken place and there are occasional sandy beaches on the western side, but the usual picture is one of patchy, unconsolidated fine material thrown into suspension by each succeeding storm, creating long stretches of turbid water near shore extending out to about a mile or so and later clarifying in calm weather. The generation of extensive turbid reaches is, as one might expect, accentuated during epochs of high lake level and active shore erosion.

On the eastern-central and southeastern shores, on the other hand, there are long stretches of sandy beaches backed by dunes with long, shore-parallel sand bars immediately offshore, commonly two (Davis and McGeary, 1965; Davis and Fox, 1971). Storm action generally produces less turbidity here than on the western shore, although some localized turbidity is to be expected wherever large waves, coupled with high lake level, erode freshly exposed glacial till.

The biological effects of beach stability, re-sorting of bottom materials and the large-scale storm-induced turbidity have received relatively little attention, but are likely to be important in the beach zone. This matter will be referred to again briefly in the section concerned with the penetration of sunlight. The growth of plants, both attached and planktonic, is strongly

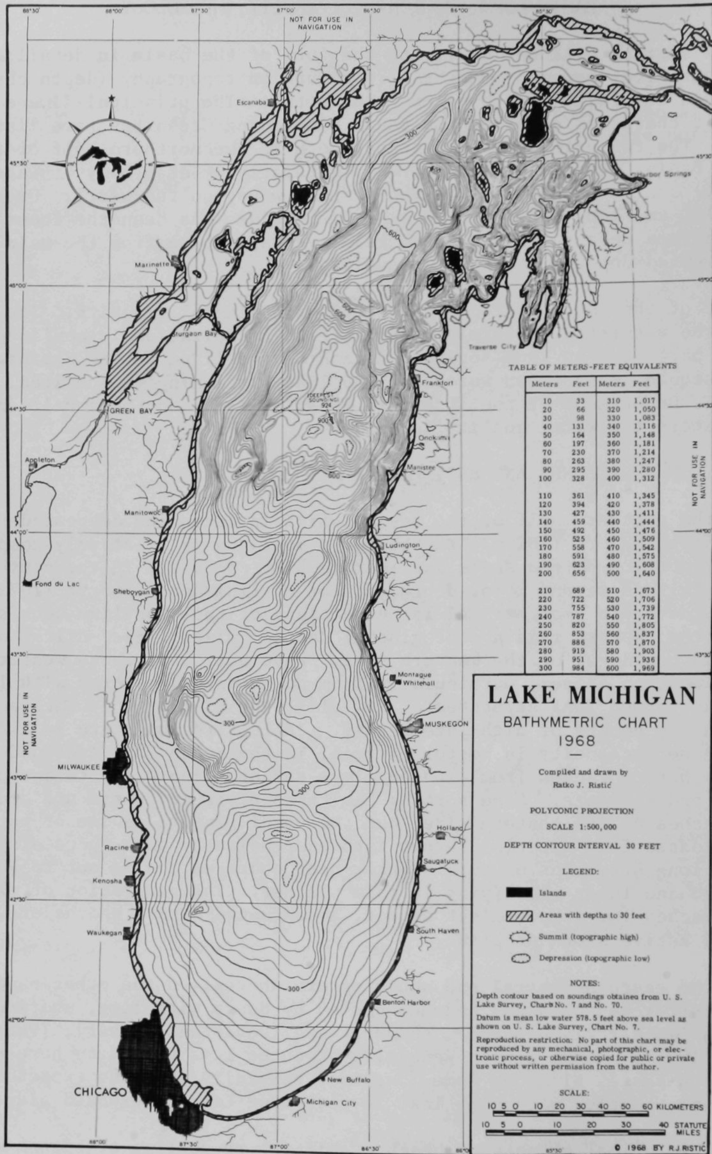

Fig. 1. Depth Contour Map of Lake Michigan. Prepared by R. J. Ristic from charts published by NOAA Lake Survey Center (with permission, see credits).

Table 1. Physical Characteristics of Lake Michigan, Including Green Bay

Lengths	*miles*	*km*
"Trough length" (medial track)[a]	350	560
Shoreline	1,660	2,670
Max. E-W line of sight (N. half)	111	179
Max. E-W width (S. half)	84	135
Depths	*feet*	*m*
Maximum (below LWD)	923	282
Mean (below LWD)	279	85
Areas	*miles*^{2}	*km*^{2}
Water surface	22,300	57,800
Drainage basin (including lake)	67,900	175,800
Water levels: 1860-1968	*feet*[b]	*m*[b]
1860-1968 mean	578.7	176.5
Highest monthly mean (June 1886)	581.9	177.5
Lowest monthly mean (March 1964)	575.4	175.5
LWD = low water (chart) datum	576.8	176.0
Volumes		
Volume (*V*)	1,180 mi^3	4,920 km^3
Approximate average discharge rate[c] (*R*)	51,000 ft^3/sec	1,444 m^3/sec
"Emptying time" (to drain *V* at rate *R*)	108 years	

[a] *Approximate length of smoothed track following the center line of the curved basin (used in seiche calculations, Mortimer 1965).*

[b] *Above International Great Lakes Datum (1955) "mean sea level" Father Pt., Quebec. These data and those for areas and volumes are those of U. S. Dept. of Commerce, NOAA, Lake Survey Center, and are taken from tables in Great Lakes Basin Commission (1972).*

[c] *Average of four estimates, ranging from 44,000 to 52,000 cfs (1246-1472 m^3/sec), was 48,000 cfs (1359 m^3/sec) (personal communication, DeCooke, U. S. Lake Survey Center). Adding to this the Chicago diversion of up to 3200 cfs (91 m^3/sec) yields an approximate mean of 51,000 cfs (1444 m^3/sec).*

influenced by the shading effect of suspended matter in the water. Some reduction of plant nutrients is also possible by adsorption on suspended particles.

Erosion, sorting, and transport of shore materials and shallow-water deposits contribute continually to the building of sediments in deeper water. A description of these sediments is beyond the purpose of this review; the reader is referred to Hough (1935, 1958), Ayers (1967), Sommers and Josephson (1968), and to Lineback, Ayer, and Gross (1970). Finer fractions of the sediment tend to accumulate under the deepest water, i.e. in the deep northern region off Frankfort and in the two broad, deep channels separated by a shallower, rockier region midlake east of Port Washington (see Fig. 1). The horizontal heterogeneity and the vertical structure of the deepwater sediments invite further investigation. As a general conclusion, we may note that the composition of shallow-water sediments is generally very heterogeneous along the western shore from Chicago to Sturgeon Bay Canal, in contrast to the western sandy beaches or the northern beaches on which rock outcropping is more common.

WATER ZONES

All the information on depth distribution, contained in Figure 1, is helpfully summarized in Figure 2, which shows the percentage of the total lake volume that lies below a given depth contour. For many purposes it is convenient to refer to various water regions, although precise and universal definitions are rarely possible. For example, inflows to the lake (natural or man-made) or waves acting on the shorelines add their load of materials or heat to a beach zone, where further dispersion takes place into nearshore coastal water. Here the added materials or heat is acted upon by biological or physical mechanisms or is further dispersed to the offshore waters of the whole basin. These regional terms are often used too loosely and with different, ill-defined meanings. There are also, as we shall see, large seasonal and short-term variations in the hydrographic conditions near shore, which means that no definition is acceptable without substantial qualification. However, there is evidence from the rates of biological production and water chemistry (Holland and Beeton, 1972) that throughout substantial portions of the year

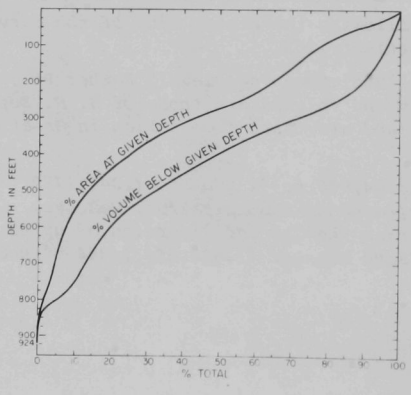

Fig. 2.

Lake Michigan: Area/Depth and Volume/Depth Relationships. Data kindly supplied by Dr. A. M. Beeton and obtained by planimetry from NOAA Lake Survey Center charts.

there are reproducible differences between coastal and offshore waters, at least in the neighborhood of large metropolitan centers. The transition between coastal and offshore water, in this sense, commonly occurs between five and ten miles (8 to 16 km) from the shore, and this is the sense in which we shall use the terms here. Chemical differences between inshore regions and deepwater or offshore water (> 10 mi offshore) are also demonstrated in other publications in which regions of major pollution are also described (U. S. Department of the Interior, 1968).

Equally difficult is the definition of the beach zone. In a hydrodynamic sense the outer limit of the beach zone coincides with the outer limit of the zone of breaking waves in severe storms, a limit determined not only by water depth, but also by the exposed fetch and prevalent wind direction on a given beach. Wave statistics obtained by Saville (1953) at certain points around Lake Michigan's shore and more recent work carried out by the Lake Survey Center* could help to define the widths of the breaker zone more precisely. Although no measurements have been made on Lake Michigan, we know from work on marine beaches (Bowen, 1969; Bowen and Inman, 1969) that longshore currents develop within the breaker zone whenever waves arrive at an angle to the beach. In regions with fine beach sediments, another definition of the beach zone might use the extent of turbid water stirred up by storms.

VARIATIONS IN WATER LEVEL

Variations in water level occur on a wide range of time scales, from seconds for breaking waves running up the beach to annual or longer fluctuations, depending on variations in the components of the water budget. The annual variations of those components are illustrated for Lake Michigan-Huron in Figure 3. The Michigan and Huron basins are joined by the Straits of Mackinac and thus are at the same average level. It is therefore convenient to consider them as a single lake for purposes of calculating water budgets. Figure 3 shows that three components of the budget (inflow from Lake Superior, precipitation on the lake, and outflow) show only minor annual variations; therefore the rate of change of lake level (ΔS, or change in storage) is mainly dependent on seasonal fluctuations in runoff from the land and on evaporation. During the interval when ΔS is positive, February to July, the lake level rises; during the remainder of the year it falls. There is therefore an annual level wave with a trough in February and a crest in July with a 113-year mean range of close to one foot (1860-1972, Fig. 4). However, as Figures 4 and 5 show, the range of monthly values around the long-term mean has been about 5 ft (1.5 m) over the 113 years of record. The highest monthly mean level was 581.9 ft (177.4 m) in June 1886 and the lowest was 575.4 ft (175.4 m) in March 1964; the 113-year average is 578.7 ft (176.4 m) which is 1.9 ft (0.58 m) above low water used as the datum on the Lake Survey Center navigational

---

*This agency, which we shall refer to as Lake Survey Center, was formerly the U. S. Lake Survey of the U. S. Army Corps of Engineers. It was and still is responsible for charting the Great Lakes and for related hydrological and scientific research. Its present address and designation are: Department of Commerce, National Oceanic and Atmospheric Administration (NOAA), Lake Survey Center, 630 Federal Building, Detroit, Michigan 48226. Some of the research activities of the former U. S. Lake Survey were transferred in 1974 to NOAA's Great Lakes Environmental Research Laboratory in Ann Arbor, Michigan.

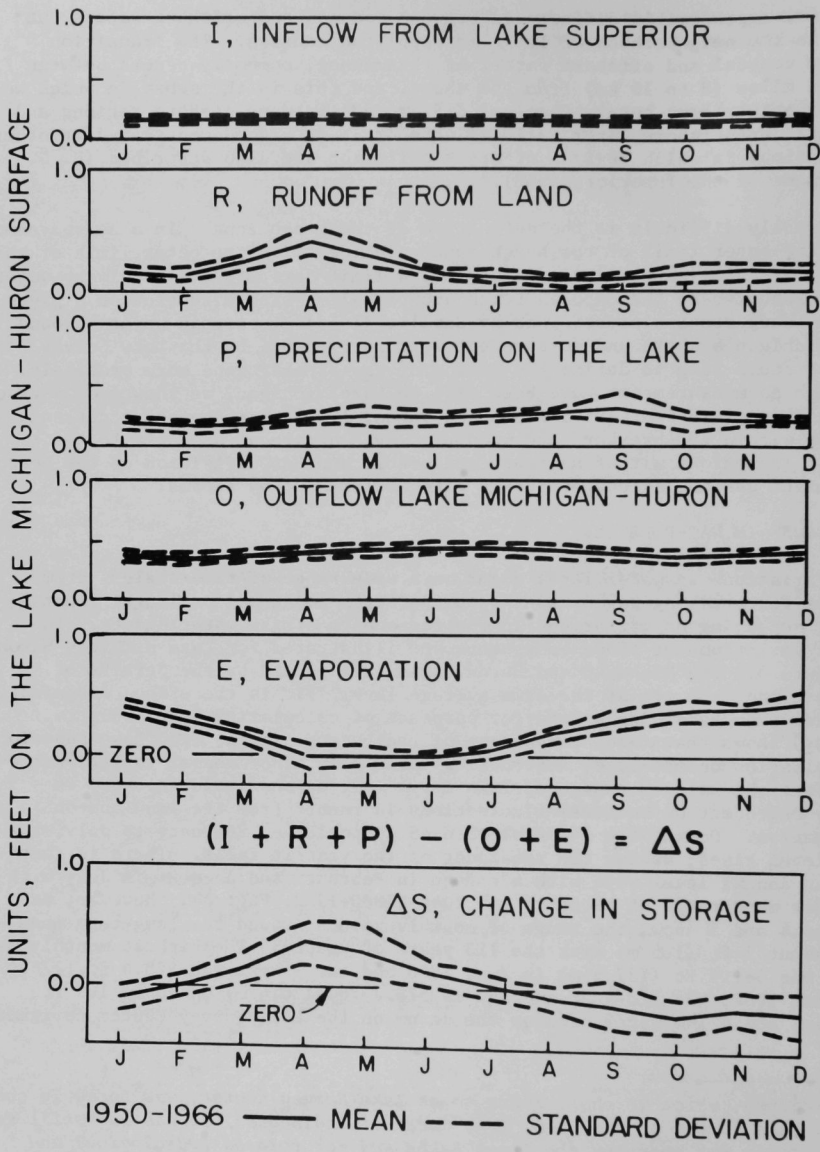

Fig. 3. Lake Michigan: 1950-1966 Mean (continuous line) and Standard Deviation (broken line) of Monthly Totals of the Components of the Water Budget. Expressed in units of feet on the Lake Michigan-Huron water surface. Data from Witherspoon (1971).

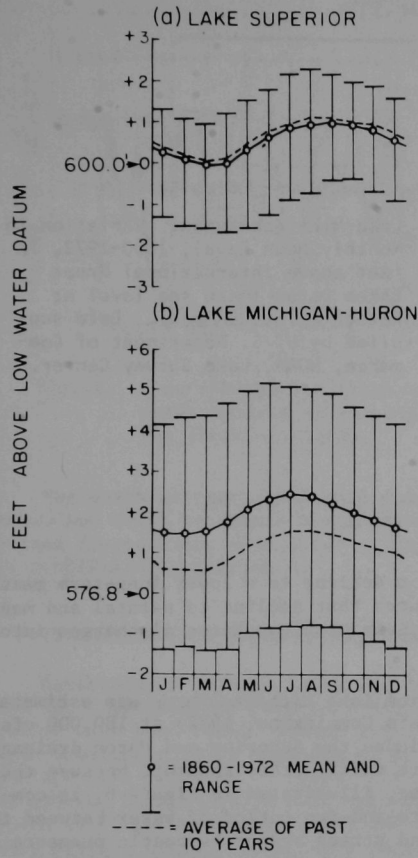

Fig. 4.

1860-1972 Averages and Extreme Ranges of Monthly Mean Water Levels in (a) Lake Superior and (b) Lake Michigan-Huron, with the Mean of the Last 10 Years (broken line). Levels are shown relative to low water datum, (a) 600.0 and (b) 576.8 ft above International Great Lakes datum. Data from U. S. Department of Commerce, NOAA, Lake Survey Center, Monthly Bulletin, April 1973.

charts of Lake Michigan. All these levels are expressed relative to an International Great Lakes Datum, adopted in 1955 as the mean sea level at Father Point, Quebec. A useful bibliography on Great Lakes hydrology is that of Beutikofer and Meredith (1972).

Figure 5 clearly shows the annual fluctuations in lake level superimposed on longer variations with time scales of decades. These long-term changes in level are related in an obvious, although not well-understood, manner. A better understanding of this phenomenon may be obtained by comparing the 1900 and 1970 graphs of annual precipitation for the Great Lakes basins in Phillips and McCulloch (1972) to variations in precipitation. It is interesting to note only nine years have elapsed between the lowest monthly mean in 1964 and the 1973 nearly record high levels.

The influence of high-level epochs on shore erosion and beach evolution must be considered when assessing man-made changes. Before leaving Figure 5 it is of interest to note that the mean levels were generally above 579 ft

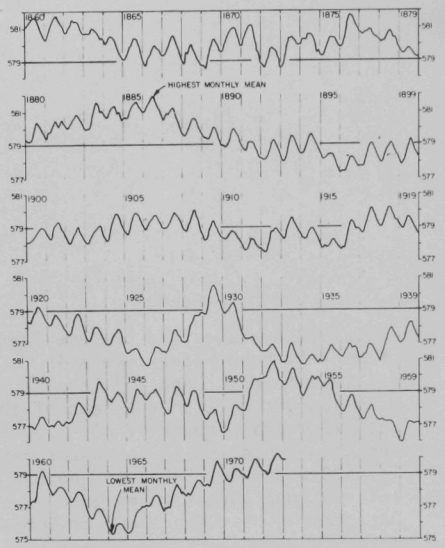

Fig. 5.

Lake Michigan-Huron: Variation in Monthly Mean Level, 1860-1972, in feet above International Great Lakes Datum (mean sea level at Father Point, Quebec). Data supplied by U. S. Department of Commerce, NOAA, Lake Survey Center.

(177 m) until 1895, after which there was a decline to a lower long-term mean by the early 1920's. Brunk (1963) attributes that decline to natural and man-made deepening of the outflow sill, where Lake Michigan-Huron discharges into the St. Clair River.

The 1937-1969 mean rate of outflow from Lake Michigan-Huron was estimated by the Lake Survey Center (Great Lakes Basin Commission, 1972) at 180,000 cfs (5097 m^3/sec). That flow, of course, includes the Superior and Huron drainage. The outflow from Lake Michigan is much more difficult to estimate because the oscillatory flow in the Straits of Mackinac, illustrated in Figure 6, is commonly 10 to 20 times the mean flow. The to-and-fro motion of water between the two basins is driven by differences in wind stress and/or barometic pressure between them, as well as by a low-frequency, two-basin oscillation (seiche) with a period of about three days. The net outflow, shown as a broken line in Figure 6, has been estimated by the Lake Survey Center on four occasions (see footnote to Table 1). The mean of those four estimates, plus the sanitary diversion of 3200 cfs (91 m^3/sec) through Chicago to the Illinois River, yields an approximate mean outflow of 51,000 cfs (1444 m^3/sec). This raises the question of the retention time of the basin, namely the average time of residence of the water particle. This is often equated with the emptying time, i.e. the basin volume divided by the mean outflow. At 51,000 cfs (1444 m^3/sec) the emptying time is 108 years. An improved but still highly simplified mathematical model is that of Rainey (1967), which predicts that if a "pollutant" has become uniformly distributed throughout the basin and the polluting supply were suddenly stopped, 90% of that pollutant would have been removed after 2.3 emptying times had elapsed, i.e. 249 years for Lake Michigan. The model applies only to a conservative pollutant, i.e. one not subject to biological purification or to removal from the water by other mechanisms, and assumes that the basin is always fully mixed.

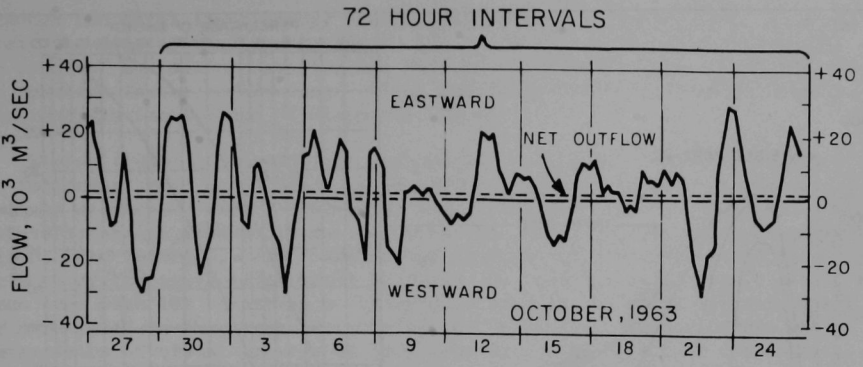

Fig. 6. Flow through the Straits of Mackinac, Estimated from Current Meter Records at the Single Station 54 (U. S. Department of the Interior, 1967).

The beach watcher sees rapid changes in water level produced by the storm waves, and beach residents are aware of annual and slower changes, but not-so-obvious fluctuations also occur at frequencies in between. Those fluctuations are considered in Section 4.

TRANSMISSION OF SOLAR ENERGY INTO THE WATER; HEAT BUDGET COMPONENTS

Surprisingly perhaps, very few investigators have concerned themselves with light penetration into Lake Michigan. In fact only two substantial studies have been made: Beeton (1962) and the Lake Survey Center (Great Lakes Basin Commission 1972, Appendix 4: p. 382), both in the northern half of the lake and both referred to later. To place the Lake Michigan findings within the general background of this subject, we must refer back to the pioneering papers of Birge and Juday (1929) and to oceanographic texts (Sverdrup *et al.*, 1942; Jerlov, 1968). Sverdrup's introductory figures, assembled in Figure 7, summarize the matter quite well for Lake Michigan also. Smoothed outlines of the spectra of energy, penetrating to various depths in pure water, are assembled in the upper part of the figure. The penetration of total radiant energy is illustrated in the top right inset. Pure water is more transparent to radiation in the blue-green region than to radiation in other parts of the spectrum. Therefore, at a 40-m depth (131 ft) in pure water for example, 40% of the blue-green light has penetrated to that depth, as against 9% for total radiation.

The transparency of natural waters, always less than that of pure water, varies greatly. This variation is illustrated, in the lower part of Figure 7, by comparisons of energy spectra at a 10-m depth (32.8 ft) in various types of marine water ranging from the clearest ocean to turbid coastal water. With increasing turbidity, not only does the transparency decrease, but the color of maximum pentration shifts from the blue-green region for pure water to the yellow-orange in very turbid waters. For example, the lower inset shows that,

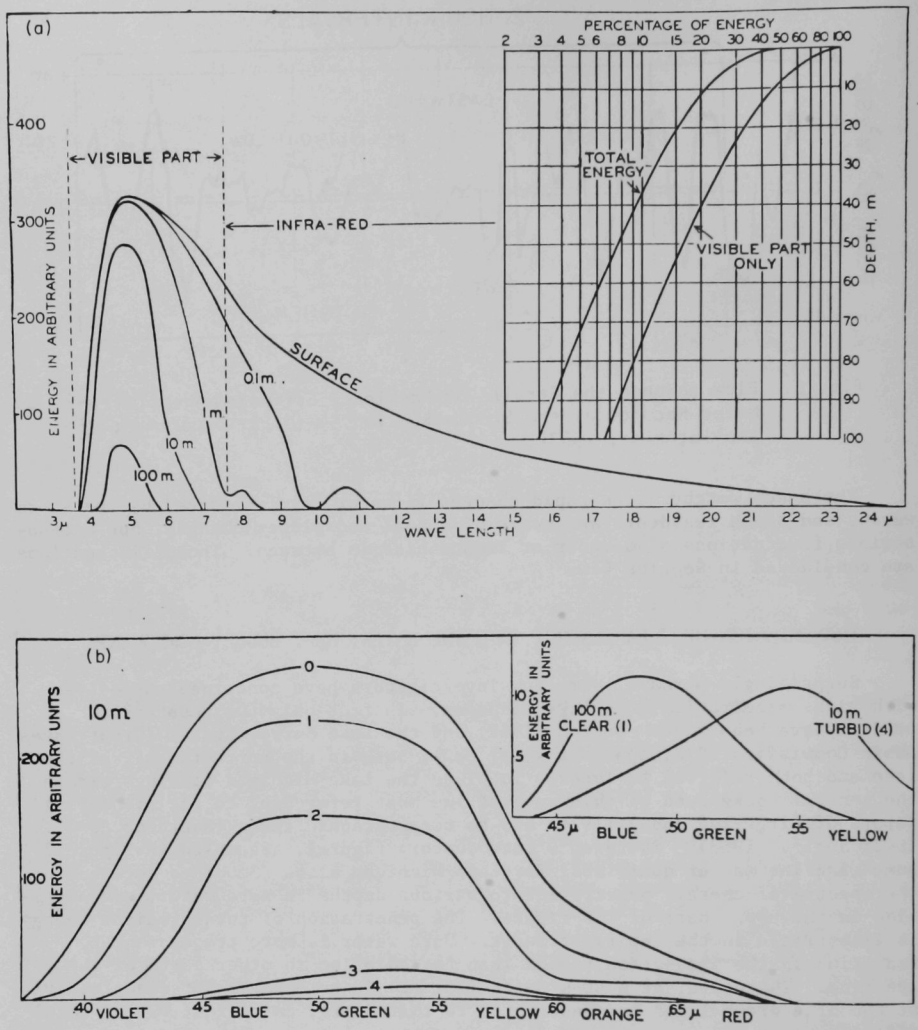

Fig. 7. Energy Spectrum of the Radiation from Sun and Sky (a) that Penetrates the Water Surface, and Spectra of the Remaining Energy after Penetration through 0.1-, 1-, 10-, and 100-m Columns of Pure Water. The percentages of total energy and of energy in the visible part of spectrum reaching different depths is shown in the inset. Energy Spectra at 10-m Depth (b) in Different Water Types: 0 Pure Water, 1 Clear Oceanic, 2 Average Oceanic, 3 Average Coastal, 4 Turbid Coastal Sea Water. Energy spectra at the depths of 100 m in clear oceanic and at 10 m in turbid coastal water are shown in the inset. Assembled from figures in Sverdrup *et al.* (1942) (with permission, see credits).

although the total light energy penetrating to 10 m in turbid water is approximately the same as that pentrating to 100 m (328 ft) in clear oceanic water, the color of maximum penetration has shifted considerably toward the red end of the spectrum in the turbid case. Birge and Juday (1929) illustrated similar relationships for a range of Wisconsin lakes.

Beeton (1962) measured light penetration in each of the Great Lakes, in the following broad color bands, approximate wavelength ranges in nanometers shown in brackets: violet (300-420); blue (440-490); green (490-540); yellow (540-590); orange (590-610); and red (610-750). His findings in the northern half of Lake Michigan, near Sturgeon Bay Canal on May 7, 1958, are illustrated for some of the above color bands in Figure 8. Maximum transparency was in the green band with 10% remaining at 10 meters. Bearing in mind that spectrum 0 for pure water in the lower part of Figure 7 represents approximately 45% transmission of visible energy at 10 m (see inset top right), Beeton's Lake Michigan spectrum lies between the spectra for average oceanic and average coastal water, i.e. spectra 2 and 3 in lower Figure 7. The percentage of total visible energy transmitted through a one-meter column was about 45% at Beeton's station, which agrees remarkably well with the results obtained for that station by the Lake Survey Center during May 23-June 8, 1970, cruise [Fig. 9(b)] (Great Lakes Basin Commission, 1972). That figure confirms that the central deep waters were the clearest, more than 70% transparent, and that the coastal waters were less transparent, down to 30% for a one-meter column. The comparison of Figure 9(a) with Church's (1945) temperature map, Figure 9(b), for the same region and time of year, suggests one possible reason for the lower transparencies near shore, namely higher plankton production in the shallower, warmer coastal waters.

In contrast to the relatively deep penetration of visible energy, infrared (heat) radiation is almost completely absorbed in the uppermost few centimeters.

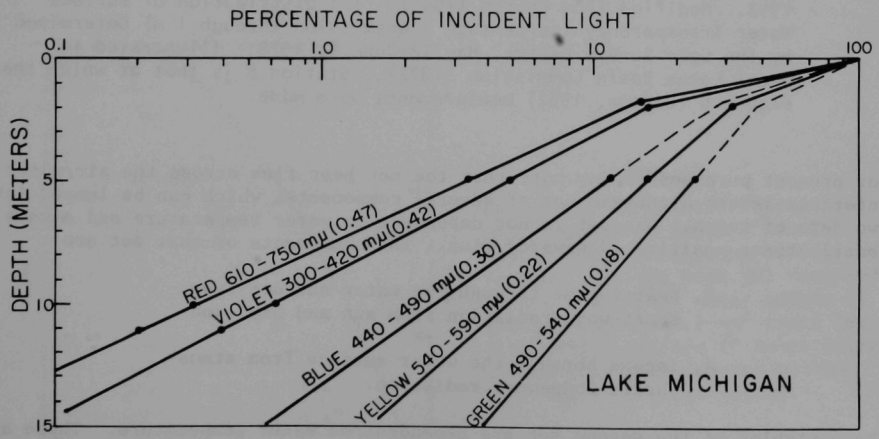

Fig. 8. Penetration of Light of Different Colors into Lake Michigan at Station B Shown in Figure 9(b). Modified from Beeton (1962).

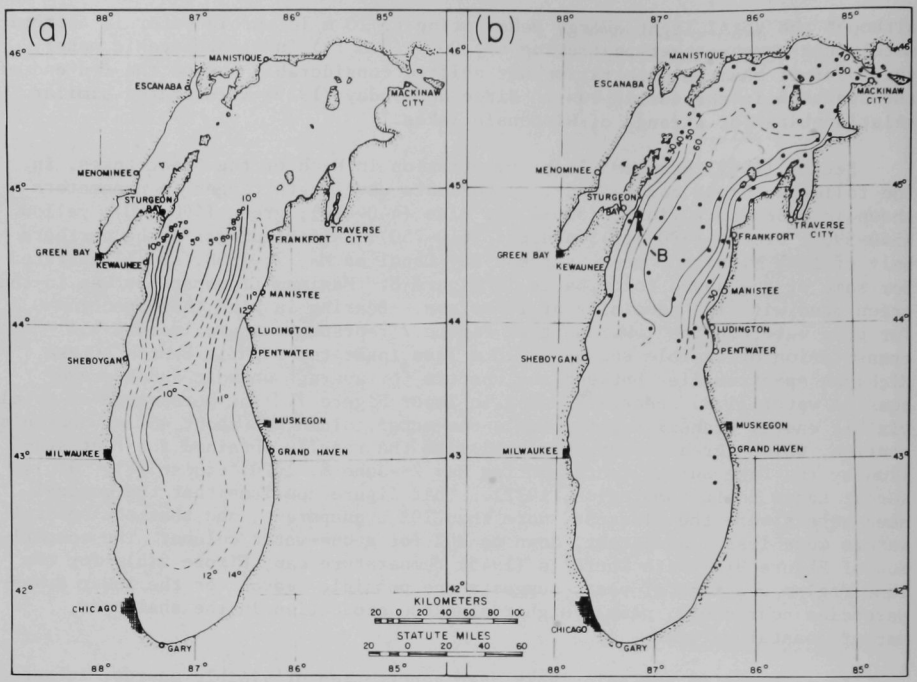

Fig. 9. Lake Michigan: (a) Distribution of Surface Temperature, °C, June 7-9, 1942. Modified from Church (1945). (b) Distribution of Surface Water Transparency (percentage transmission through 1 m) Determined by the Lake Survey Center, May 23-June 8, 1970. Illustrated in Great Lakes Basin Commission (1972). Station B is that at which the Figure 8 (Beeton, 1962) measurements were made.

For present purposes we may note that the net heat flux across the air/water interface is the algebraic sum of several components, which can be lumped into two sets of terms. One set is not dependent on water temperature and always contributes a positive (downward) flux. The components of that set are

S, heat income through the water surface from short-wave radiation from sun and sky; and

A, income through the water surface from atmospheric long-wave radiation.

The variables of the second set are dependent on water temperature. These are

B, outgoing, long-wave back radiation, radiating from a very thin surface layer only and always negative (upwards);

C, heat gain (or loss) by conduction from or to the atmosphere; and

E, heat lost by evaporation (or gained by conduction).

Neglecting heat exchanges with the shores and bottom sediments, which are small in terms of the exchanges across the air/water interface, the rate of change, ΔH, of the heat content of the lake, is equal to the net heat flux defined by

$$\Delta H = (S + A) - (B \pm C \pm E) .$$

When translating the heat gains and losses into temperature, and therefore into buoyancy which influences motion, we may ignore the small temperature dependence of the specific heat of water; but we can by no means ignore the strong temperature-dependence of density. Figure 10 illustrates the well-known nonlinear dependence of density on temperature, with a density maximum at 4° (39.2°F). The important role played by this nonlinearity will become clear during later discussion of the factors which create stratification and control its course through the seasons. Also important for that discussion is the fact that all terms except S (incoming visible radiation for which the water is relatively transparent) in the above expression for ΔH act out their heat exchange function at or very near the surface. Modifying a treatment by Edinger and Geyer (1965), Asbury (1970) has expressed the temperature-dependent terms B, C, and E as functions of commonly measured meteorological variables: wind speed, air and water surface temperature, and humidity. He was therefore able to analyze and estimate the effects of thermal discharges on the mass and energy balances of Lake Michigan as a whole.

We may note that Asbury's analysis predicts a whole-basin annual temperature increase of 0.01°C (0.019°F) and an annual evaporation loss rate of 125 cfs (3.5 m^3/sec) for 1975, resulting from an anticipated 13.9 Gw (13.9×10^9

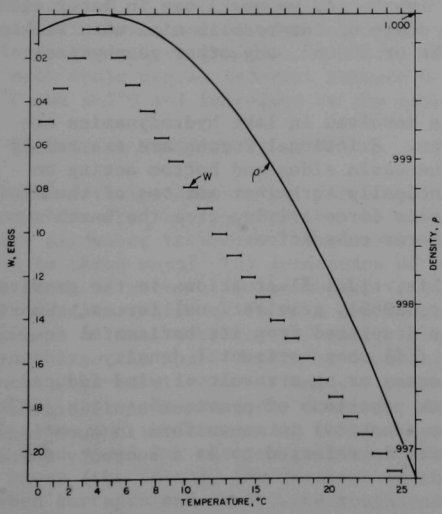

Fig. 10.

Density of Pure Water Plotted over the Temperature Range 0° to 26°C. Also shown, for each whole degree interval, is the work (W) required to mix a vertical water column of 100-cm length and 1-cm^2 cross section with a uniform 1° temperature gradient between top and bottom. Modified from Birge (1910).

watts) of thermal discharge, almost all from electric power stations. The predicted figures for the year 2000 (66.4 Gw) are 0.05°C (0.09°F) and 600 cfs (17 m^3/sec). If those heat additions were confined to a strip of water bounded by the shore and the 10-m depth contour (covering 8% of the total lake area), the temperature rises would be 12.5 times those given above. Asbury's illuminating analysis of the sources of error in these calculations suggests that the temperature estimates are accurate to ± 30% and the evaporation water losses to ± 20 percent. Even so, these estimates are very useful and based on what is known of the physics of the Lake. Improved estimates of temperature increase for nearshore waters, where they are most needed, must await a better understanding of the physical mechanisms and the natural variability of the applied forces.

Following a discussion of the heat budget components, it is customary to describe seasonal changes in the thermal regime. But, in order that treatment of Lake Michigan's annual heat budget shall be interpretative rather than descriptive, that treatment is postponed until the section titled *The Seasonal Cycle of Heat Distribution*.

FORCES ACTING ON THE WATER BODY; SOME REPRESENTATIVE RESPONSES

For an understanding of later sections, a brief excursion into the theory of fluid motion as it applies to large lakes will be helpful. In common with other physical systems, a lake's response to applied force may be immediate or delayed, periodic or steady. The type of response depends on whether the force has periodic components, on whether one or more of those components matches one or more of the possible (normal) modes of oscillation of the system, and on the degree of the braking effect due to internal and external friction. What an observer sees as a response also is strongly dependent on the time scale of interest. For example, a lake makes an obvious annual periodic response to seasonal changes in weather, but (except very near the surface) does not respond immediately to diurnal changes in heat input. As we shall see in later examples, it is necessary to keep the time scale of interest in mind when seeking answers to questions concerning the lake or indeed, any other geophysical system.

The two principal classes of force involved in lake hydrodynamics are gravitational force and frictional force. Frictional forces are exerted by wind acting on the water surface, by the basin sides and bottom acting on moving water, and by the internal, principally turbulent motions of the fluid. To these forces must be added the Coriolis force arising from the earth's rotation. This force is treated in a later subsection.

Neglecting the small, but measurable, tidal fluctuations in the gravitational force in Lake Michigan (Mortimer, 1965), gravitational forces primarily originate (*i*) when the water surface is displaced from its horizontal equilibrium position, by wind for example, or (*ii*) when horizontal density gradients are set up by heating and cooling processes or as a result of wind-induced displacement of stable water masses from positions of previous equilibrium. The horizontal distribution of buoyancy (density) is nonuniform in such cases and the corresponding gravitational force is referred to as a buoyancy force.

THE BUOYANCY FORCE

To understand the nature of this force, as it is applied to the seasonal thermal cycle of a lake, one must remember that the density of fresh water is at its maximum at 4°C (39.2°F) and decreases not only as the temperature rises above 4°C, but also as it falls below 4°C to the freezing point at 0°C (32°F) (see Fig. 10). In fact, the density of water at 0°C equals that of water at 8.1°C (46.6°F) and is 0.013% less than that of water at 4°C. Figure 10 shows that temperature change near 4°C produces very little change in density, but that as the temperature diverges from 4°C (up or down) the density change corresponding to unit temperature change increases. For example, starting at 6°C (42.8°F), it is necessary to raise the temperature to 11°C (51.8°F) to bring about a density decrease equal to that produced by only a one-degree temperature rise from 34°C (93.2°F). The generation of the buoyancy force can be visualized by taking a simple hypothetical example of a lake initially at uniform temperature near 4°C. If one region of the lake were then heated by the sun to, say, 16°C (60.8°F) throughout the whole of the water column, a thermal expansion of one part in a thousand would take place, and the center of gravity of the column would consequently be raised by 1/500 of its total depth. With the rest of the lake remaining cold, the expansion in the hot region would generate a horizontal pressure gradient, directed from the hot region to the cold, which would set currents (gradient currents or density currents) in motion. If the hot and cold masses did not mix appreciably, the result would be a new equilibrium with a vertical density stratification, with less dense warmer water lying on top of the colder denser water, and with a more or less sharp interface (vertical density gradient or thermocline) between them. Although not developed in the simple manner described above, a similar stratification is set up in lakes in summer as a result of the interaction of heat input and wind energy (see the next major section).

To mix any stratified column in a lake, the wind must perform work in overcoming the corresponding (gravitational) buoyancy force, or as Birge (1910) called it, the thermal resistance to mixture. He calculated the work required to mix a column of water 1 cm^2 in area and 1 m high with an initial uniform temperature gradient of 1°C/m. That work, plotted in ergs in Figure 10 for each whole degree interval between 0 and 26°C, is minimal for the intervals 3-4°C and 4-5°C and increases as the temperature moves above or below 4°C.

THE MECHANICAL FORCE OF THE WIND

The principal mechanical force applied to a lake arises from the transfer of momentum from air to water by the imperfectly understood action of the wind at the air/water interface. Mechanical energy is transferred from wind to water in three ways: (*i*) generation of waves and the turbulence associated with particle motions in the waves, (*ii*) frictional drag of the wind on the water surface, which is in turn dependent on the wave topography and the roughness of that surface, and (*iii*) sporadic injections of momentum and turbulence into the upper layers by breaking waves. In any given set of circumstances, the relative contributions of wave effects, frictional drag, and wave breaking cannot be precisely defined. The relative magnitudes of these contributions and their relation to wind speed is strongly dependent not only on mean wind speed but also on gustiness, the water distance over which the wind has blown (the fetch), the duration of the storm, the partition of wind energy between currents and waves, the roughness of the water surface and the previous

history of the waves, and vertical temperature gradients in the air. Water colder than air will produce a stratification in the moving air layer (stable flow) which in turn decreases the mechanical effects (drag) at a given wind speed.

We need not be surprised, therefore, that estimates of energy transfer from wind to water must still rely on empirical or semi-empirical data and equations which await experimental verification. Energy transfer across the air/water interface is a very topical theme in physical oceanography, and much of the experimental work is being done on the ocean. However, some valuable results are expected to appear from the IFYGL Program (International Field Year on the Great Lakes), for which field work was completed on Lake Ontario in 1972. Lake Michigan and the other Great Lakes require more research into the contribution of breaking waves to the generation of mechanical energy and turbulence.

TURBULENCE AND FRICTION

The ultimate fate of mechanical energy introduced into the water is, as every high school student knows, to perform work against viscous forces and to become dissipated into heat. The pathway towards that final energy sink is, however, complex and associated with eddying motions covering a wide range of scales. Therefore, to understand these motions it is necessary to acquire at least a qualitative impression of the nature of turbulence. With very rare exceptions, flow is always turbulent in lakes, although the intensity of the turbulence varies enormously. Anyone who tries to hold an umbrella on a windy day recognizes the essential properties of turbulent flow: a mean flow, moving in a more or less steady direction, upon which are superimposed apparently random fluctuations of velocity directed randomly in space. It is also evident that the random motions occur in a wide range of sizes and frequencies, i.e. a "spectrum of eddies" is involved, ranging from very large eddies which threaten to lift the umbrella over the rooftops, to small ones which make it vibrate like a leaf. Similar chaotic properties with a widely ranging eddy spectrum are characteristic of turbulent flow in wide pipes, open channels, and natural water bodies, in contrast to the organized streamlined laminar flow in narrow pipes.

Turbulent flow can be conceptually separated into (*i*) a mean flow, responsible for the transport of fluid properties and materials carried in the fluid, and (*ii*) irregular fluctuations in velocity superimposed on the mean flow, and responsible for the diffusion of fluid properties and materials carried with the fluid. Dispersal of those materials can be defined as the combined effects of transport and diffusion.

The chaotic and irregular character of the turbulent fluctuations present severe difficulties in predictive applications. Prediction is only made possible by statistical models and concepts which average contributions of the individual random motion. The simplest model, analogous to that for molecular diffusion, is the "random walk model" described by Csanady in the essay which follows. The model is analagous to diffusion across a given plane; the rate of diffusion of material or heat is the product of the concentration gradient normal to that plane and a diffusion coefficient. At the molecular level the diffusion coefficient is small and constant; whereas in turbulent flow the coefficient is much larger and varies in magnitude with the intensity of the turbulent motion.

More realistic models, also presented in Csanady's essay, take account of the fact that the turbulent diffusion coefficient (eddy diffusion coefficient) varies not only with the intensity but also with the scale of the turbulent motions. This result, which has a far-reaching influence on the properties of our natural environment, is derived from another useful statistical concept, that of the "eddy spectrum" of turbulence. That concept, discussed more fully in Csanady's essay, envisages the cascading of mechanical energy from the largest eddies, generated by the stirring agent (the wind), down through the eddy spectrum of motions of ever-decreasing scale into the molecular, viscous range where the energy is finally dissipated by viscous forces and appears as heat. These viscous forces represent the system's frictional brake, either as internal friction (water viscosity) or boundary friction at the side or bed of the lake. If the motion achieves a steady state, as it rarely does in nature, the driving or stirring forces at the large eddy input end are balanced by the frictional forces at the molecular output end of the cascade.

THE INFLUENCE OF THE EARTH'S ROTATION

Because of Lake Michigan's large dimensions, some motions in the Lake are strongly influenced by the earth's rotation. In order to understand such motions, a general account must be given of the Coriolis force, which is a consequence of the rotation.

An empirically correct description of fluid motion in pipes or small basins is provided by the simple equations of motion (without the terms involving rotation) in a coordinate system rotating with the earth, i.e. the everyday coordinate system which we earthbound observers use. Since the motion is controlled by the boundaries of the pipe or basin, which are rigidly connected with the rotating earth, we do not have to take rotation into account in such cases. However, for motion not so constrained, the simple equations of motion only apply in an inertial coordinate system connected, not to the rotating earth, but to the fixed stars. The transformation from fixed to rotating coordinates is treated in textbooks of classical mechanics or physical oceanography or meteorology, most simply in terms of vector algebra; but the following descriptive account will help us to understand important types of motion in Lake Michigan.

Let us start by considering, in Figure 11, three level surfaces, one at the north pole, one on the equator, and one at latitude ϕ. If we confine our consideration to the horizontal components of motion, we can use a horizontally directed telescope at each of the three positions to determine how the local horizontal plane rotates relative to the fixed stars, i.e. to the inertial system of coordinates. At the pole, the telescope will rotate relative to the fixed stars once every sideral day, i.e. at frequency Ω, the angular frequency of the earth's rotation. At the equator, there is no rotation in the horizontal plane relative to the stars. At an intermediate latitude ϕ the local horizontal plane rotates, relative to the stars, at an angular frequency $\Omega \sin \phi$. Therefore, to determine the horizontal component of unconstrained motion (i.e. motion of a projectile, or an air of water mass not connected to the earth) we have to solve the equations for a turntable rotating at angular speed $\Omega \sin \phi$. This can be done by considering, in Figure 12, how the horizontal component of the unconstrained motion is seen by (a) a space observer poised in a satellite above the horizontal plane in question and conscious only of the coordinates linked with the fixed stars, and (b) a terrestrial observer whose coordinates rotate with the earth.

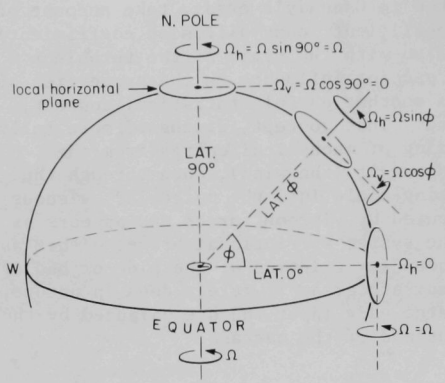

Fig. 11.

Diagram of the Northern Hemisphere for Explaining the Coriolis Force (see text).

Ω = angular speed of earth's rotation, 7.29×10^{-5} rad/sec.

ϕ = angle of latitude.

$\Omega_h = \Omega \sin \phi$ = horizontal
$\Omega_v = \Omega \cos \phi$ = vertical
} component of earth's rotation.

Therefore, the angular speed of rotation of the local horizontal plane at latitude ϕ, relative to the inertial co-ordinate frame, is $\Omega \sin \phi$, and the period of rotation is $2\pi/\Omega \sin \phi \sin = 24/\sin \phi$ hours. (The vertical component is usually not considered in oceanographic applications.)

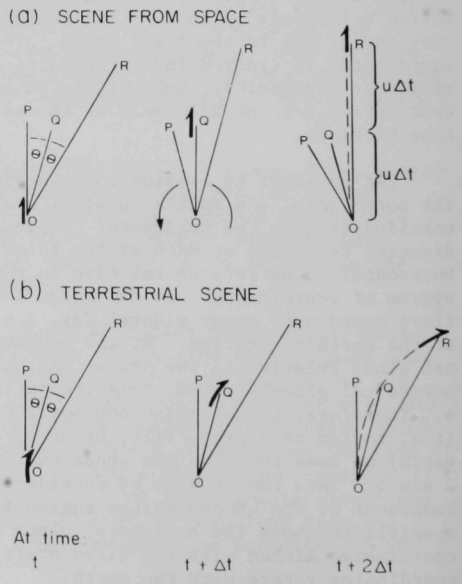

Fig. 12.

Explanatory Diagram of Coriolis Force (see text).

Let us assume that at time $t = 0$ a mass is moving under inertial forces alone at a velocity u through O, which in the figure is the center of the turntable, but could in fact be any point on the turntable. After a small time interval Δt, the space observer sees that the turntable has rotated through a small angle θ and that the mass has arrived at point Q, such that length $OQ = u\ \Delta t$. OP and OQ can be regarded as spokes of the turntable, so that during the next interval Δt the space observer sees the mass continuing its progress in a straight line to arrive at R on the next spoke. On the other hand, the terrestrial observer, not aware of the rotation of his local horizontal platform plane, sees the spokes as fixed and the track of the mass (moving under inertial forces) as continually curving to the right in the manner shown in Figure 12(b). Continued projection of this track shows it to be a circle, the inertial circle, completed during half the period of rotation of the turntable.

This not immediately obvious result can be obtained in another way by considering, in Figure 12(b), the force which the terrestrial observer has to invoke to explain the observed curvature of the inertial track. Because the mass maintains its constant speed u, there can be no force acting in the direction of motion. Therefore, the force bringing about the curvature must be directed always normal to the inertial track, toward the right in this example in the Northern Hemisphere. In Figure 12(b) the inertial motion can be broken down into components along OP (displacement $u\ \Delta t$) and along PQ. As Δt approaches the limit zero, the angle OPQ approaches a right angle. The displacement component PQ is a result of acceleration a acting over interval Δt. The mean velocity in direction PQ is therefore $a\ \Delta t/2$, and the displacement PQ is $a(\Delta t)^2/2$. The ratio PQ/OP is therefore $(a\ \Delta t)/2\ u$; and, as Δt tends toward zero, that ratio ($\simeq \tan POQ$) approaches the angular measure POQ, which is Δt multiplied by the angular speed of rotation, $\Omega \sin \phi$. Therefore the Coriolis acceleration is

$$a = 2\ \Omega \sin \phi\ u\ .$$

The parameter $2\ \Omega \sin \phi$, which has the dimensions of a frequency (the inertial frequency), is usually referred to as f, the Coriolis parameter. The Coriolis force is therefore $f\ u$ per unit mass, directed always at 90° to the right (Northern Hemisphere) of the direction of motion at any instant.

As already suggested, the mass, moving only under its own inertia in the terrestrial frame (i.e. with no other forces acting upon it), follows a circular track of radius r. The observer on earth can interpret this track as the resultant of a balance between the Coriolis force, $f\ u$ per unit mass, and the centrifugal force corresponding to the circular motion, u^2/r per unit mass. Therefore,

$$r = u/f\ .$$

Taking a typical value of u of 10 cm/sec (0.328 ft/sec) the radii of the corresponding inertial circles at latitudes 20°, 40°, and 60°, are 2.00, 1.06, and 0.79 km (1.24, 0.66, and 0.49 mi) respectively.

These results, to be found in textbooks of physical oceanography, are summarized here to make the point that a lake must be of width order greater

than about 5 r before rotational effects become significant, and greater than about 20 r before they become dominant. As we shall see, rotational effects are significant for surface long waves and dominant for internal long waves in Lake Michigan. The circumference of the inertial circle, $2\pi r$, equals $2\pi u/f$. At velocity u, the circle is therefore completed in period $2\pi/f$, the inertial period, which is $2\pi/2\Omega \sin\phi$ sec, or $12/\sin\phi$ hours. This confirms the result mentioned earlier that the inertial period is half the period of the local horizontal component of the earth's angular speed. At the latitude of Milwaukee, the inertial period is close to 17.5 hr and, although the Coriolis parameter at Mackinaw City differs by some 8% from that at Chicago, the value of f may be taken as constant, for our purposes, over the whole basin.

REPRESENTATIVE RESPONSES TO APPLIED WIND FORCE

If the applied wind force is of sufficient steadiness and duration, a relatively stable response develops in the form of wind-driven currents. In offshore regions of basins as large or larger than Lake Michigan, the wind-driven currents are initially constrained by the Coriolis force to flow to the right of the wind direction. When wind-driven currents are generated near shore, the boundaries also provide a constraint and the water piles up to form a slope, or set-up. In small lakes, this slope extends over the whole basin with the surface sloping upward toward the downward end. If the wind blows long enough for a steady-state condition to be established, the gravitational force acting down the slope balances the wind stress on the water surface. In large basins such as Lake Michigan, Coriolis force comes into play, and a nearshore set-up slope is established across the wind, with the higher water surface on the right of the wind direction. If, in long basins such as Lake Michigan, the wind begins to blow along the basin axis, circulation is established with water moving with the wind in the shallower parts of the basin, i.e. near the wind-parallel shores, and with a return circulation moving against the wind in the deeper parts, as described later in connection with Figure 62. Models of this type of circulation, applied for example to a cross section of Lake Ontario (Bennett, 1973b; Csanady, 1973; and Simons, 1973, reviewed by Boyce, 1974), suggest that the direction reversal occurs at a depth equal to the mean depth of the cross section. Because transport averaged over the whole basin must be zero in this model, and approximately zero in actual lakes, the fastest currents will be found in the shallower regions. This relatively simple circulation pattern may be expected to hold generally after about 12 hr of applied wind stress. Later, after the wind stress is removed, the pattern will become more complex, particularly if the water is stratified (see Periodic Responses below).

In fact, in small and large basins, the circulation pattern can be regarded as a combination of primary, wind-driven currents, and secondary gradient currents driven by the horizontal pressure gradients produced by the set-up slopes. When wind stress is removed, primary currents die down fairly quickly; but the set-up slopes take more time to disappear, and associated gradient currents decay less rapidly. In Lake Michigan, nearshore gradient currents are geostrophic or nearly so, i.e. the component of gravity acting along the set-up slope balances the Coriolis force and permits the current to travel in a straight (shore-parallel) line.

Examples of relatively steady currents have been observed in Lake Michigan, particularly in nearshore regions. Their directions are strongly correlated

with wind direction: they frequently appear to be generated by wind, and persist for several days in their original, usually shore-parallel direction after the wind has stopped. But, as we shall note, observations of steady circulation patterns are fragmentary at best, and this reveals a serious gap in knowledge and methodology. We defer further discussion of currents until the section on characteristic responses of the stratified lake.

PERIODIC RESPONSES

Except in very shallow basins or nearshore regions, where friction at the solid boundaries is a dominant force, the dissipation of set-up slopes after the wind ceases is not a steady decrease but is coupled with oscillations in the form of long waves, i.e. waves of length much greater than water depth. In closed basins, these long waves are constrained by the boundaries and take the form of standing waves or seiches. These conform to standing-wave patterns familiar to anyone who has made waves in his bath. In the simplest mode of seiche oscillation, a rise in water level at one end of the basin is accompanied by a fall at the other end, with a nodal region in the center where the water level does not oscillate. The simplest model, to which we shall refer later, is a seiche in a rectangular tank, i.e. a basin of constant depth. The seiche is a standing wave characterized by (*i*) one or more nodal lines or nodes, at which wave elevation is always zero and particle motion is entirely horizontal, with no vertical component; and (*ii*) two or more antinodal lines or antinodes at which wave elevation is maximal and particle motion is entirely vertical, with no horizontal component. The basin ends must coincide with antinodal lines because only along those lines can the boundary condition, of no flow normal to the ends, be met.

Lake Michigan also executes seiche oscillations, with the simplest single-noded variety being the most strongly excited. Seiches are set in motion during wind disturbance and during the degeneration of the wind-induced set-up mentioned earlier. After the wind has ceased, these pulsations continue for several cycles of oscillation; the number depends upon the rate of frictional damping. A simplified diagram showing the mode of generation and subsequent progress of a surface seiche oscillation in a small lake is presented in Figure 13(a) for the single-noded variety. This is the form most commonly encountered. Although higher harmonics with more than one node may also be generated, they tend to be damped out by friction more quickly than is the uninodal component. Flow associated with the seiche oscillates to and fro and attains its highest velocity and largest horizontal excursion in the nodal region. As the basin ends are approached, the horizontal component of flow falls to zero; some vertical components remain, thereby satisfying the obvious and universal boundary conditions that flow normal to any solid boundary is impossible.

Figure 13(b) refers to an analogous interface seiche in a small stratified lake, to be discussed in the section on characteristic responses of the stratified lake.

An example of the most common (single-noded or uninodal) variety of surface seiche in Lake Michigan is illustrated in Figure 14, which is based on extracts of water level record from six stations around the basin. Except for the record from Green Bay, placed at the top of the diagram and discussed later, the level traces occupy vertical positions on the diagram roughly

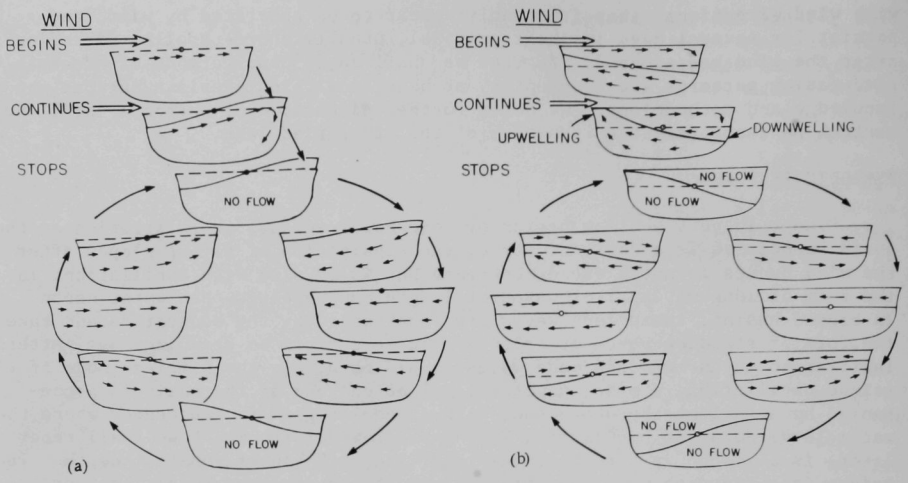

Fig. 13. Models of (a) a Surface Seiche in a Homogeneous Lake and (b) an Internal Seiche in a Two-Layered Lake. The initial action of the wind and one cycle of the ensuing oscillation is shown. The broken line represents the equilibrium position of the water surface in (a) and of the interface in (b).

proportional to their spacing around the shore. This method is used to draw attention to a counterclockwise progression of high water. Depending on the design and location of the recorder stilling wells, the records show a greater or lesser degree of high frequency decoration. On the diagram, smooth curves have been drawn through the decorations by eye to follow the low-frequency tide-like wave generated during the wind storm starting at the left side of the diagram. This not only set the seiche in motion but also induced a north-south set-up, apparent as a reduction of mean level at Mackinaw City, accompanied by an increase in mean level at the southern end (Milwaukee and Chicago). The set-up corresponded to a one-foot ($\sim$ 30 cm) water-level difference between the basin ends, which gradually equalized during the following day or so. In addition, there was a seiche wave of about a 6-in ($\sim$ 15-cm) range (trough to crest) and a period close to nine hours. At the other stations the seiche range was less. The range was the least at Ludington, which, as we shall see, lies close to the nodal region for this particular seiche node.

The very large seiche ranges observed at the southern extremity of Green Bay represent a resonant oscillation between that bay and the 9-hr seiche in the main Michigan basin. Compared with the records at Mackinaw City, the Green Bay resonance response is magnified by a factor of about 6 and is opposite in phase, i.e. high water at Mackinaw City coincides with low water at Green Bay. The nature of this resonance and of a second resonance with the semidiurnal tide is discussed by Mortimer (1965).

Although a great deal of information about higher frequency oscillations (i.e. higher seiche modes) is contained in water-level records of the kind illustrated in Figure 14, it is rather rare that single or multiple seiche

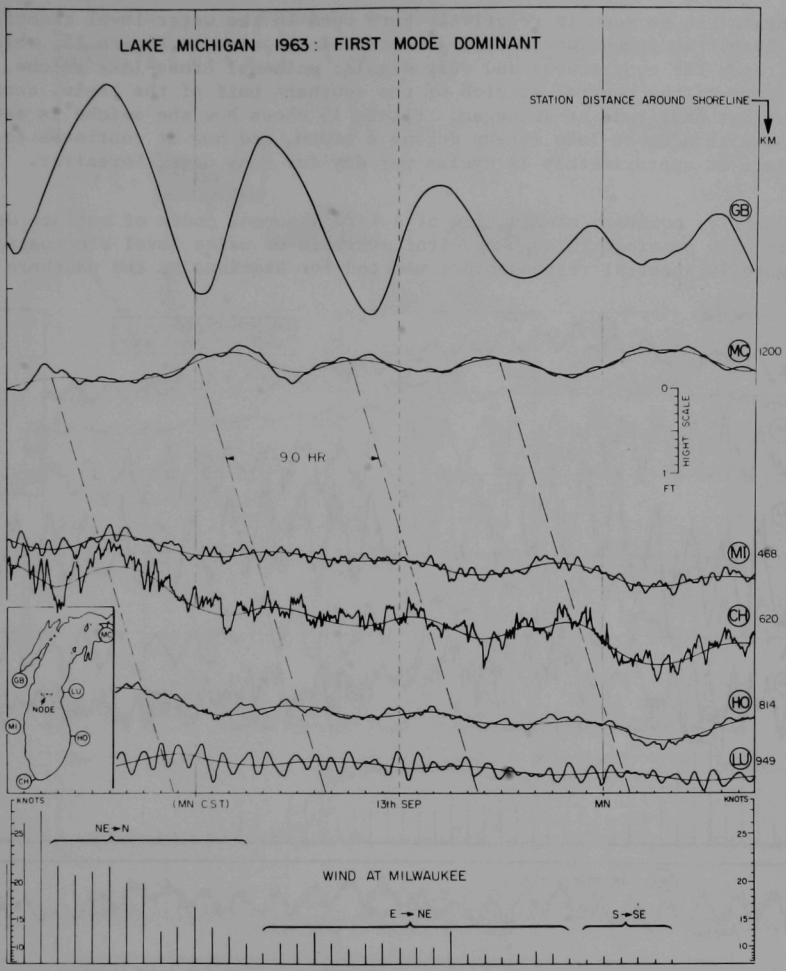

Fig. 14. A Two-Day Extract of Water Level Records at the Following Stations in Lake Michigan: GB Green Bay, MC Mackinaw City, MI Milwaukee, CH Calumet Harbor, HO Holland, LU Ludington. Except for GB, the vertical spacing of the water-level traces approximately represent the spacing of the stations around the shoreline to show the counter-clockwise progression of the first seiche mode (period 9.0 hr) indicated by the thin line drawn by eye through each record. The origin of the large amplitude at GB is discussed in the text. The diagrams here and in Fig. 15 are modifications of those in Mortimer (1965) prepared from records made available by the Lake Survey Center.

components can be seen in relatively pure form in the water-level records themselves. An exception to this general rule is seen in Figure 15, which illustrates the conspicuous and very regular uninodal cross-lake seiche, characteristic of the central stretch of the southern half of the basin, seen at its largest amplitude at Waukegan. Figure 15 shows how the seiche is set in motion, with a cross-lake set-up during a storm, and how it continues to oscillate at approximately 11 cycles per day for many days thereafter.

Usually, however, elucidation of a lake's normal modes of surface oscillation is only possible through spectral analysis of water level fluctuations. In Figure 16 spectral responses are plotted for stations at the southern

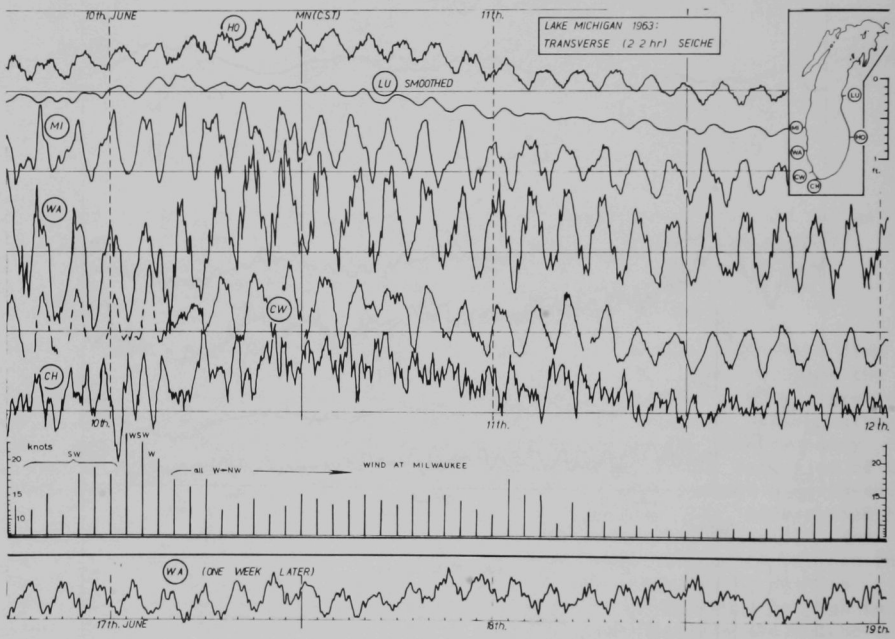

Fig. 15. Extracts of Water Level Records (Lake Survey Center) June 10-12, 1963, at Lake Michigan Stations HO Holland, LU Ludington, MI Milwaukee, WA Waukegan, CW Chicago Wilson Avenue, CH Calumet Harbor. The smooth curve for LU was obtained from the original record as a moving average of five consecutive readings at 15-min intervals, advancing in steps of 15 min, in order to remove large local oscillations. The figure demonstrates the dominance and persistence of the first transverse surface seiche mode in the southern basin. Also plotted are wind speed and direction at Milwaukee and extract from the WA record of one week later, on which the transverse seiche still persists. The diagrams here and in Fig. 14 are modifications of those in Mortimer (1965) prepared from records made available by the Lake Survey Center.

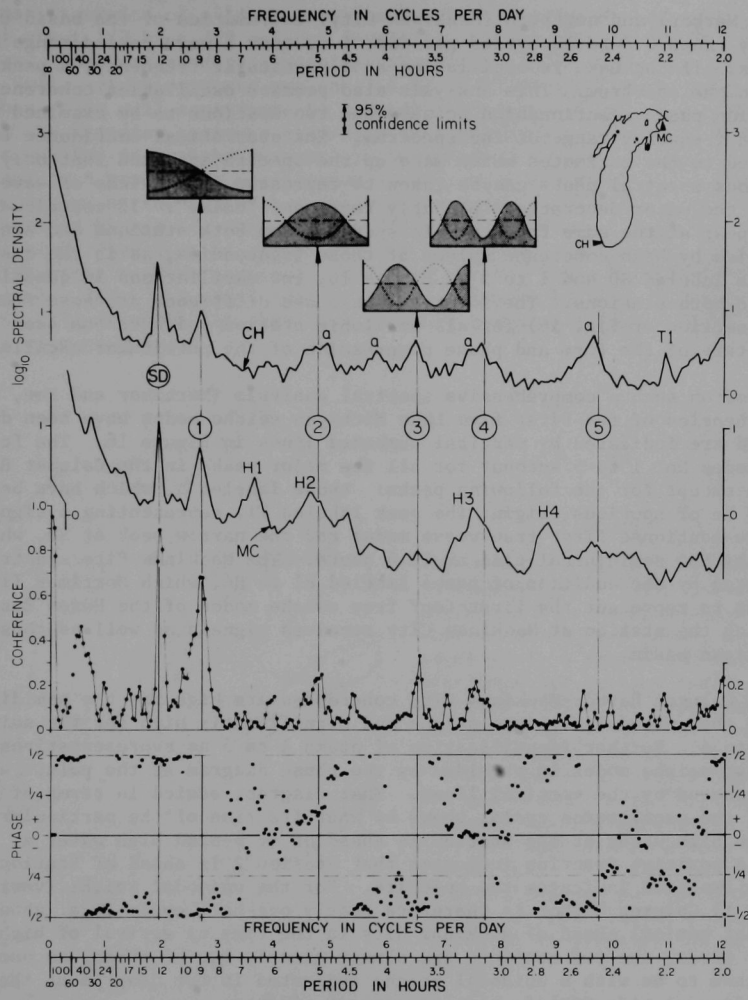

Fig. 16. Spectra of Water Level Fluctuations at Lake Michigan Stations CH Calumet Harbor and MC Mackinaw City (13,152 hourly readings June 1962-November 1963, supplied by Lake Survey Center). Illustrated are power spectra (after removal of the mean and a linear trend) for stations CH and MC, interstation coherence, and interstation phase difference as explained in the text. Spectral peak SD represents the semidiurnal tide and peaks 1 to 4 represent the first four surface seiche modes, the forms of which are illustrated in the model basins at the top of the figure.

(Calumet Harbor) and northern (Mackinaw City) extremities of the basin over the frequency range 0.2 to 12 cycles per day, i.e. over a wave period range of 2 to 120 hours. If the Lake is oscillating at a particular frequency, a peak will appear in the spectrum. This analysis also permits oscillation coherence and oscillation phase relationships between the two stations to be examined over the whole frequency range of the spectrum. The statistical confidence to be attributed to the estimates which make up the spectra are such that only the conspicuous spectral peaks can be taken to represent real seiche or wave oscillations; the minor decorations probably represent "noise". If conspicuous peaks appear at the same frequency in spectra from both stations and are accompanied by high coherence values at those frequencies, as is the case for the peaks labeled SD and 1 to 5 in Figure 16, the oscillations in question are common to both stations. The interstation phase difference at those frequencies (bottom section of Fig. 16) for all available station pairs can be used to build up a picture of the form and phase progression of the particular oscillation.

Based on such a comprehensive spectral analysis (Mortimer and Fee, 1973), the frequencies of the first five Lake Michigan seiche modes have been determined and are indicated by vertical numbered lines in Figure 16. The free seiche modes No. 1 to 5 account for all the major peaks in the Calumet Harbor spectrum except for the following peaks: those labeled α, which have been shown to be of spurious origin; the peak labeled T1, representing a signal from the above-mentioned first transverse mode; and the narrow peak at SD, which represents the semidiurnal tide at 12.4 hours. The Mackinaw City spectrum is complicated by the addition of peaks labeled H1 to H4, which Mortimer (1965) has shown to represent the first four free seiche modes of the Huron Basin, from which the station at Mackinaw City receives signals as well as those from the Michigan basin.

The Calumet Harbor-Mackinaw City coherences are high for the semidiurnal tide and the uninodal Michigan seiche and significantly high for the seiche modes 2 to 4. Further identification of peaks 1 to 5 as representatives of the first five seiche modes is provided by the phase diagram at the points where it is intersected by the vertical lines. That diagram, scaled in terms of fractions of the oscillation cycle, shows by what fraction of the particular seiche cycle the high water at one station is ahead of or behind high water at the other. A positive fraction indicates that Station 2 is ahead of Station 1; a negative fraction indicates the opposite. For the uninodal seiche (vertical line No. 1) Calumet Harbor is therefore nearly one-half cycle (i.e. about 4.5 hr at that period) ahead of Mackinaw City in the time of arrival of high water. In other words, the two stations are almost exactly out of phase, as one would expect them to be with a uninodal seiche indicated in the diagram at the top. The semidiurnal tide (SD) is also almost out of phase.

The same out-of-phase condition also holds very closely for the other odd-numbered modes, 3 and 5; while the even-numbered modes, 2 and 4, are approximately in-phase (i.e. with the phase estimates near the zero line of the diagram), which is in agreement with the relationships predicted for those modes in the sketches at the top of the figure.

The currents induced by wind set-ups and seiches in Lake Michigan are not negligible, but are only generated occasionally during and after storms. For example, a uninodal seiche with a range of 3 ft at Chicago would induce a horizontal to-and-fro motion in the middle reaches of the basin with a total

water mass excursion of a little over half a mile (∿ 0.8 km) and a peak current speed of about 1/3 knot (18 cm/sec) involving the whole water column from top to bottom. The current direction alternates every half period, i.e. every 4.5 hours. While seiche currents are not likely to be of more than occasional importance, they will contribute to general turbulence, and in some cases they may modulate steadier currents generated in other ways. Even so, the basin is large enough for the seiche currents to be modified by the Coriolis force, which imposes a transverse oscillation in the central region of the basin, with the same period as the seiche but delayed in phase by one-quarter cycle. As illustrated in Figure 17, this has the effect of changing the motions of the surface seiche from that of a plane seesaw in Figure 13 to a form of motion in which high water rotates counterclockwise around the basin (in the Northern Hemisphere). Also, the nodal line in Figure 13 is replaced by a single point (P in Fig. 17) at which the elevation does not change and around which the rotating wave progresses.

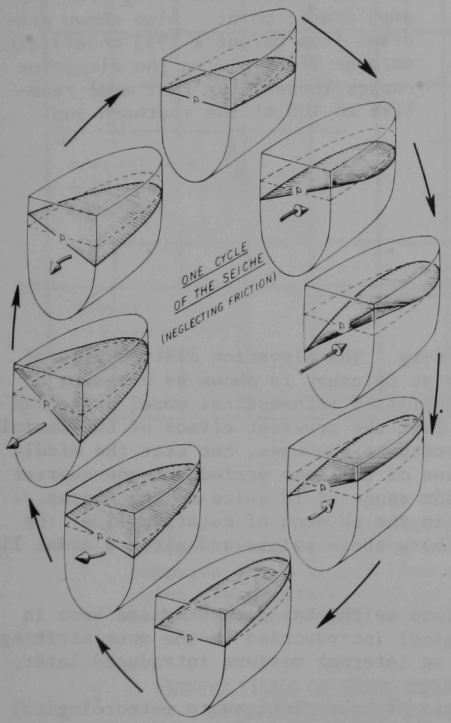

Fig. 17.

The Effect of Basin Rotation on the Surface Seiche. Eight stages in the oscillation cycle of an amphidromic surface seiche are shown, with the water surface shaded and the equilibrium water surface indicated by a broken line. For illustrative convenience, the basin is shown bisected through the amphidromic point P (nodal point of zero elevation change) around which "high water" rotates counterclockwise in the northern hemisphere, as explained in the text. A rough indication of the direction and speed of the seiche current flowing through the P section is given by the solid arrows.

Interstation comparisons of seiche amplitudes and phases using all available Lake Michigan water-level records confirm the Figure 17 picture. The result for the 9-hr uninodal seiche is illustrated in Figure 18, which shows a pattern of cotidal lines radiating from a central point of zero elevation change (the amphidromic point P). Cotidal lines are those along which high water occurs at the same hour, and they are drawn in Figure 18 at half-hour

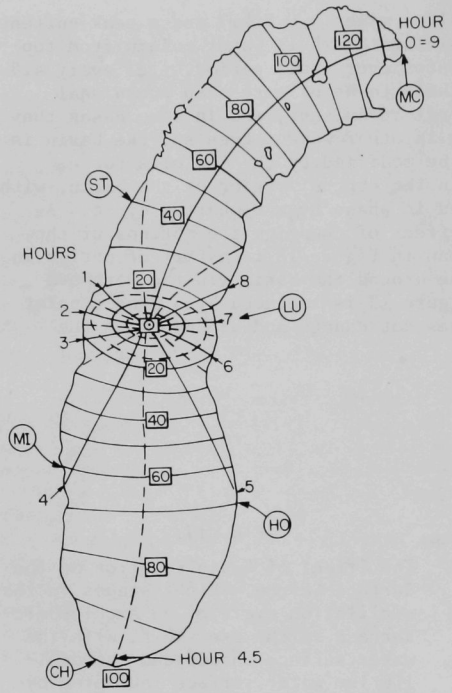

Fig. 18.

Lake Michigan: Phase Progression of the First Longitudinal Seiche Mode of Period 9.0 Hours. Relative to 0 at MC, cotidal lines, at which high water occurs at the same time, are shown for each hour and half hour (broken lines), radiating from the amphidromic point. Also shown (redrawn from Defant's 1953 model) are corange lines giving the elevation ranges (boxed) for that mode relative to 100 at the southern end.

intervals starting at 0 hr at Mackinaw City. The elevation distribution of this seiche mode, relative to 100 units at Chicago, is shown by a series of cross-lake corange lines, based on a simplified mathematical model presented by Defant (1953). Figure 18 demonstrates that the greatest effect of the Coriolis force on the seiche pattern is found, not near the ends, but near the middle of the basin, where a transverse oscillation of the same period but one-quarter cycle out of phase generates an elevation range of 18 units on the shores opposite the amphidromic nodal point. In the absence of rotation (i.e. the Fig. 13 case) the elevation change at those shore points and along a nodal line joining them would have been zero.

The effect of rotation of the surface seiche has been examined here in some detail, because it serves as a logical introduction to the more striking and more important effects of rotation on internal motions introduced later.

Another surface (long) wave response of Lake Michigan to meteorological forcing must also be mentioned, namely the surge often associated with summer squall lines (barometric pressure jumps) traveling eastward or southeastward across the basin. If the pressure jump is large, and if the squall line travels at a critical speed equal to the speed of the water wave at the depth concerned, a large amount of energy passes from the air to the water and waves of large amplitude are built up. These progressive tidal waves, often confused with seiches in the popular press, can cause damage and drownings; and the

effect is accentuated between Chicago and Waukegan by reflection of the eastward-traveling wave by the eastern shore of the southern basin. An example, analyzed and modeled by Platzman (1958), is illustrated in Figure 19. The range of water level fluctuation in the lake at Chicago (Wilson Avenue crib) was over 3 ft (∿ 92 cm) and the surge waves recurred at about 20-min intervals. On that day (June 26, 1954) the level in some harbors rose higher [local focusing effects? . . . "a seven foot (2.1 m) rise" at Montrose] and at least seven lives were lost. Small surges are common all summer and probably contribute to the generation of seiches.

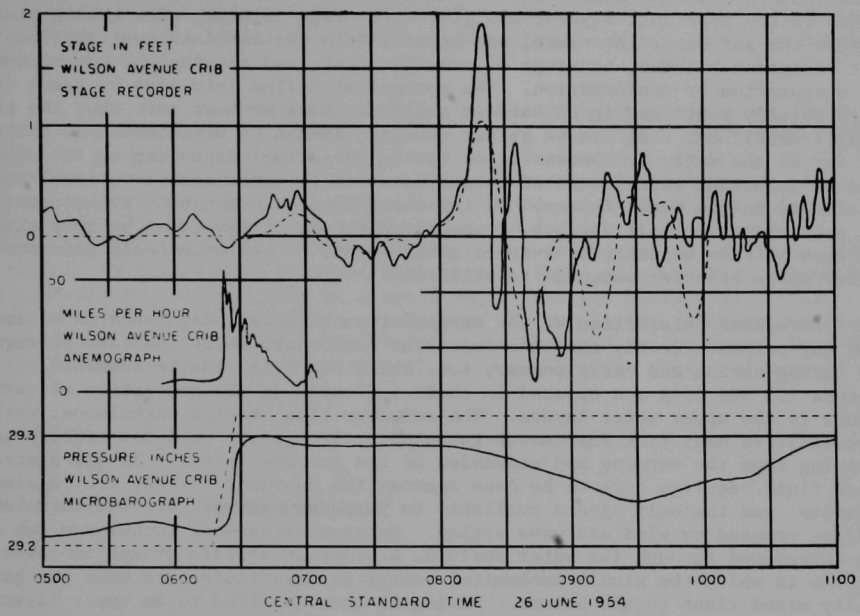

Fig. 19. Lake Michigan: the June 26, 1954, Surge. Illustrated are the lake level, wind, and atmospheric pressure records at Chicago Wilson Avenue Crib. The broken line represents lake level computed for a squall line speed of 54 kn in Platzman's model, using the pressure jump indicated by the lower broken line. From Platzman (1958) (with permission, see credits).

INTERACTIONS OF WIND-INDUCED TURBULENCE AND THE BUOYANCY INDUCED BY HEATING AND COOLING

The practical usefulness of this essay, and indeed any present-day treatise on physical limnology, is severely limited by the fact that it is much more difficult to measure turbulence and turbulent flow and dispersal in water than it is to measure water temperature or to record the standard meteorological variables in the air: wind speed, air temperature, humidity, and radiation into or out of the water surface. Therefore, much more is known about the heat energy budgets of the world's lakes than about the motions and momentum transfers

that take place below the surface. We know, for example, from Birge's pioneering work in Lake Mendota (1897, 1904) that the peculiar temperature-density relationships of water (Fig. 10), influencing the interplay of wind and solar heating in spring, produced "a warmed surface layer of nearly uniform thickness . . . with a transition layer immediately below it--the thermocline" (Birge, 1904), a term which Birge himself first introduced in 1897. As we shall see when we examine the seasonal and shorter term changes in heat distribution in Lake Michigan, there are five or six distinct seasonal phases, the succession of which depends on the interaction of two principal agents: (*i*) a flux of wind-induced momentum across the air-water interface, thereby generating turbulence in the uppermost layers; and (*ii*) a net flux of heat, also taking place across the air-water interface, and arising from the combined contributions of net radiation balance, exchange of sensible heat, and the thermal consequences of evaporation or condensation. The mechanisms called into play by agent (*ii*) were briefly mentioned in an earlier section. Here we must note that the net (daily mean) heat flux can be either downward (which we will define as positive as far as the water is concerned) or upward (negative) depending on the season; and an important consequence of these fluxes is the creation of vertical buoyancy gradients in the water column. On the other hand, the momentum flux, agent (*i*), is predominantly positive, i.e. downward, although it may often be very close to zero in calm weather, or even slightly negative when previously generated water waves transfer momentum to still air.

Air-water interaction is the target of much present-day research effort. For our purposes we may note the important fact that, while the lake is warming up during spring and early summer, i.e. while the heat flux is downward, agents (*i*) and (*ii*) are opposed in their influence on the generation of turbulence in the upper water layers. The momentum flux creates turbulence, while the positive heat flux suppresses turbulence through the creation of buoyancy, arising from the warming and expansion of the surface layers. To mix a stratified fluid requires work to be done against the buoyancy forces, i.e. against gravity, and the only agents available to perform that work are the turbulent eddies created by wind and wave action. Because mechanical turbulence can only be introduced through the water surface, a state of affairs arises in lakes and oceans in which the wind's mechanical energy is insufficient to keep the basin fully mixed right to the bottom. Mixing is then confined to an upper layer (epilimnion) extending down to the thermocline, where stratification resists the further penetration of turbulent mixing into deeper layers. The principle governing the growth or suppression of turbulence in stably stratified fluids is of such fundamental importance that I have chosen to discuss it here before describing and interpreting the seasonal changes in Lake Michigan's density structure.

The initial insight into this matter must be attributed to Richardson (1920), who examined conditions under which turbulence increases or decreases in an air mass, typically near the ground, and characterized by a vertical change in wind speed and a stable density stratification. To demonstrate the simplicity of Richardson's concept we must use mathematical shorthand and define the vertical velocity gradient, or the shear as the differential du/dz where u is the wind velocity varying with height and z is the height coordinate. Similarly, the intensity of stratification can be expressed as a vertical density gradient, $d\rho/dz$, where ρ is the density of the fluid. The buoyancy force is therefore associated with the vertical density gradient and can be expressed as $g(d\rho/dz)$, in which g is the acceleration of gravity.

Richardson reasoned that turbulent eddies lose energy in two ways: through viscous dissipation into heat and through work performed against the buoyancy force. To maintain turbulence, the rate at which the eddies lose energy must equal or be less than the rate of supply of energy from the shearing flow. Supply and loss are in balance when the following nondimensional parameter (the Richardson Number),

$$R_i = \frac{g(d\rho/dz)}{\rho(du/dz)^2} ,$$

is approximately equal to 0.25. The energy loss and supply terms are respectively represented by the numerator and denominator, supply being proportional to the square of shear.

At values of R_i greater than 0.25, turbulence is suppressed and, as we shall see, shearing flow remains stable. As R_i falls below the critical 0.25, there is a sudden increase in turbulence as illustrated in Thorpe's (1969) experiment, described in Figure 20. A long rectangular, transparent tube, closed at both ends, was placed horizontally and carefully filled with two layers, brine and water. The steepness of the density gradient could be varied by allowing diffusion between the layers to proceed for different time intervals while the tube remained horizontal. Shear flow was then introduced by suddenly tilting the tube at a small angle from the horizontal. This induced an increasing rate of shear between the two layers, because the denser brine layer accelerated down the slope, to be replaced by the upper, less dense water layer flowing in the opposite direction. When the shear had reached a

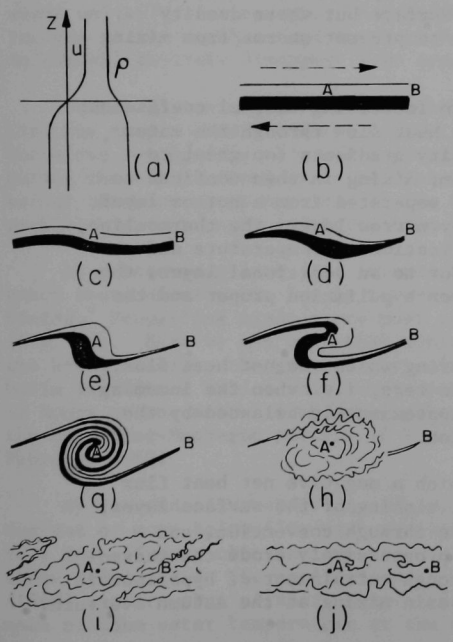

Fig. 20.

The Growth of Shear Instability Leading to Turbulent Mixing in a Stratified Fluid, Subject to Shear, with the Velocity and Density Distribution Shown in (a). A and B are fixed points, the arrows indicate direction of flow, and the lines represent isopycnals (surfaces of equal density). Modified from Thorpe (1969).

critical level, which Thorpe's theoretical treatment showed to be equivalent to a value of R_i = 0.25, short and nearly stationary internal waves appeared on the interface and, as R_i fell further with increasing shear, these waves grew in amplitude. The waves then broke into the spiral vortices illustrated in (g) of Figure 20. The vortices later disintegrated into patches of turbulence which elongated and coalesced, as in the sequence (h) to (j). Although this experiment may seem to the reader to be somewhat removed from events in Lake Michigan, I assure him that it is not, and that it exhibits a property of flow in stratified fluids of great fundamental importance. Although similar behavior has not been directly observed in natural lakes, its consequences have been inferred, and it is basic to the interpretation of observations we shall examine later.

THE SEASONAL CYCLE OF HEAT DISTRIBUTION

As a starting point for discussion of the seasonal thermal regime in Lake Michigan, the stages in a typical temperate small-lake sequence are listed below. After disappearance of ice cover in the spring, the stages are listed below.

1. Wind-induced turbulent mixing of the whole basin from top to bottom, as long as the water temperatures remain at or within a few degrees of maximum density (4°C), and heat gains produce little change in density.

2. An initial warming phase in which temporary thermal stratification is established near the surface but where density gradients are not strong enough to prevent storms from mixing the water column to the bottom.

3. A main warming phase in which an increasing thermal coefficient of expansion and a net positive heat flux through the water surface combine to produce density gradients too great to permit wind mixing to the bottom; mixing is then confined to an upper layer, the epilimnion, separated from a bottom layer, the hypolimnion, by a relatively narrow layer, the thermocline, characterized by marked stratification of temperature and density. Some limnologists refer to an additional layer, the metalimnion, transitional between hypolimnion proper and the steepest thermocline gradient.

4. A midsummer stratified phase during which the net heat flux, averaged over 24 hr, is close to zero, i.e. when the incoming short-wave solar radiation is approximately balanced by the outgoing long-wave back radiation.

5. An autumnal cooling phase in which a negative net heat flux contributes to surface cooling, sinking of the surface layer, producing epilimnetic turbulence through convection, and during which successive storms progressively erode the thermocline and push it downward, through entrainment of hypolimnetic water culminating in complete basin mixing at the autumn overturn.

6. A phase of progressive cooling of the fully mixed lake, isothermal water column, leading in some cases to an inverse temperature stratification and ice formation, if the lake temperature falls below that of maximum density.

For Lake Michigan, Church's (1942, 1945) monograph is still the best and most complete description of the thermal regime and its seasonal progress. Four principal phases can be recognized.

WINTER COOLING

During the fall, the condition described in Paragraph 5 above prevails; the thermocline is pushed progressively deeper, probably in a series of steps as one storm follows another. Noble's (1966) analysis of temperature records obtained at various stations and depths over two years by the Federal Water Pollution Control Administration (see U. S. Department of the Interior, 1967) demonstrated that when surface waters have cooled to approximately 10°C (50°F) the thermocline has been pushed down to about 30 meters (∿ 98 ft). By the end of November (Fig. 21), when the surface temperature is about 7°C (44°F), the thermocline has descended to below 60 meters (197 ft), preparatory to complete mixing by the next big storm. That overturn produces a nearly isothermal water mass in the temperature range 4 to 6°C (39.2 to 42.8°F) (Fig. 22). Although some temperature gradients may persist a little longer near the shore, mixing of the main basin is completed in December, and this is the time of year when the lake is most thoroughly mixed. We should note, however, that although the water columns in various regions of the lake will each be very thoroughly mixed in the vertical, the extent of horizontal mixing is still an open question. It seems unlikely, for example, that differences in water quality between the deep regions of the northern and southern basins, although small and probably smallest in winter, entirely disappear (see Ayers, 1963).

Continued cooling during the month of January affects coastal waters more than the deeper offshore water masses; and horizontal temperature gradients are therefore set up (Fig. 23) which persist throughout the winter (Noble, 1966). During the early winter it is possible that mixing of colder coastal water with warmer offshore water may lead to the formation of a thermal bar, similar but probably less strongly developed than the spring thermal bar, described later.

As winter progresses, an inverse stratification is established in the beach zones where shore ice is formed or where drift ice accumulates in ice fields. Prevailing winds carry most of the drift ice to the eastern shore (Fig. 24). Here we may note that winter ice is formed regularly every year in the bays, covering the greater part of Green Bay for example, but the main basin is skimmed by ice only in exceptional years and then only for a few days or hours at the most. A thin but ephemeral ice cover, probably complete across the Milwaukee-Muskegon portion of the lake, persisted for a day or so in February 1963.

By the end of March (Figs. 23 and 25) the whole water mass has cooled two degrees or more below 4°C, with the coldest waters remaining near the shores. Very few offshore observations are available for the late winter season, but those presented in the publication by the U. S. Department of the Interior (1967) confirm that offshore waters are well mixed right to the bottom. The mean minimum water temperature at the end of the winter varies somewhat from

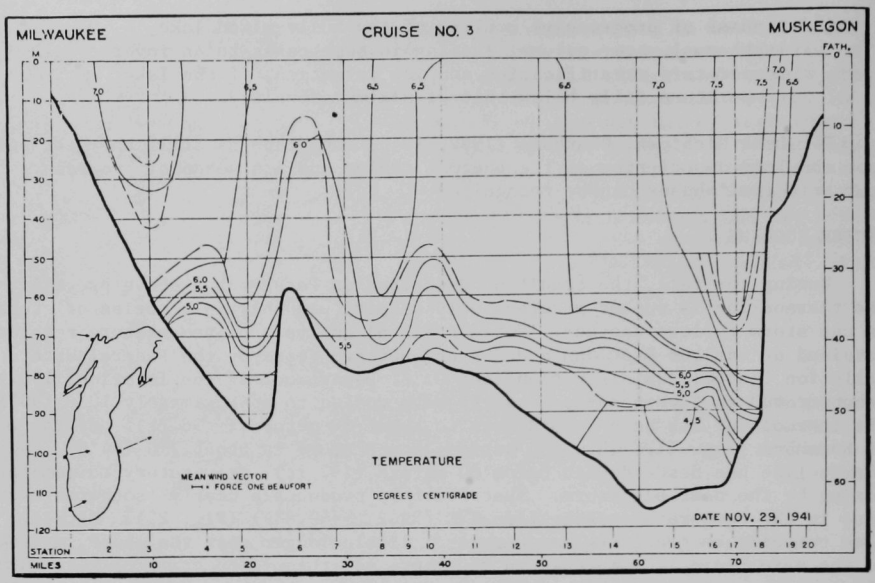

Fig. 21. Lake Michigan, November 29, 1941. Distribution of Temperature, °C, along the Milwaukee-Muskegon Transection; see Fig. 1 (Church, 1942) (with permission, see credits).

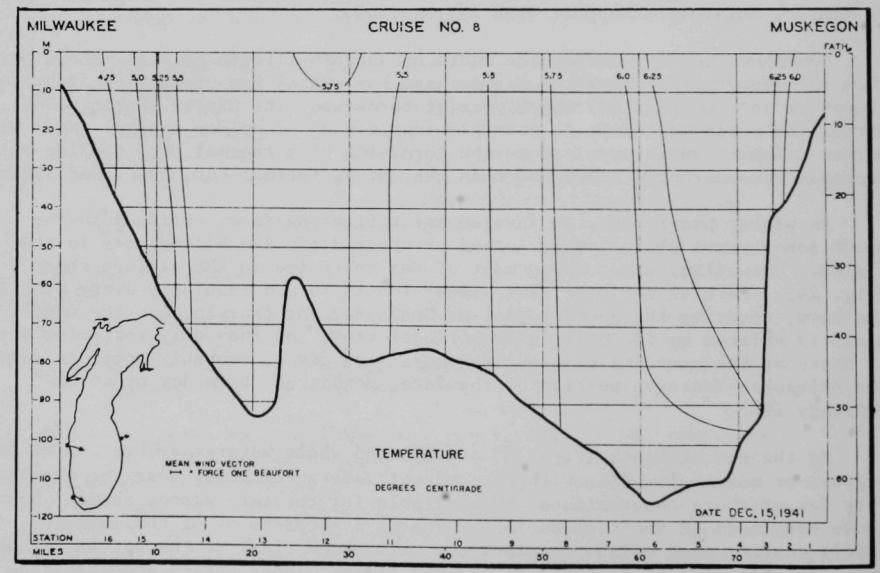

Fig. 22. Lake Michigan, December 15, 1941. Distribution of Temperature, °C, along the Milwaukee-Muskegon Transection (Church, 1942) (with permission, see credits).

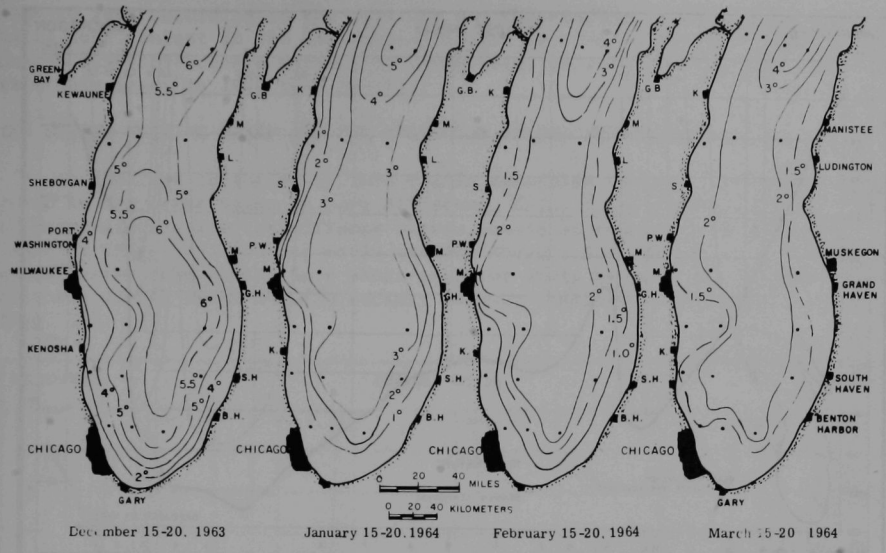

Fig. 23. Distribution of Temperature, °C, at 10 m Depth in the Southern Two-Thirds of Lake Michigan, Representative for December 15-20, 1963, and January, February, and March 1964. Drawn from data in Noble and Michaelis (1968).

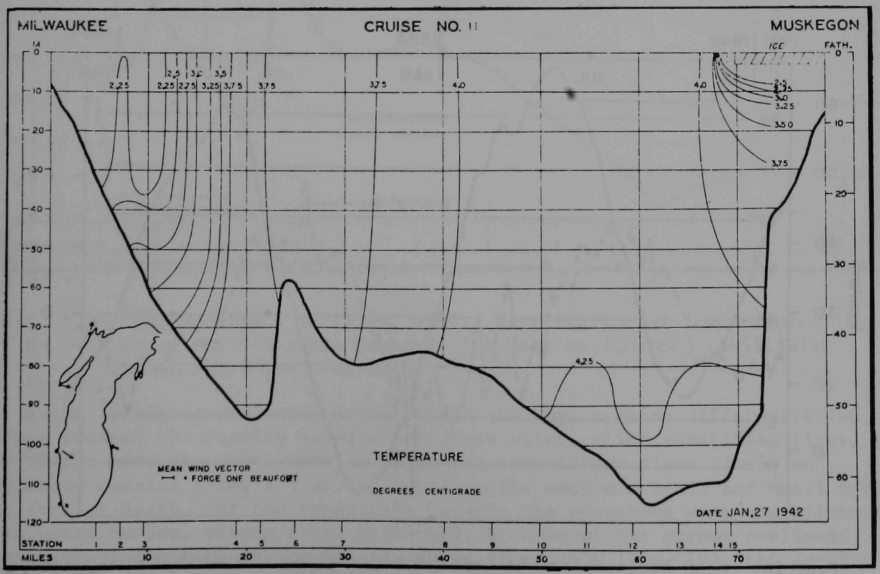

Fig. 24. Lake Michigan, January 27, 1942. Distribution of Temperature, °C, along the Milwaukee-Muskegon Transection (Church, 1942) (with permission, see credits).

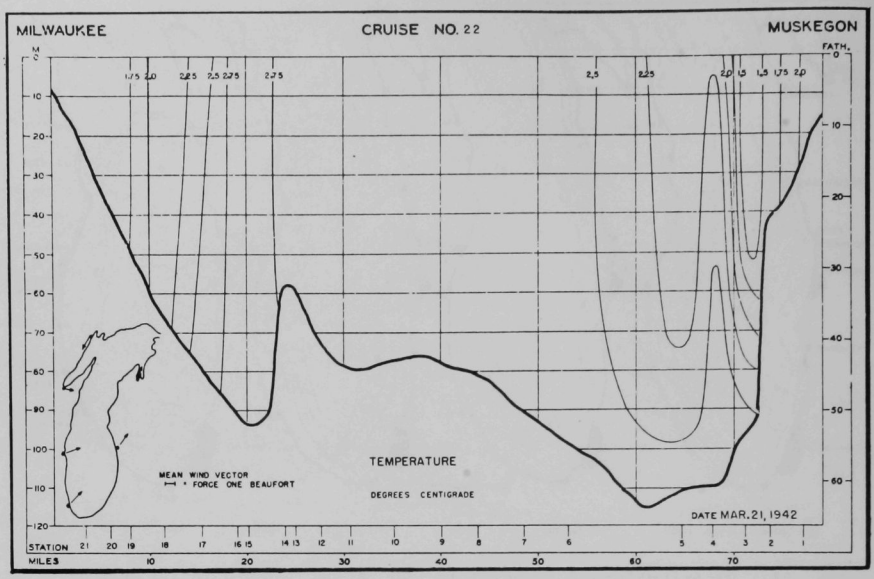

Fig. 25. Lake Michigan, March 21, 1942. Distribution of Temperature, °C, along the Milwaukee-Muskegon Transection (Church, 1942) (with permission, see credits).

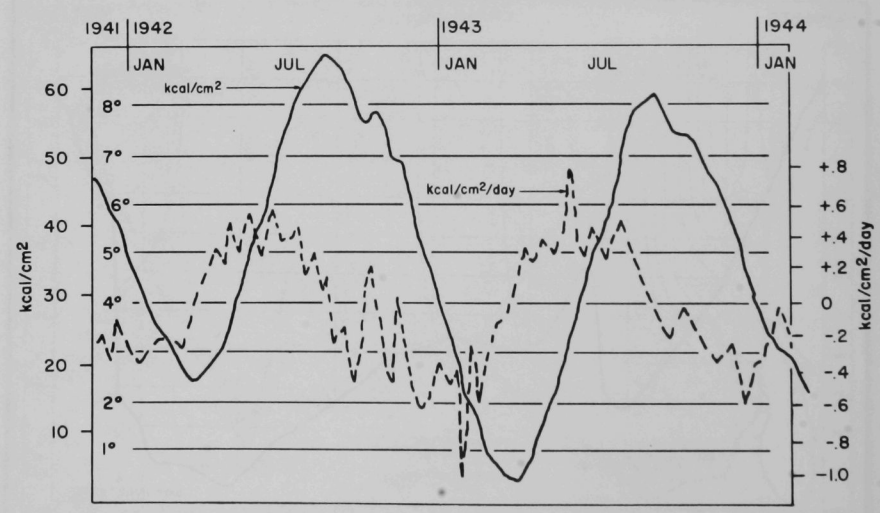

Fig. 26. Mean heat content of Lake Michigan along the Milwaukee-Muskegon Section at 72 meters (average depth of transect), 1941-1942. A scale of the mean temperature (°C) is shown on the left; 0°C is equated to 0 kcal. Daily rates of change are also shown. Modified from Church (1947).

year to year according to the severity and the windiness of the winter. The total heat content in the Milwaukee-Muskegon section of the lake computed by Church (1947) reaches a minimum in March (Fig. 26), and that minimum was considerably lower in 1943 than in 1942.

THE SPRING HEATING PHASE AND THE EVOLUTION OF THE THERMAL BAR

In contrast to the small lake regime described earlier, the spring warming phase in the Great Lakes is very different, being first confined to shallow inshore waters while the offshore waters remain at temperatures below 4°C (39.2°F) (Fig. 27). During early warming stages, the remains of the coldest winter water come to lie in a shore-parallel strip between the slightly warmer offshore winter water and the rapidly warming shallows of the beach zone (Fig. 28).

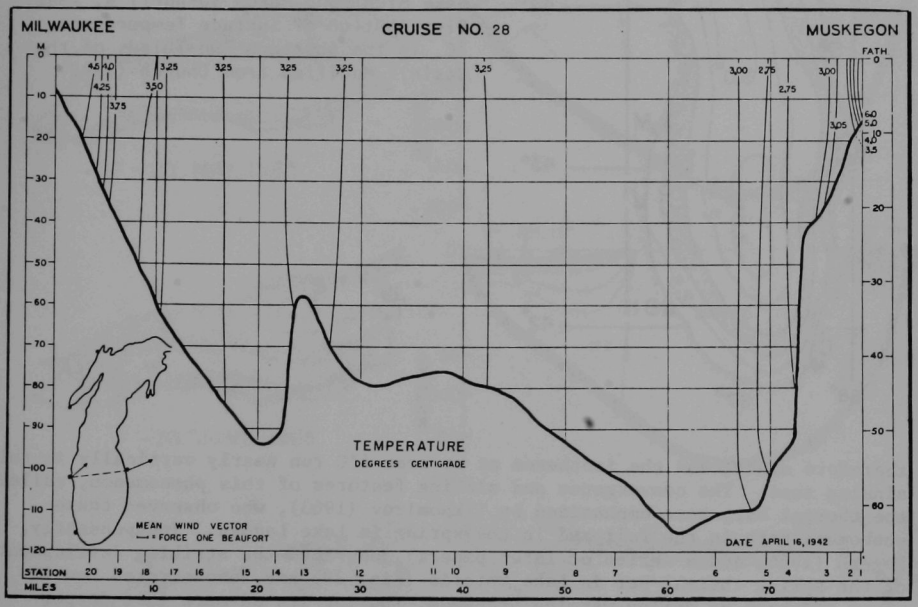

Fig. 27. Lake Michigan, April 16, 1942. Distribution of Temperature, °C, along the Milwaukee-Muskegon Transection (Church, 1945) (with permission, see credits).

With accelerated heating during April and May, a sharp differentiation arises between the rapidly warming nearshore water, which stratifies first, and the deeper offshore water mass in which the temperature rises slowly and, typically remains below 4°C during April in the southern basin and until early May further north. At the transition between the nearshore warm and offshore cold water masses, mixing takes place and, because of the strong nonlinear convexity of the temperature-density curve around 4°C (Fig. 10), the density of the mixed water is greater than that of either parent water mass. The mixture

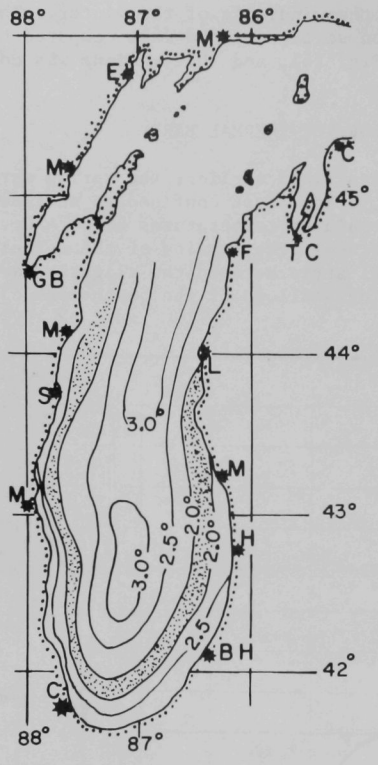

Fig. 28.

Lake Michigan, March 30-April 4, 1942. Distribution of Surface Temperature, °C, in the Southern Two-Thirds of the Basin. Modified from Church (1942).

therefore sinks, and the isotherms at or near 4°C run nearly vertically in this sinking zone. The convergence and sinking features of this phenomenon, called the thermal bar, were emphasized by Tikhomirov (1963), who observed these phenomena both in the fall and in the spring in Lake Ladoga. Independently, Rogers (1966, and a series of later papers) described the striking development of the spring thermal bar in Lake Ontario (Fig. 29) and demonstrated how it moves offshore as spring warming proceeds. During its advance into deeper water, the bar maintains an extremely sharp front, often conspicuous as a color difference between the two water masses. The two common causes of that color difference are related to the fact that the water is thermally stratified on the inside of the bar. First, the relatively warm inflowing streams, silt-laden when in flood, add suspended material and plant nutrients to the upper layer; second, because of stratification, the rate of phytoplankton (diatom) growth is much greater and starts earlier inside the bar than outside in the deeper unstratified water. The question of the degree and duration of entrapment of shore-introduced materials and heat inshore of the bar remains the subject of debate. Although increases in turbidity and phytoplankton crop in the warm epilimnion inside the bar may be viewed as evidence of temporary entrapment, the large natural additions (and smaller man-made additions) of heat to the system result in a progressive offshore transport of heat as the

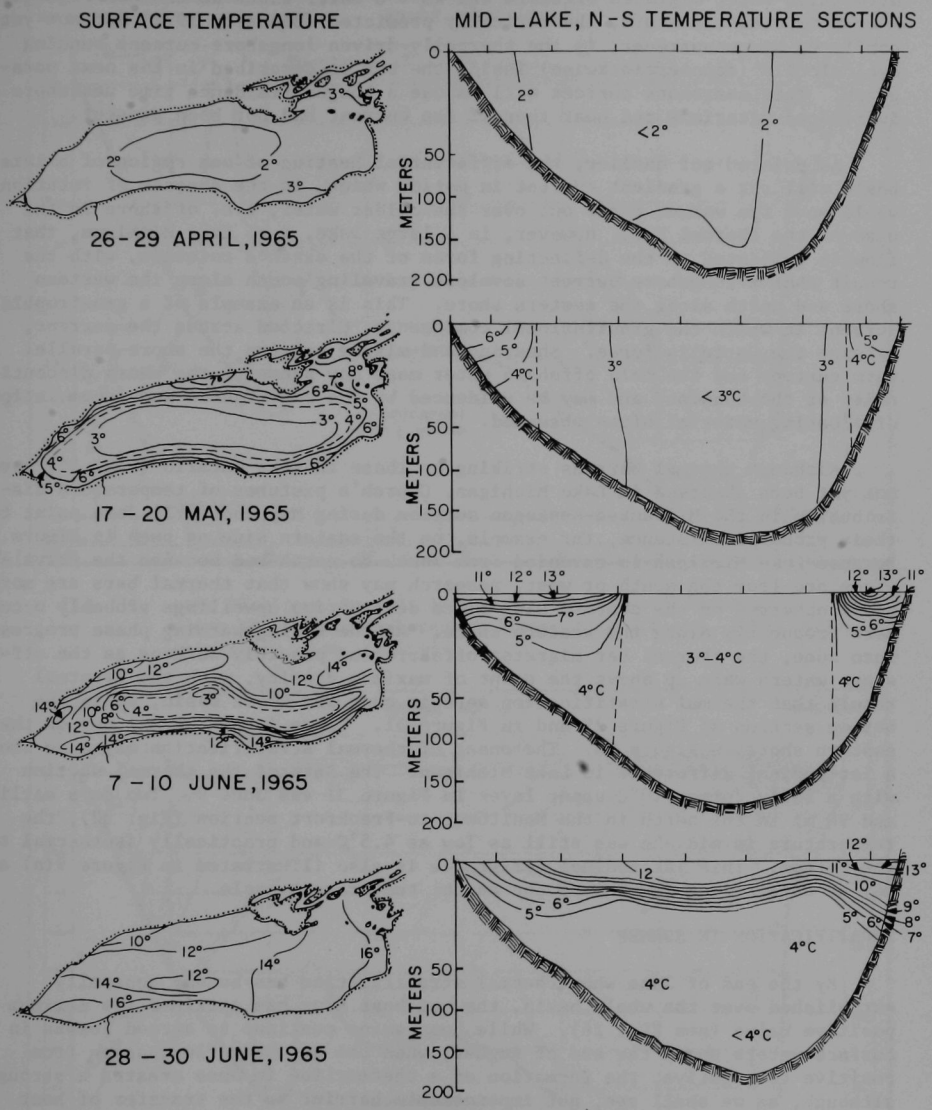

Fig. 29. Formation and Development of the Thermal Bar in Lake Ontario. Redrawn from Rodgers (1966).

stratified water migrates offshore and as 4°C water sinks at the convergence. A more important feature, theoretically predicted (Bennett, 1971) but not yet confirmed by measurement, is the thermally-driven longshore current running cyclonically (counterclockwise) inside the bar as described in the next paragraph. This nearshore current will impose a longer residence time nearshore of introduced materials and heat than if the current had not been present.

As pointed out earlier, the differential heating of one region of a lake basin will set a gradient current in motion which, in the absence of rotation, would move the warmer water out over the colder water, i.e. offshore in the case of the thermal bar. However, in a large lake, e.g. Lake Michigan, that flow is subjected to the deflecting force of the earth's rotation, with the result that a longshore current develops traveling south along the western shore and north along the eastern shore. This is an example of a geostrophic current in which the gravitational components, directed across the current, balance the Coriolis force. Shearing and mixing between the shore-parallel warm current and the cold offshore water mass may preserve the sharp discontinuity of the boundary and may be evidenced by the convergence and accumulation of floating material often observed.

Although thermal bars as striking as those in Lake Ontario (Fig. 29) have not yet been observed in Lake Michigan, Church's pictures of temperature distribution in the Milwaukee-Muskegon section during May and early June point to their probable existence, for example, on the eastern side as seen in Figure 30. Because Lake Michigan is extended from south to north and because the prevalent winds are from the south or west, research may show that thermal bars are more often observed on the eastern side since destructive upwellings probably occur more frequently along the western shore. As the spring warming phase progresses into June, the thermal bar migrates offshore and possibly weakens as the offshore waters warm up above the point of maximum density, with the eventual result that thermal stratification sets in over the whole basin, as in the bottom section of Figure 29 and in Figure 31. There is no thermal bar on the eastern shore in Figure 30. The onset of thermal stratification may also show a latitudinal difference in Lake Michigan. The date of the thermal section with a fully formed 10°C upper layer in Figure 31 was June 9. Two days earlier and 90 mi to the north in the Manitowoc-to-Frankfort section (Fig. 32), the temperature in midlake was still as low as 4.5°C and practically isothermal to the bottom. This latitudinal difference is also illustrated in Figure 9(a) and may be a recurring feature of the annual temperature cycle.

STRATIFICATION IN SUMMER

By the end of June when thermal stratification has become generally established over the whole basin, the net heat flux has attained its maximum positive value (see Fig. 26). While heat gains continue to exceed losses in surface waters until the end of August, when the net heat flux passes from positive to negative, the formation of a thermocline in June creates a strong although, as we shall see, not impenetrable barrier to the transfer of heat through the thermocline to the layers below. The lake is effectively divided into two layers by an interface characterized by a relatively steep density gradient, which means that turbulence is strongly suppressed (high local Richardson Numbers). The friction associated with turbulence is also suppressed, and the upper layer of the thermocline, where the density gradient is steepest, acts as a slippery surface permitting the upper and lower layers to

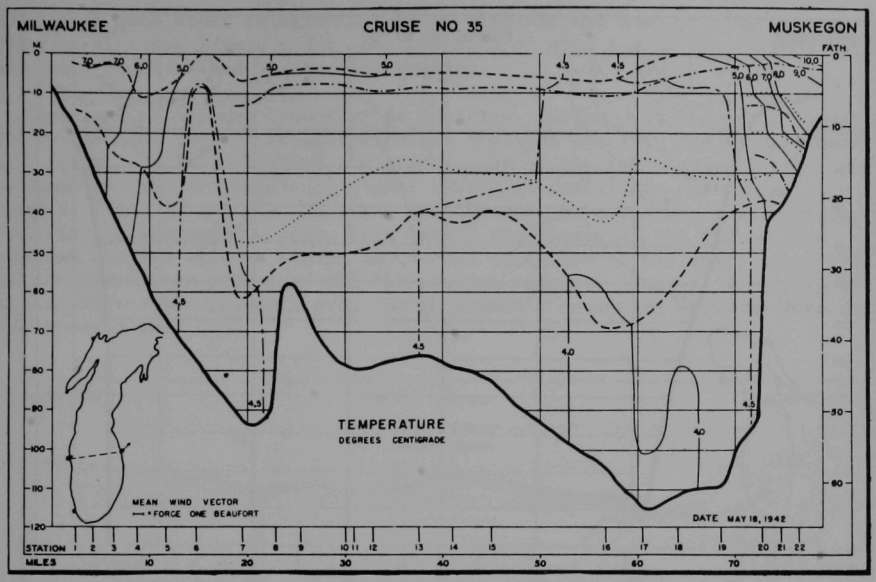

Fig. 30. Lake Michigan, May 18, 1942. Distribution of Temperature, °C, along the Milwaukee-Muskegon Transection (Church, 1945) (with permission, see credits).

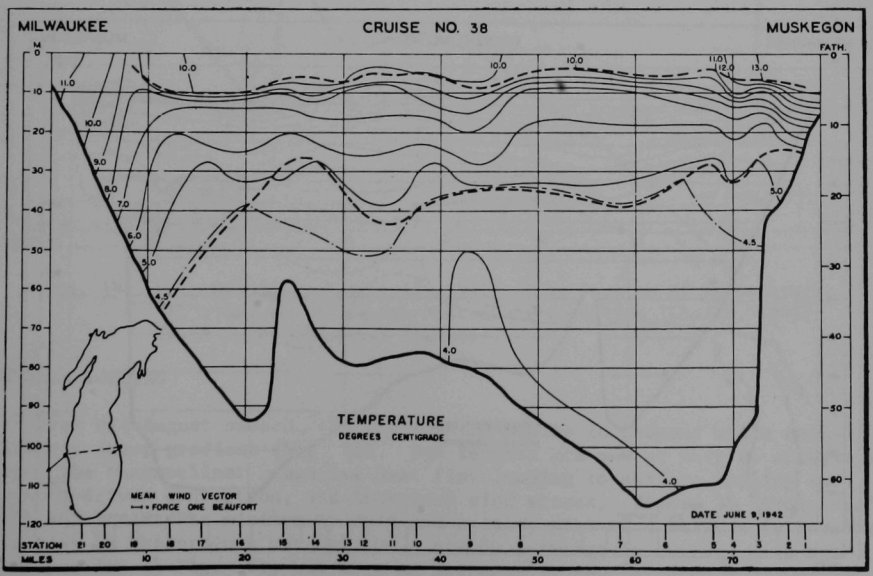

Fig. 31. Lake Michigan, June 9, 1942. Distribution of Temperature, °C, along the Milwaukee-Muskegon Transection (Church, 1945) (with permission, see credits).

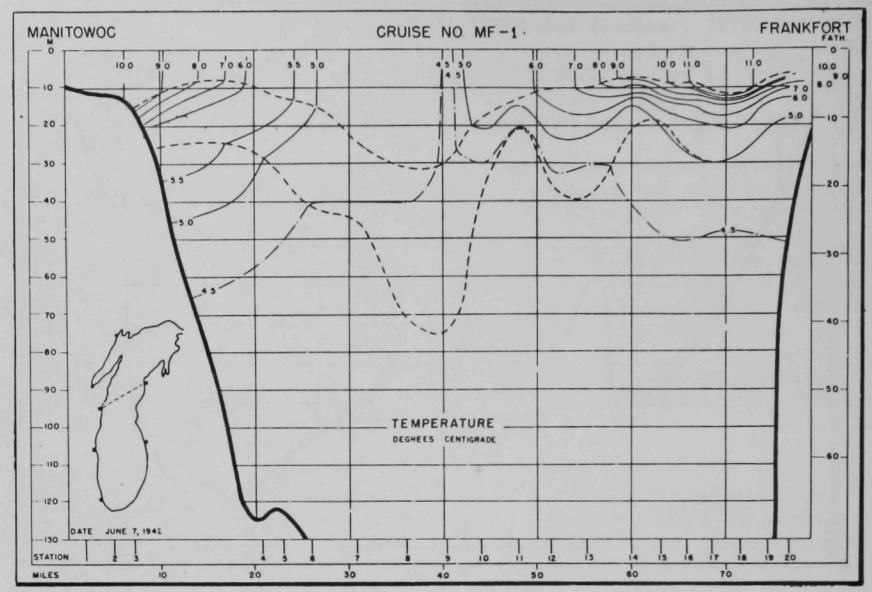

Fig. 32. Lake Michigan, June 7, 1942. Distribution of Temperature, °C, along the Manitowoc-Frankfort Transection (Church, 1945) (with permission, see credits).

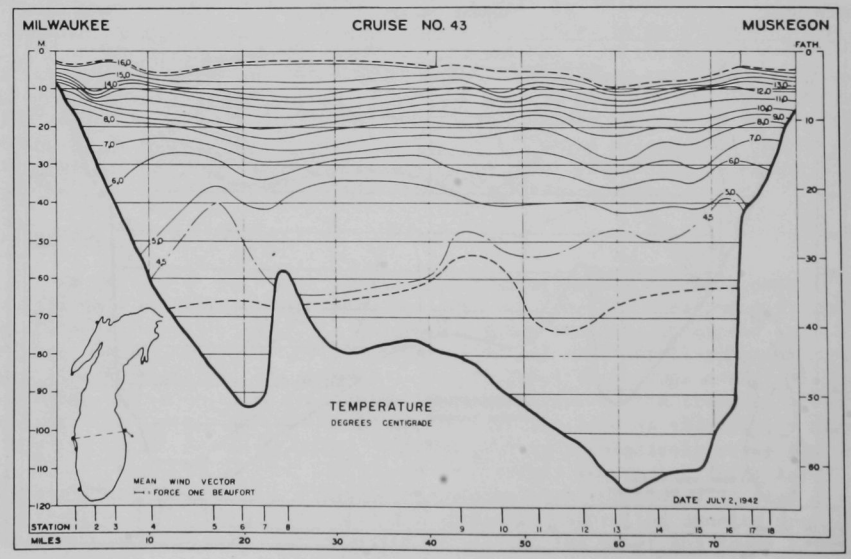

Fig. 33. Lake Michigan, July 2, 1942. Distribution of Temperature, °C, along the Milwaukee-Muskegon Transection (Church, 1945) (with permission, see credits).

slide over each other relatively easily, with minimal mixing. The motions executed by these layers under the influence of wind and of the earth's rotation will be described in the next section.

As long as the net heat flux is positive, during July and early August, the thermocline remains at approximately the same level in the neighborhood of 10 m (Figs. 33, 34), although the steady rise of the temperature in the upper layer means that progressively higher isotherms constitute the thermocline (compare Figs. 31 and 34). A later development, at about the time when the net heat flux is approaching zero, is a marked steepening of the thermocline gradient coupled with an almost isothermal condition in the upper layer (Fig. 34). The corrugated topography of the thermocline suggests internal waves (to be treated later) are present, even though Church's measuring stations were rather widely separated.

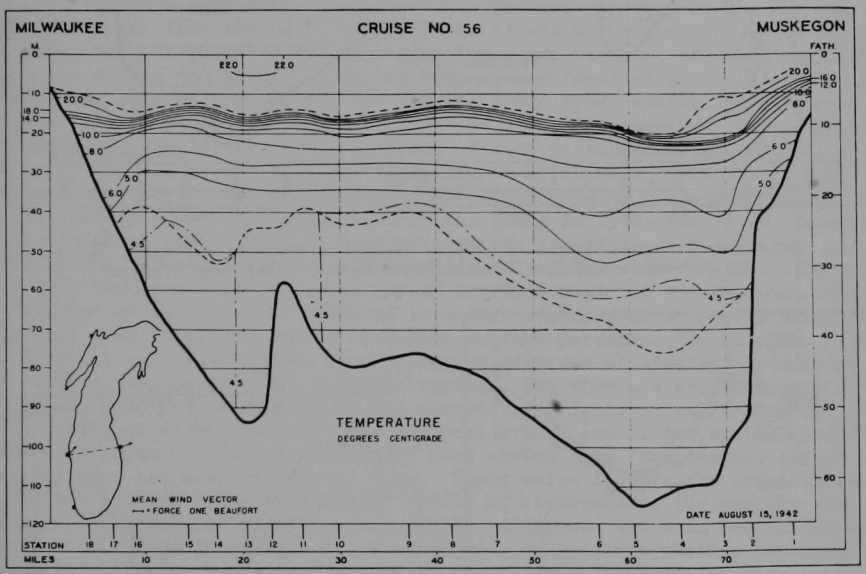

Fig. 34. Lake Michigan, August 15, 1942. Distribution of Temperature, °C, along the Milwaukee-Muskegon Transection (Church, 1945) (with permission, see credits).

AUTUMNAL COOLING

From mid-August onward, the thermocline begins to descend while maintaining a steep gradient (Fig. 35). Two factors are now at work to steepen and deepen the thermocline: negative heat flux leading to surface cooling and buoyancy-driven convection, and increased wind stress. Figure 36 (from Asbury, 1970) shows a stress minimum in July and a steep rise to a maximum in November. This rise is the product not only of a steady increase in average wind speed (left portion of Fig. 36), but also an increase in the correction factor required to derive wind speeds over water from those measured at land stations.

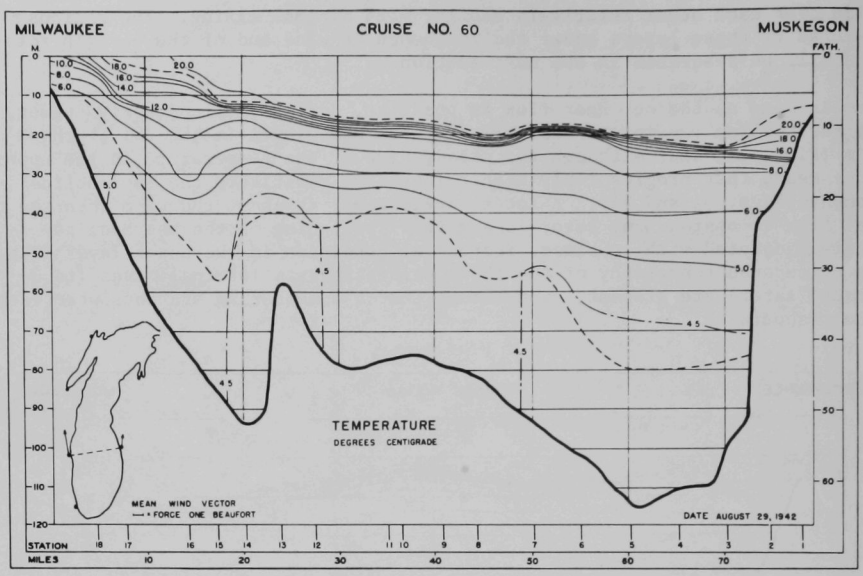

Fig. 35. Lake Michigan, August 29, 1942. Distribution of Temperature, °C, along the Milwaukee-Muskegon Transection (Church, 1945) (see credits).

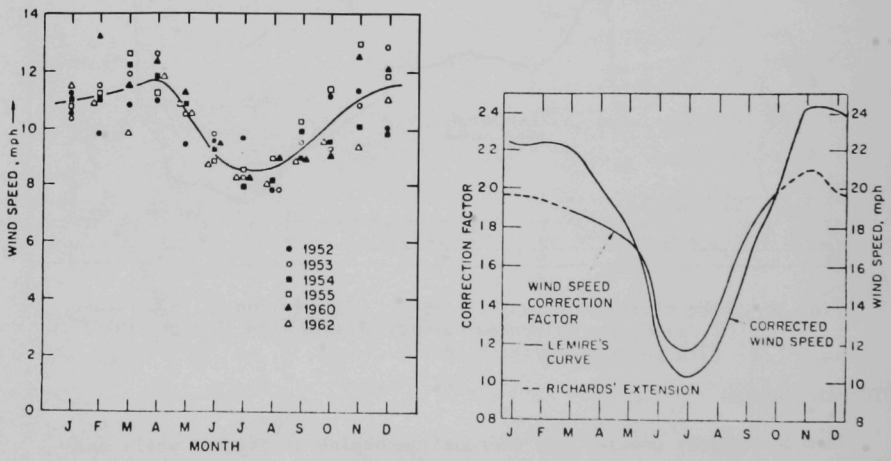

(a) Month-average Wind Speeds

(b) Corrected Wind Speeds

Fig. 36. Annual Variation of Wind Speed for Lake Michigan. (a) "Monthly wind speed" for six years at six weather stations (Chicago, South Bend, Escanaba, Muskegon, Sault Ste. Marie, Green Bay, and Milwaukee); (b) corrected wind speed using factors (Lemire, Richards) taking into account the systematic monthly variations between lake and land wind speeds. From Asbury (1970).

During the fall the water-air temperature difference becomes increasingly positive (the water is warmer), which in turn increases the wind stress on the water for a given wind speed. In spring and early summer, the reverse is true. A better measure of stress would have been given by plotting the data in Figure 36 on a speed-squared scale to illustrate the sixfold increase in average stress between July and November.

Continued surface cooling and increasing (average) wind stress during the fall combine to push the thermocline progressively downward (Fig. 37, note apparent large-amplitude waves, and Fig. 38), probably in an intermittent manner during storms, until the final mixing (overturn) takes place in December.

CHARACTERISTIC RESPONSES OF THE STRATIFIED LAKE

The relative ease with which water temperature can be measured and the fact that, over time scales of days, it can be viewed as a conservative property have made it possible to infer some important features of lakewide patterns of motion during the season of spring warming and later stratification. Proof of the existence of the thermal bar and its associated coastal (geostrophic) currents is one example of the usefulness of such measurements. Other examples are upwelling and internal wave motions. Direct measurements of current, on the other hand, are much more difficult and prohibitively expensive on anything approaching lakewide scales. The most ambitious program of such measurements in Lake Michigan was that undertaken by the FWPCA in 1962-1964 (U. S. Department of the Interior, 1967) with an array of moored, recording current meters and thermographs. Some of the results are illustrated in later figures. But even with this monumental effort, a series of detailed regional and seasonal charts of circulation could not be produced in a form appropriate to answer pressing practical questions, concerning nearshore current patterns, for example. The FWPCA report referred to does indeed present diagrams of average circulation for various seasons, depths, and wind regimes, but they are of little use for day-to-day prediction, because of the overriding effects of short-term fluctuations (internal waves and responses to local winds) and of the spatial complexity of these motions, particularly near shore. For that reason, those diagrams have not been reproduced here. Their value lies in the comparisons which they provide between numerical models of circulation, for example the steady-state models of Murty and Rao (1970), discussed below in connection with steady circulation patterns. It is still an open question whether anything resembling a steady state is found in Lake Michigan. Recognizing this as a serious gap in our knowledge and methodology, we need fleets of "talking drift bodies", trackable in the lake for weeks or months. We now turn to some significant perturbations of the steady state.

UPWELLING RESPONSES

Upwelling is a good example of a conspicuous lakewide response to wind stress, made visible by a network of temperature measurements, for example: thermographs on water works intakes, or research vessel cruises. Forcing of subsurface water masses towards the surface, as a result of wind stress at the surface, occurs to some degree in all lakes at all seasons, but it becomes more obvious during seasons of stratification when cold sub-thermocline layers are

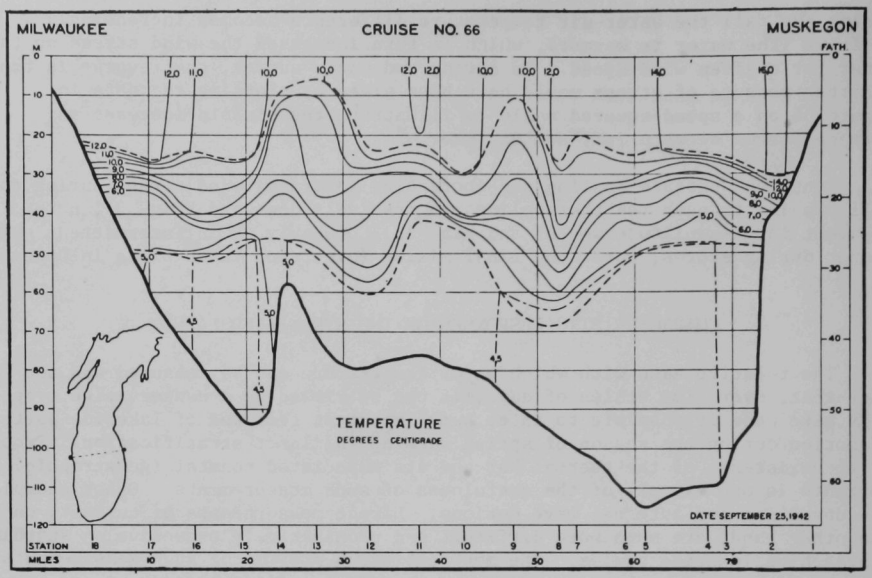

Fig. 37. Lake Michigan, September 25, 1942. Distribution of Temperature, °C, along the Milwaukee-Muskegon Transection (Church, 1945) (with permission, see credits).

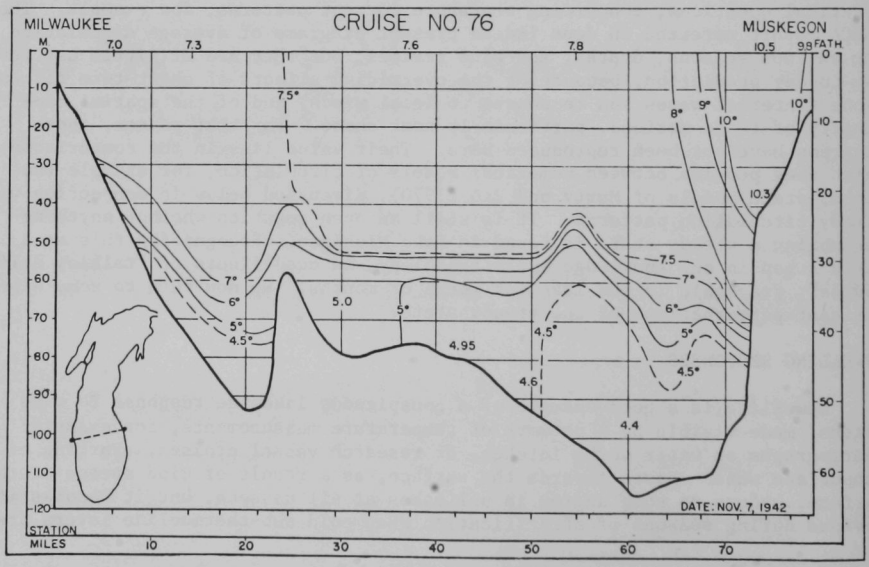

Fig. 38. Lake Michigan, November 7, 1942. Distribution of Temperature, °C, along the Milwaukee-Muskegon Transection (Church, unpublished figure)(with permission, see credits).

forced upward, in some cases right up to the surface. This forcing is a consequence of the application of wind stress over the whole or over larger parts of the lake, and in small stratified lakes the response is a tilting of the isotherms (the thermocline) directed downhill toward the downwind end of the basin, as illustrated in the upper portion of Figure 13(b). The angle of the tilt is a function of the wind stress. If the basin is long enough and the wind strong enough, hypolimnetic water is pulled up to the surface at the upwind end, and the thermocline is depressed below equilibrium level at the downwind end. There, strong currents circulating in the upper layer exert a shear on the thermocline, which steepens the density gradient in that region. At the upwind end of the basin, the thermocline gradient is typically much less pronounced. Such temporary upwelling provides a mechanism for introducing heat and oxygen into the hypolimnion and of transferring some of the accumulated nutrient materials from the lower layer into the upper illuminated layers, thereby constituting a leak, as long as the normal thermocline barrier to these exchanges remains partially open.

Large-scale upwellings are a common occurrence in Lake Michigan, particularly during late summer and fall, a consequence (as seen in Fig. 36) of the large increase in average wind stress from a minimum in July to a maximum in November. If the thermocline tilts are correlated with wind stress, as is the case, it is easy to see that upwelling must commonly occur in large basins and that in Lake Michigan the incidence of such a response will be increased during the fall. The upwelling motions in large basins are also strongly modified by the Coriolis force, which imposes a rightward deflection on the wind-induced currents, so that the thermocline becomes depressed on the right-hand side of the wind direction and raised on the lefthand side. The strongest wind stresses on Lake Michigan are applied either from the southwest or from the northeast quadrant, therefore the greatest upwellings of sub-thermocline water are found along the eastern shore with a north wind and along the western shore with a south wind. Figure 39(b) from Church (1945) shows evidence of a relatively weak upwelling on the western shore, extending from Sheboygan to Kewaunee in early July, following an interval of moderate wind. The accompanying cross section, Figure 39(a), shows a corresponding but slight depression of the isotherms on the eastern shore and, incidentally, a wave-like topography across the thermocline. An example of a moderate upwelling on the eastern shore is shown in Figure 40, and a more typical mid-summer picture is that in Figure 41, after strong winds had thoroughly mixed the upper layer and imposed a cross-lake set-up on the thermocline.

The indications of upwelling in Church's Milwaukee-Muskegon cross sections are fully confirmed by Figure 42 (Mortimer, 1963; redrawn 1971) showing water intake temperatures at pairs of stations at approximately the same latitude, one on either side of the basin. Upwelling at a given intake is shown by a sharp drop in temperature, and this is usually accompanied by a rise in temperature (downwelling) at the intake on the opposite shore. In Figure 42 the temperatures shown in Church's (1945) figures, at the positions of the Milwaukee and Muskegon intakes, are superimposed on the respective intake temperature traces. They show remarkably close agreement. The strong correlation between upwelling and wind activity is also illustrated. A plot of wind speed squared would have given a better picture of wind stress, but since a general indication of the principal storms was needed for the figure, a linear scale suffices. The wind coding is explained in the figure legend. The Figure 42 example is interpreted in more detail in Mortimer (1971). Similar correlations were found during many other years.

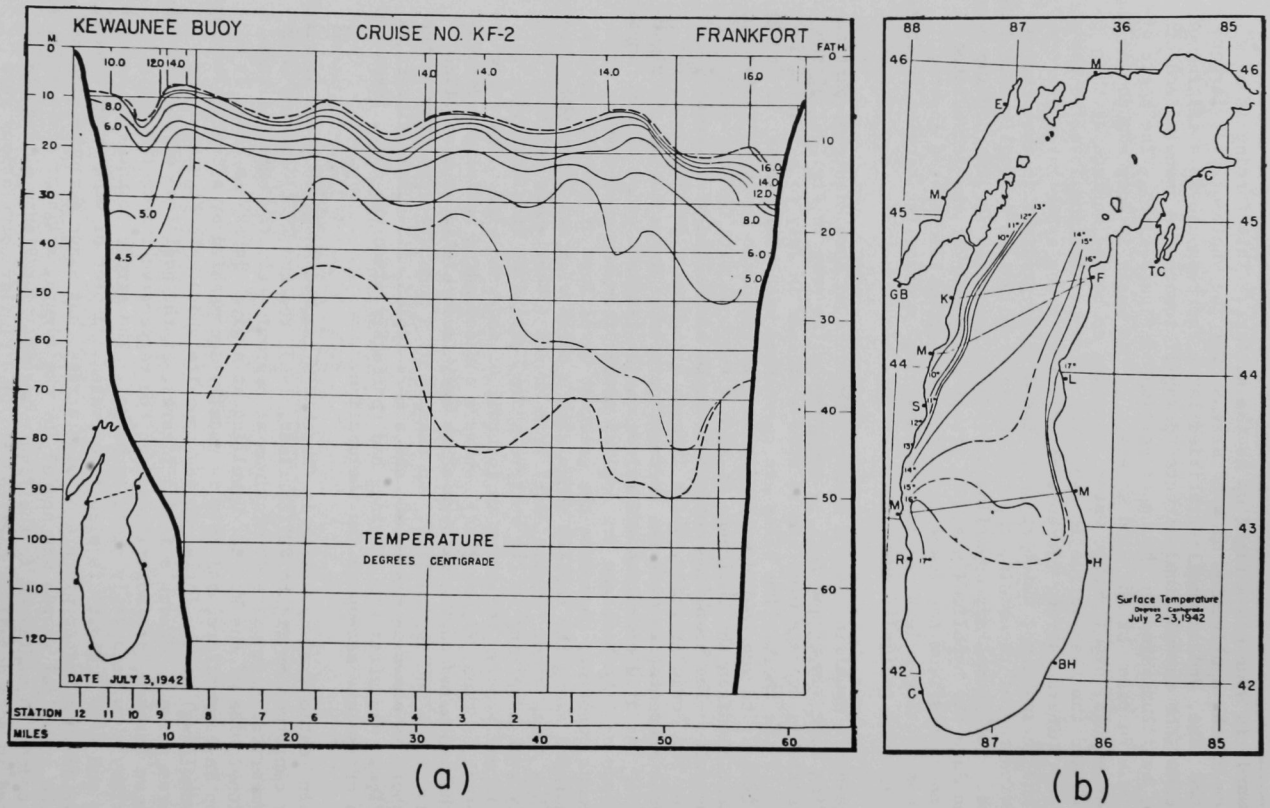

Fig. 39. Lake Michigan: (a) Distribution of Temperature, °C, along the Kewaunee-Frankfort Transection, July 3, 1942; (b) Distribution of Surface Temperature, July 2-3, 1942 (Church, 1945) (with permission, see credits).

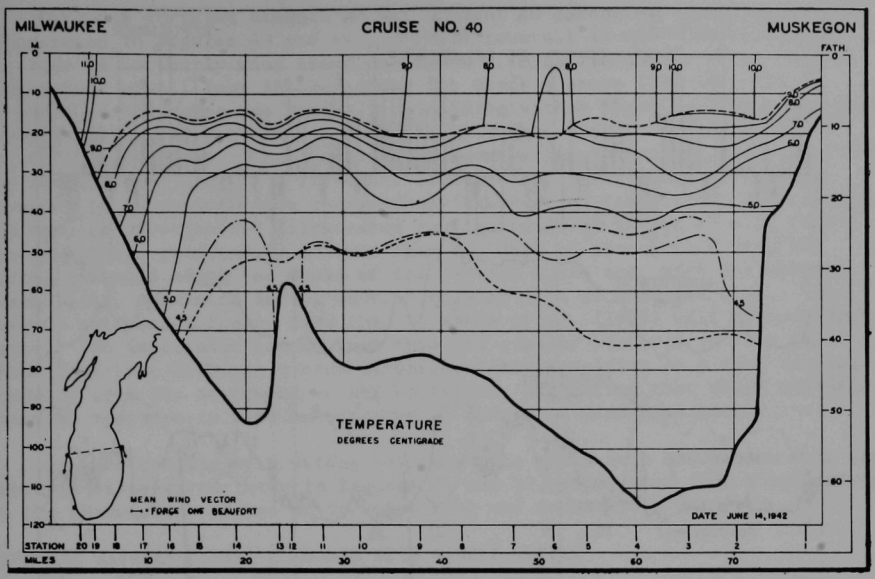

Fig. 40. Lake Michigan, June 14, 1942. Distribution of Temperature, °C, along the Milwaukee-Muskegon Transection (Church, 1945) (with permission, see credits).

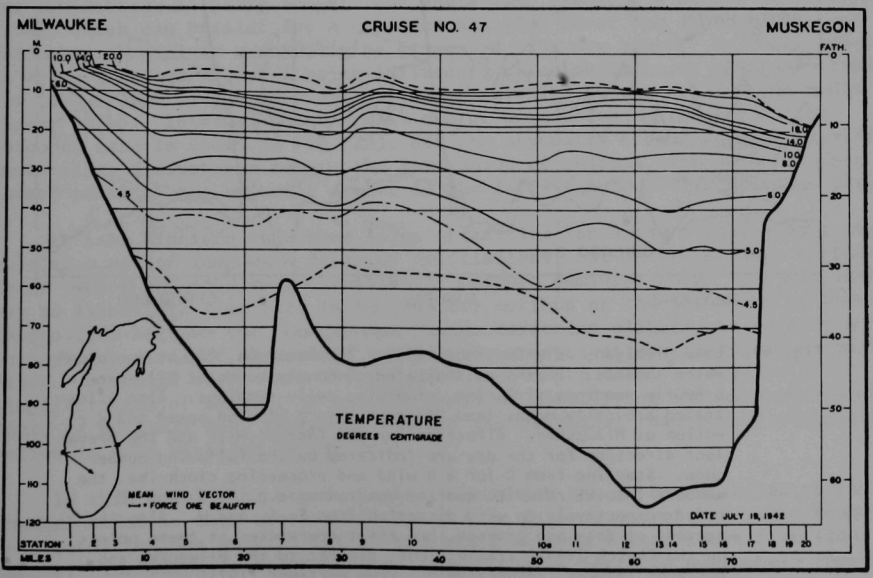

Fig. 41. Lake Michigan, July 19, 1942. Distribution of Temperature, °C, along the Milwaukee-Muskegon Transection (Church, 1945) (with permission, see credits).

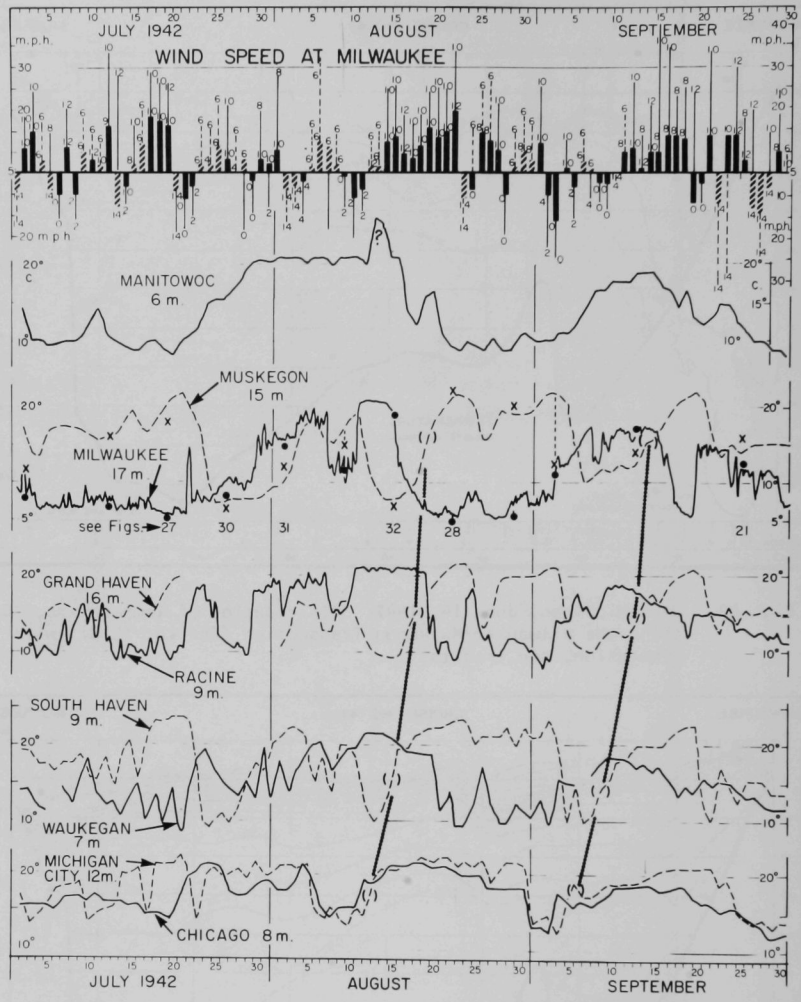

Fig. 42. Lake Michigan, July-September 1942: Temperatures, °C, at Municipal Water Intakes. Depths as indicated, 6-hourly means at Milwaukee, 6-hourly readings at Racine, otherwise daily readings. Also illustrated are daily means (and "fastest mile") of wind speed and direction at Milwaukee. Direction for the fastest mile and the prevalent direction for the day are indicated by the following number code. Starting from 0 for a N wind and proceeding clockwise, the numbers 1 to 15 refer to quarter quadrants, e.g. 4, 8, and 12 refer respectively to wind direction from E, S, and W. Also inserted, as dots and crosses, are the temperatures at these points on the Church (1945) transections, nearest to the Milwaukee and Muskegon intakes, respectively. From Mortimer (1971).

The most striking example we yet have of an extensive upwelling is that illustrated in Figures 43 and 44. A rapid reversal in wind direction and increase in northerly wind speed on August 7, 1955, induced a sharp rise in temperature at all four intakes along the western shore [8°C (46.4°F) in 12 hours at Milwaukee and Racine], coinciding with a sharp fall in temperature (upwelling) at the eastern stations from Michigan City to Ludington [11°C (51.8°F) in 6 hours]. The upwelling and downwelling situation then persisted for several days and, by a fortunate coincidence, seven research vessels happened to be conducting a quasi-synoptic survey of temperature distribution, the results of which are illustrated in Figures 44-46 (Ayers *et al.*, 1958). The upwelling, produced by no more than two days of strong wind from the north, extended along the whole of the eastern shore and, with the western downwelling, persisted during several ensuing days of moderate wind. The current patterns inferred from this by Ayers *et al.* (1958) will be described later. The impression gained from this and similar pictures is that the stratified Lake Michigan system is particularly sensitive to a wind veering suddenly from the southwest to the northeast, suggesting that there may be a resonant response to particular rates of change of wind direction.

Another example of a strong response to a rapid veer and a blow from the north is illustrated later in Figures 51 and 52, which also show a persistence in the thermocline slopes of the upwelling and downwelling regions.

INTERNAL WAVE RESPONSES COMPARED WITH SIMPLE MODELS

The Models

When the wind stops, the stress producing the upwelling is removed, and the displaced water masses are released to seek a new equilibrium. While that new equilibrium is being sought, the whole lake executes a series of oscillations, which can persist for a considerable time after the disturbance, and which may themselves eventually be disturbed by a new storm. In small lakes, in which rotation is not a major influence, these oscillatory responses take the form of the simple internal seiche represented by the two-layered model in Figure 13(b). Internal seiches with one or more nodes can co-exist (the uninodal case is shown in Fig. 13), but the asymmetry of the initial upwelling-downwelling disturbance favors the generation of seiches with an odd number of nodes, of which the uninodal member is the largest and usually the most persistent.

In Lake Michigan and other large stratified lakes the response to a storm is also a set of long-wave internal oscillations, but in these cases Coriolis force cannot be neglected. In fact, it plays a dominant role. The simplest way to illustrate that role is to consider motions on the interface or model thermocline between two homogeneous fluids differing slightly in density and occupying a straight channel of rectangular cross section, therefore of uniform depth. Although such a two-layered, constant-depth model is a gross over-simplification of nature, it has the merit of simplifying the mathematics and does, as we shall see, reproduce some of the principal features of thermocline motion in Lake Michigan fairly well.

In this model, the boundary condition which has to be satisfied at the channel sides is that there shall be no flow into or out of the solid boundary. This condition can only be met by two kinds of long waves, known from tidal theory. The first is so shaped that the Coriolis force is everywhere cancelled

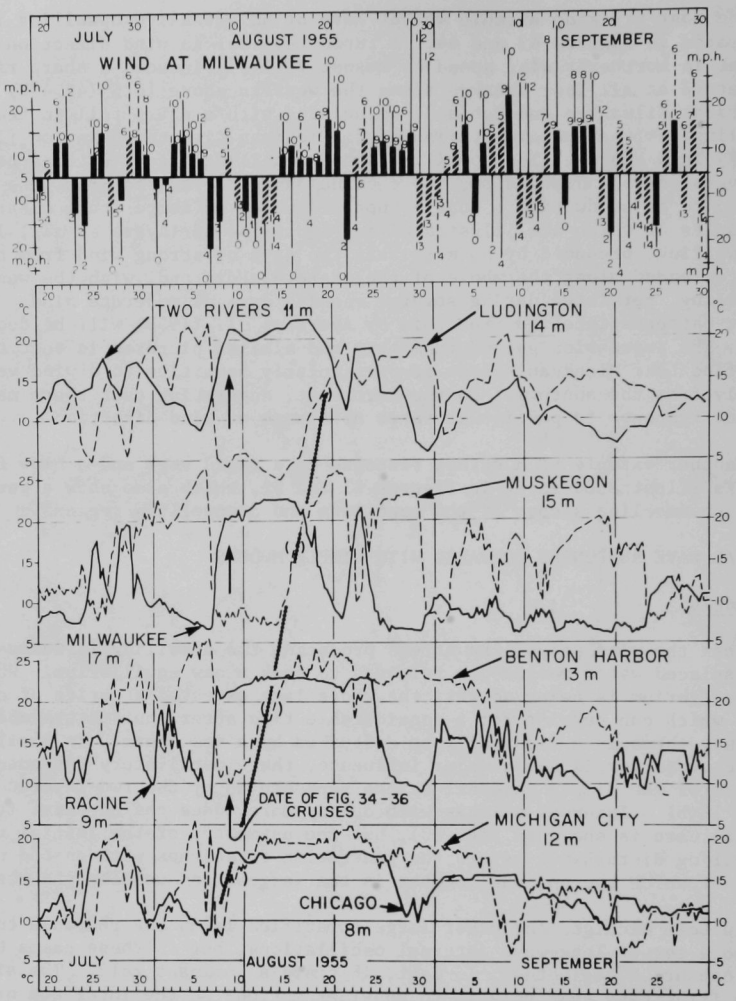

Fig. 43. Lake Michigan, July-September 1955: Temperatures, °C, at Municipal Water Intakes. Depths as indicated, 6-hourly means at Milwaukee, 6-hourly readings at Racine, otherwise daily readings. Also illustrated are daily means (and "fastest mile") of wind speed and direction at Milwaukee, as explained in the legend to Figure 42. Vertical arrows indicate the date, August 9, of the Figure 44-46 cruises. The heavy dotted line is referred to in the text. From Mortimer (1971).

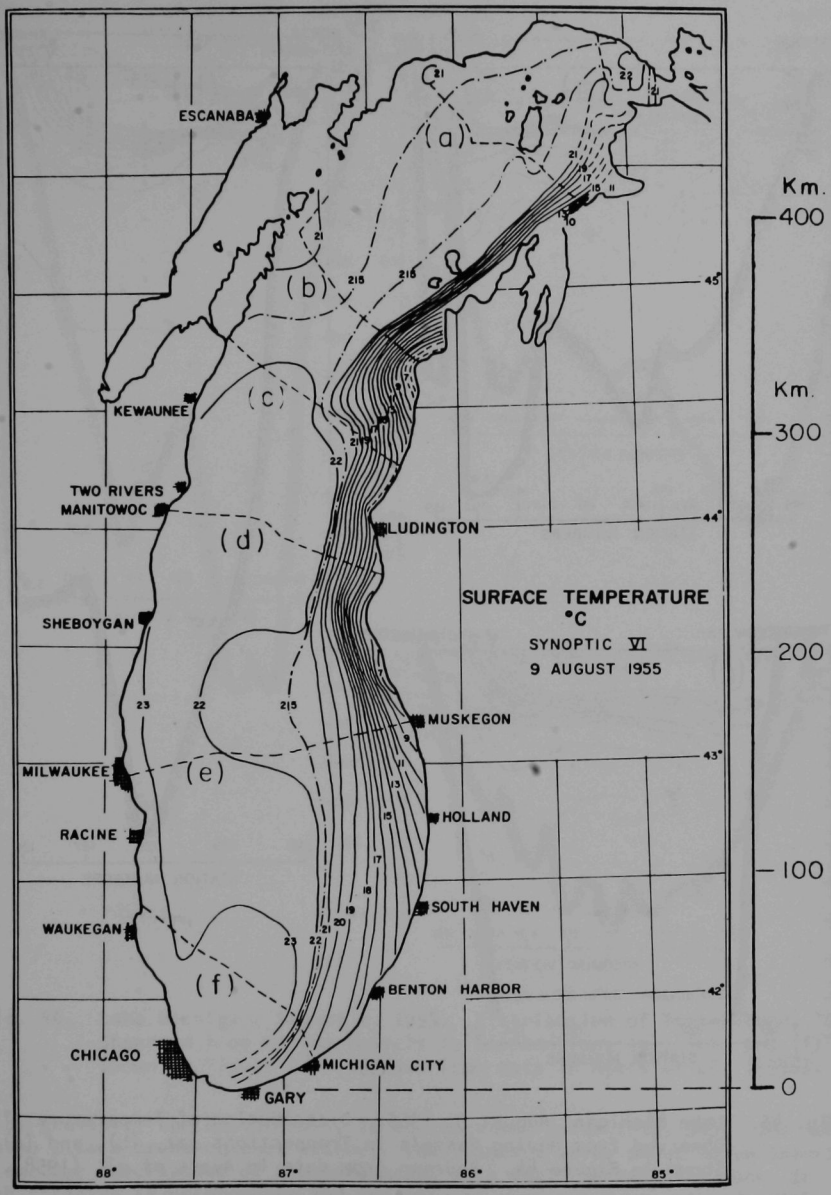

Fig. 44. Lake Michigan, August 9, 1955: Coastal Upwelling after Northerly Winds, as Shown by the Distribution of Surface Temperature °C. Derived from concurrent research vessel cruises. Tracks shown as broken lines (modified from Ayers *et al.*, 1958).

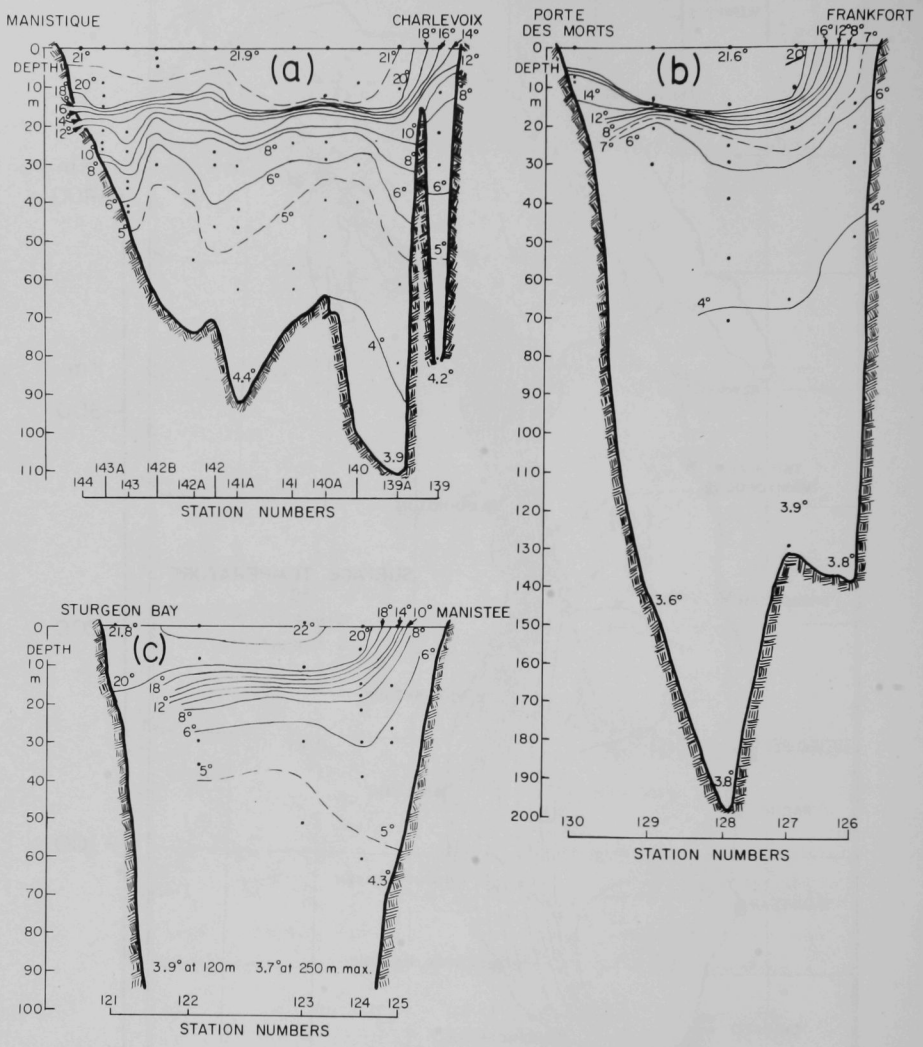

Fig. 45. Lake Michigan, August 9, 1955. Distribution of Temperature, °C, Observed from Moving Vessels in Transections (a), (b), and (c) Shown in Figure 44. Redrawn from data in Ayers *et al.* (1958).

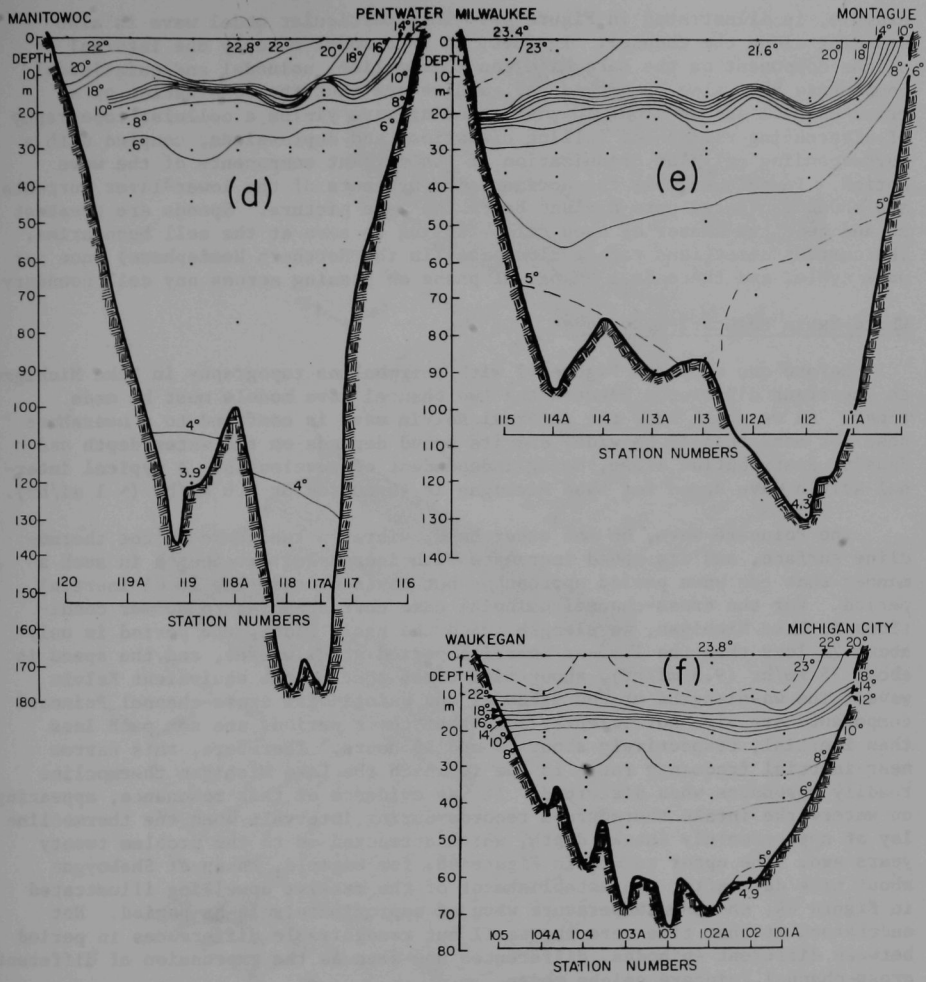

Fig. 46. Lake Michigan, August 9, 1955. Distribution of Temperature, °C, Observed from Moving Vessels in Transections (d), (e), and (f) Shown in Figure 44. Redrawn from data in Ayers *et al.* (1958).

out by gravity: the Kelvin wave, to be described later (Fig. 54). The second behaves like a cross-channel seiche: the Poincaré wave, about to be described. Our earlier description of a seiche model in a small rectangular tank, in which rotation is unimportant and the ends of the tank must coincide with antinodes, is applicable to Lake Michigan, but with a notable difference introduced by the rotation. In the large-lake model the sides of the channel must coincide with antinodes. One type of Poincaré wave, a trinodal cross-channel

example, is illustrated in Figure 47. This particular model wave is also standing along the channel. In fact, it is a model of only one internal seiche component on the Lake Michigan thermocline, uninodal and quintinodal components have also been observed, and we see that the combination of a cross-channel and an along-channel standing wave yields a cellular topography of alternating rising and falling elevations and depressions, coupled with a corresponding cellular organization of the current components of the wave motion. In this example the horizontal components of the lower-layer currents are shown projected onto a plane below the wave picture. Speeds are greatest at and near the center of each cell, falling to zero at the cell boundaries. The current directions rotate clockwise (in the Northern Hemisphere) once per wave cycle, and there is a change of phase on passing across any cell boundary.

Whole-Basin Poincaré-Type Waves

Before one compares Figure 47 with thermocline topography in Lake Michigan, an important difference between the two channel wave models must be made clear. As we shall see, the internal Kelvin wave is confined to a nearshore zone not more than 15 km wide, and its speed depends on the water depth and density distribution alone, being independent of wavelength. A typical internal Kelvin wave speed for Lake Michigan is 45 cm/sec or 1.6 km/hr ($\sim$ 1 mi/hr).

The Poincaré wave, on the other hand, vibrates the whole of the thermocline surface, and its speed increases with increasing wavelength in such a manner that the wave period approaches but never exceeds the local inertial period. For the cross-channel uninodal case corresponding to summer conditions in Lake Michigan, wavelength twice the basin width, the period is only about 2% less than the 17.5-hr inertial period at Milwaukee, and the speed is about 15 km/hr (9.3 mi/hr), about nine times that of the equivalent Kelvin wave. The wavelengths of the trinodal and quintinodal cross-channel Poincaré components are also sufficiently long that their periods are not much less than inertial, respectively about 16 and 15 hours. Therefore, this narrow near-inertial frequency range is one in which the Lake Michigan thermocline readily resonates when disturbed. It was evidence of this resonance, appearing on waterworks intake thermograph records during intervals when the thermocline lay at approximately intake depth, which attracted me to the problem twenty years ago. The upper record in Figure 48, for example, taken at Sheboygan about nine days after the establishment of the massive upwelling illustrated in Figure 44, shows a temperature wave of approximately 16-hr period. Not understood at that time were the small but recognizable differences in period between different episodes, differences now seen as the expression of different cross-channel Poincaré seiche modes.

The Poincaré model (Mortimer, 1963) predicts not only a thermocline wave with a dominant near-inertial periodicity, but also a clockwise rotation of current direction in a particular phase relationship with the wave. Two examples confirming these theoretical predictions are given here. One was provided by FWPCA (U. S. Department of the Interior, 1967) recordings of currents and temperature at a number of stations and depths in Lake Michigan (Figs. 49 and 61). Mortimer's (1968) measurements of the depth distribution of current speed, current direction, and temperature at midlake anchor stations provided another confirmation (Fig. 50).

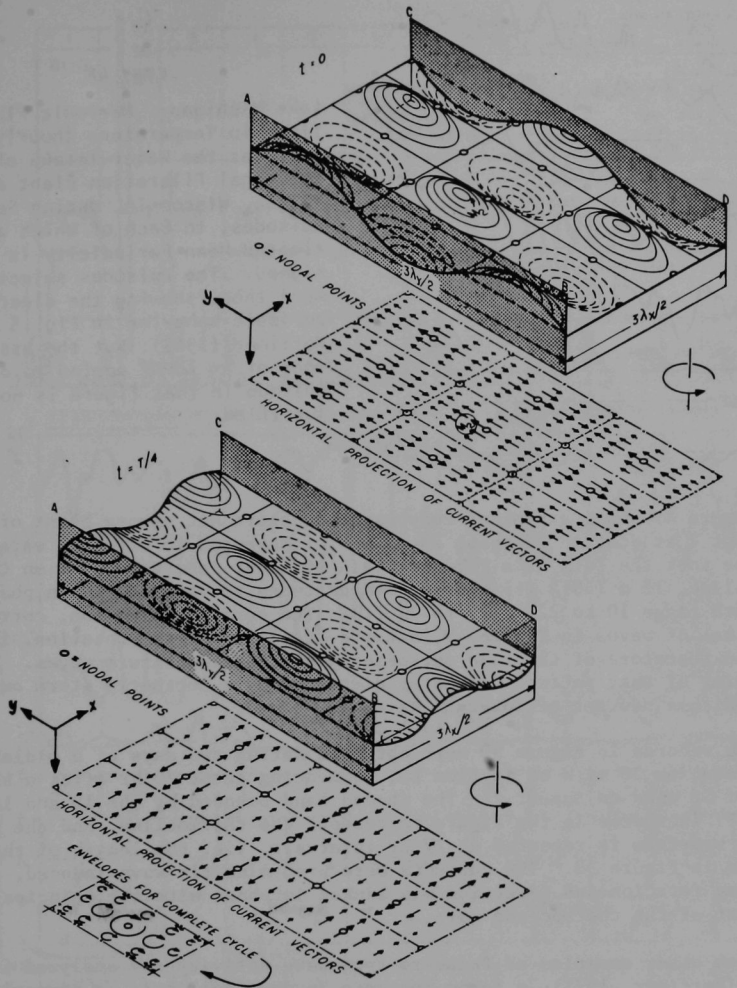

Fig. 47. A Standing Poincaré Wave in a Wide, Rotating Channel of Uniform Depth. Two phases (separated by 1/4 cycle) of the oscillation are shown for the cross-channel trinodal case, with a ratio of long-channel to cross-channel wavelengths of 2/1. The clockwise rotation and distribution of the current vectors in the Poincaré wave "cells" are explained in the text. The elevation topography in this figure may be envisaged either as that of the water surface or as that of the interface in a two-layer model, in which case current vectors shown are those in the lower layer. From Mortimer (1968).

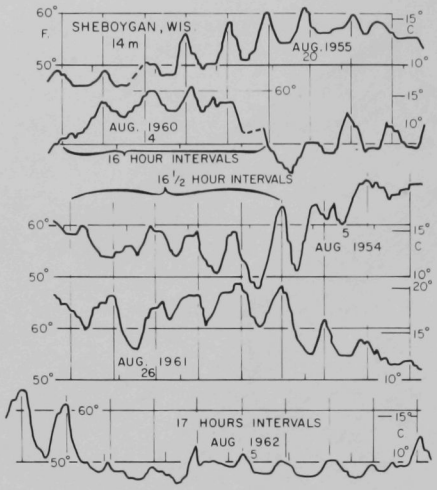

Fig. 48.

Lake Michigan: Periodic Fluctuations in Temperature (hourly readings) at the Water Intake of the Municipal Filtration Plant at Sheboygan, Wisconsin, during Selected Episodes, to Each of Which an Estimated Mean Periodicity is Assigned. The episodes selected were those showing the clearest periodic behavior in Fig. 5 of Mortimer (1963), but the assignment of an 18-hr period to one episode in that figure is not justified.

Figure 49 shows a typical response to a short but strong burst of SE wind on August 2 at station 20 about 20 mi WSW of Muskegon in offshore water. The response took the form of a regular train of 17-hr internal waves on the thermocline, 15 m (49.2 ft) causing temperatures to vary nearly in phase over the depth range 10 to 22 m (33 to 72 ft). The current direction, corresponding to the set of waves in Figure 49, shows a steady clockwise rotation, in phase with and therefore of the same periodicity as the temperature waves. The regularity of that pattern was later disturbed by a northerly storm on August 9, after which a new set of internal waves developed.

The records in Figure 50 were obtained during two days at a midlake anchor station 20 mi W of Station 20, commencing about 30 hr after a short burst of SE wind on August 2. The shaded band bounded by the 10 and 15°C (50 and 59°F) isotherms in the figure represents the thermocline, and the somewhat complex waveform is repeated at 17-hr intervals, i.e. the length of the two sections in Figure 50. The currents were predominantly wave-induced, as their clockwise rotation and direction was linked in phase with the principal 17-hr component of the thermocline wave.

When other examples of Poincaré-type wave activity are analyzed in more detail (Mortimer, 1971), a large increase in wave amplitude is commonly seen after a strong wind has produced extensive upwelling along one shore and downwelling along the opposite shore. The upwelling-downwelling perturbation is an obvious source of potential energy for generating internal waves, and the cross-lake asymmetry of the perturbation explains why the odd-numbered cross-lake internal seiche modes are the ones most often seen. For example, Figures 51 through 53 illustrate a particularly clear case.

Two northerly storms on August 13 and 17 deepened the thermocline, increased the temperature gradient [compare sections (b) and (d) in Fig. 51], produced strong upwelling on the eastern shore and downwelling on the western shore occupying coastal strips approximately 15 mi (24 km) wide, and increased

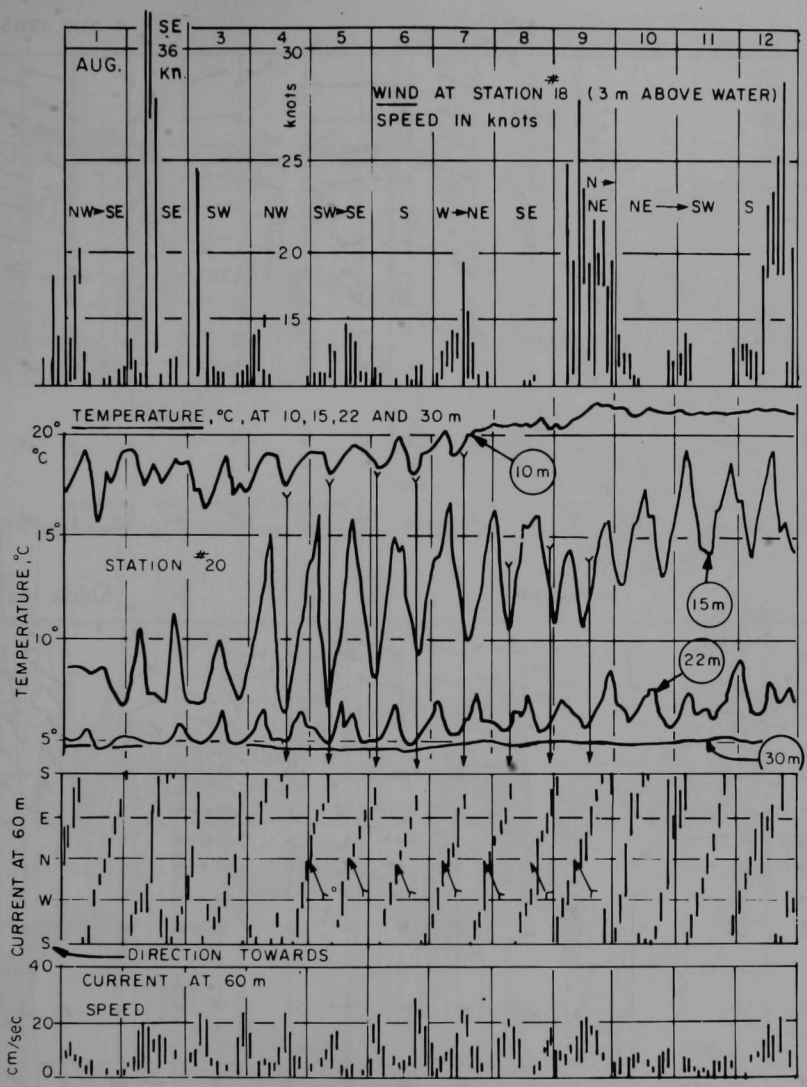

Fig. 49. Lake Michigan, Station 20 (43°08'N and 86°31'W), August 1-12, 1963. Temperature, °C, (hourly) at Depths 10, 15, 22, and 30 m; Current Speed and Direction (two-hourly ranges) at 60-m depth; Wind Speed and Direction at a Buoy Station 43°09'N and 87°28'W. Data provided by the U. S. Department of the Interior, Federal Water Quality Control Administration, and illustrated in Mortimer (1971).

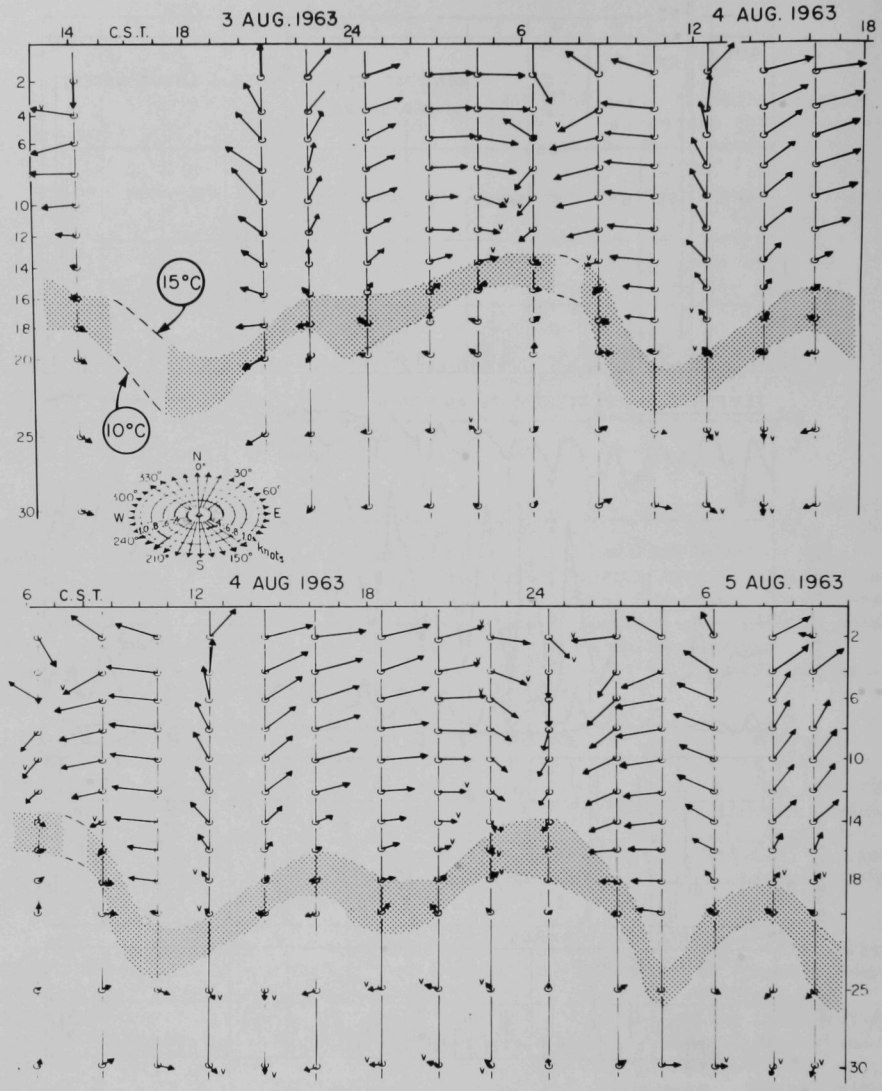

Fig. 50. Lake Michigan, August 3-5, 1963. Distribution of Current Speed and Direction, at Roughly 2-hr Intervals in the Upper 30 m at Anchor Station M_2 (43°14'N, 87°08'W). Also shown (shaded) is the thermocline layer, defined as bounded by the 10 and 15° isotherms. The figure is composed of two overlapping portions to show how current and thermocline patterns follow an approximately 17-hr cycle. Redrawn from Mortimer (1968).

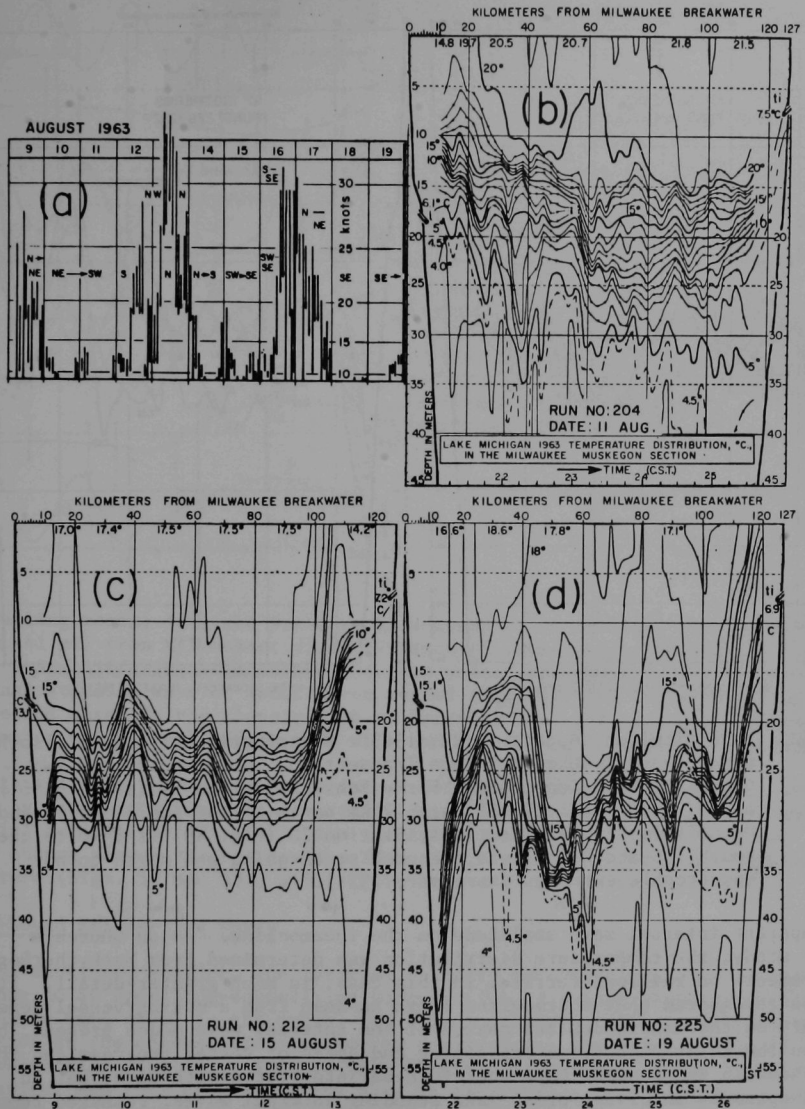

Fig. 51. Lake Michigan 1963: (a) 2-hr Ranges of Wind Speed at a Buoy Station 18 (43°09'N, 87°28'W); (b), (c), and (d) Distribution of Temperature, °C, along the Milwaukee-Muskegon Transection on August 11, 15, and 19. "i" and "ti" shows positions of Milwaukee and Muskegon water intakes, respectively. From Mortimer (1968).

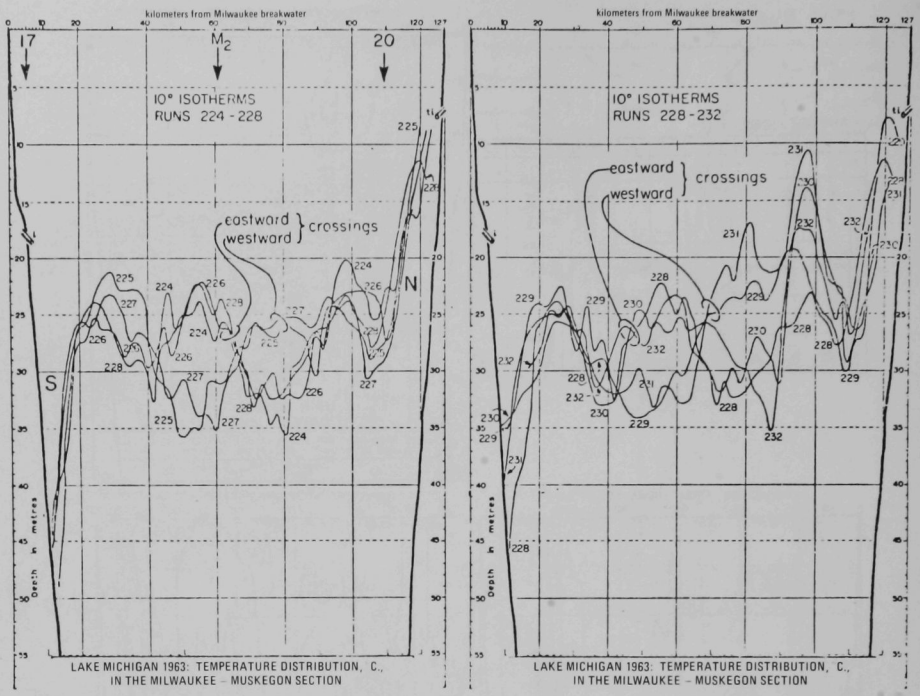

Fig. 52. Lake Michigan, August 19-22, 1963. Distribution of the 10° Isotherm along the Milwaukee-Muskegon Transection, Superimposed for Two Groups of Five Consecutive Ferry Runs. Stations 17 (see Fig. 61) and M_2 (see Figs. 50, 56) are 12 km north of the positions 17 and M_2 on this figure's sections; Station 20 (Fig. 49) is 6 km to the south. S and N indicate presumed south-going and north-going geostrophic currents (Mortimer, 1971).

the apparent internal wave amplitude on the thermocline. As in Church's (1945) study, the temperature distribution was determined from bathythermograph measurements on railroad ferries, in this case, in much greater detail. It must be remembered that thermocline depth as seen from a moving vessel depends not only on the amplitudes and phases of the internal wave modes present, but also on the relation between the timing and speed of vessel progress and the wave phases. The results must therefore be interpreted with care, but in simple episodes involving cross-lake standing internal waves, repeated temperature transects can provide information on the positions of the internal nodes and on phase differences which occur when passing from one side of the node to the other. The overlay of all the 10°C isotherms traced by the moving vessel on repeated crossings in Figure 52, and the derived depth variation of the thermocline at selected, fixed points on the crossing (Fig. 53), show several significant features: (*i*) the persistence, over three days, of the mean upward and downward deflections of the thermocline in the upwelling and

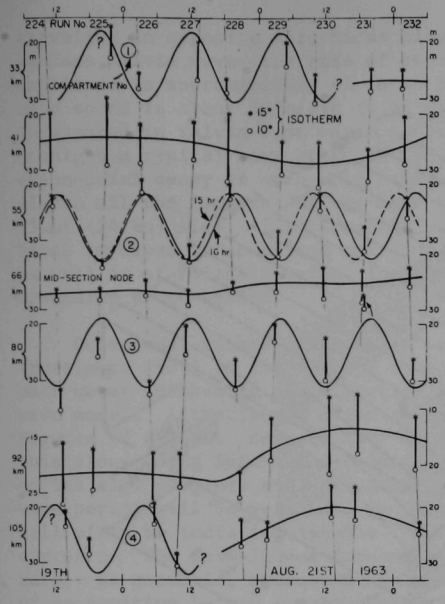

Fig. 53.

Lake Michigan, August 19-20, 1963. Oscillations in Depth of the Thermocline (bounded by the 10° and 15° isotherms) at Selected Distances from Milwaukee, Observed on Nine Consecutive Ferry Runs across the Milwaukee-Muskegon Transection. Where appropriate, a sinusoid (thin line) corresponding to a 16-hr period (also to a 15-hr period, broken line, at the 55-km station) is fitted to the observations (Mortimer, 1971).

downwelling zones; (*ii*) the presence of a conspicuous mid-lake node at about 66 km (41 mi) from Milwaukee; (*iii*) evidence of other nodes; and (*iv*) a very clear phase difference across the mid-lake node. The observations fit an internal standing wave of about 16-hr period (Fig. 53) and the observed pattern and period agree fairly closely with an internal Poincaré wave model consisting of a major quintinodal seiche mode with smaller tri- and uninodal components.

In spite of the complexities introduced by the mixture of internal wave modes by non-wave currents and variable depth, we may conclude that the near-inertial periodicity (Fig. 49), the clockwise rotation of current and the phase change across the thermocline (Fig. 50), as well as the cross-lake nodal structure (Figs. 52 and 53), all fit the Poincaré wave model quite well.

Shore-Bound Kelvin-Type Waves

As mentioned earlier, the internal Poincaré wave model is one possible response to an upwelling-downwelling perturbation of a large-lake thermocline; the Kelvin wave model is the other. In this model (Fig. 54) the solid boundary condition at the channel sides is met by constraining the flow so that it is everywhere side-parallel. This is only possible if Coriolis force is balanced by gravity, and this constrains the wave to travel in a side-parallel direction, with greatest wave height on the side lying to the right of the direction of progress (North Hemisphere case), and with wave height decreasing exponentially in the cross-channel direction. Under these conditions, and only under these conditions, is the Coriolis force exactly cancelled everywhere by the component of gravitational force acting on the cross-channel wave slopes.

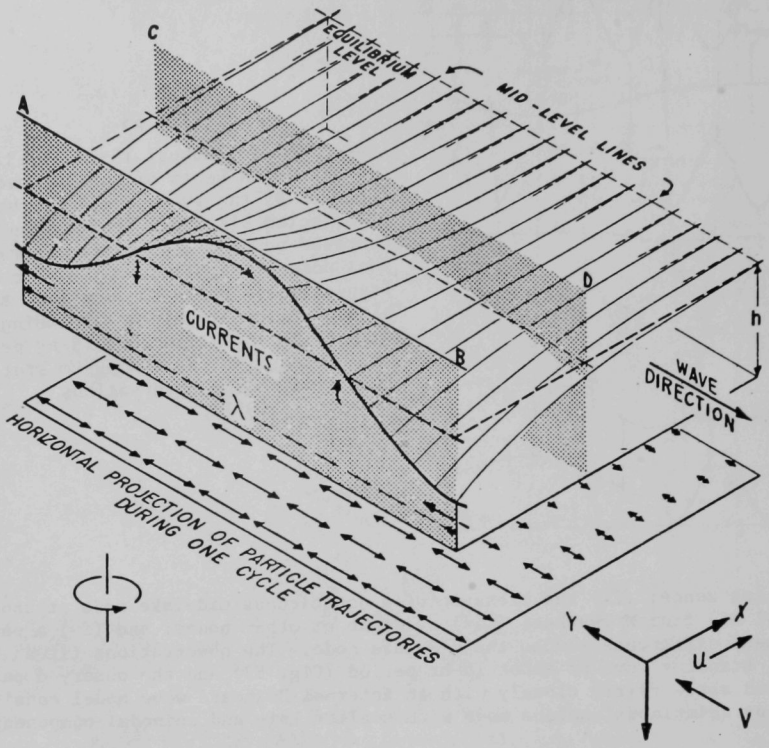

Fig. 54. One Wavelength, λ, of a Kelvin Wave Traveling along One Side (AB) of a Semi-infinite Ocean (or of a very wide channel, only one side of which is shown) of Uniform Depth and Rotating Counterclockwise about a Vertical Axis. The elevation topography may be envisaged either as that of the water surface or as that of the interface in a two-layer model, in which case current vectors shown are those in the lower layer. The amplitudes of wave elevation and current decrease exponentially in a direction normal to AB. Currents are always and everywhere parallel to AB. Therefore, a second vertical side, for example CD parallel to AB, can be inserted without disturbing the wave. Adapted from Mortimer, 1968.

Kelvin waves can be generated on the water surface as well as on the thermocline interface. In fact, the rotating (amphidromic) surface seiche pattern in Lake Michigan illustrated earlier in Figure 17 can be modeled as a combination of two surface Kelvin waves of equal wavelength and frequency

traveling in opposite directions along the two shores. In the case of the surface Kelvin wave, the rate of cross-channel exponential decrease in wave amplitude is approximately 4% in 10 km (6.2 mi) (28% across the basin) and the wave speed is about 30 m/sec (∿ 67 mi/hr) at Lake Michigan depths. Here we are interested in Kelvin-type waves on the thermocline interface and for Lake Michigan a typical wave speed is about 2 km/hr (∿ 1.2 mi/hr) and the rate of exponential decay is much more rapid, approximately 90% in 10 km. Therefore, almost all the internal Kelvin-type wave energy is confined to a coastal strip 15 mi (24 km) wide. Significantly, this is also the width of the coastal bands involved in upwelling and downwelling. Generation of Kelvin-type waves, as well as of Poincaré waves, is therefore an expected consequence of the upwelling perturbation.

Occasional rather fragmentary evidence for such generation has been seen (Mortimer, 1963) in the form of steep-fronted thermocline waves progressing past water intakes in the direction and at the speed predicted for a Kelvin wave model. Attention is drawn to this type of progression by dotted lines in Figures 42 and 43. Bennett (1973a) interpreted the steep-fronted nature of this slow-moving internal wave as a consequence of nonlinear dynamics. Because of its slow progress and, presumably, its long wavelength, the Kelvin-type wave period will be very long in Lake Michigan, and the associated currents will often be indistinguishable from other types of nearly steady longshore currents. The unambiguous demonstration of a Kelvin-type wave will therefore rarely be possible, because a new wind-induced disturbance will change it out of recognition before a substantial fraction of a wave cycle has been completed.

Although upwelling-downwelling perturbations of the Lake Michigan thermocline elicit a joint Kelvin- and Poincaré-wave response, with shore-parallel currents dominant near shore and rotary currents dominant offshore, it is not yet clear how the energy is partitioned between the two wave responses in any given episode, or indeed whether upwelling is the sole generating mechanism. Both are required responses, however, in the sense that they form interdependent components of the normal mode solutions of rectangular basin models (Lauwerier, 1960).

Short Internal Waves

Although our focus has been on long internal waves, which generate conspicuous rotating or shore-parallel currents during stratification, internal oscillations of much shorter wavelengths are also seen if the temperature structure in Lake Michigan is monitored in sufficient detail in space (Fig. 55) or time (Fig. 56, Mortimer *et al.*, 1968). Internal waves of widely differing wavelength and period are found between two limits: the long-period limit, earlier identified as the local inertial period; and a short-period limit, the Brunt-Väsäla period, physically determined by the magnitude of the vertical density gradient $\partial\rho/\partial z$. Under summer conditions in Lake Michigan, the Brunt-Väsäla period, $[4\ \pi^2\rho/g\ (\partial\rho/\partial z)]^{\frac{1}{2}}$, in which p is the density and g the acceleration of gravity, lies typically in the range two to five minutes, and is inversely proportional to the square root of the density gradient. It should be noted that the often-observed tendency for short internal wave energy to be concentrated just above the Brunt-Väsäla resonance period is comparable to the concentration at long internal wave energy just below the inertial resonance period. In Figure 56, for example, the energy was concentrated near the thermocline and in a period range little greater than the local Brunt-Väsäla period.

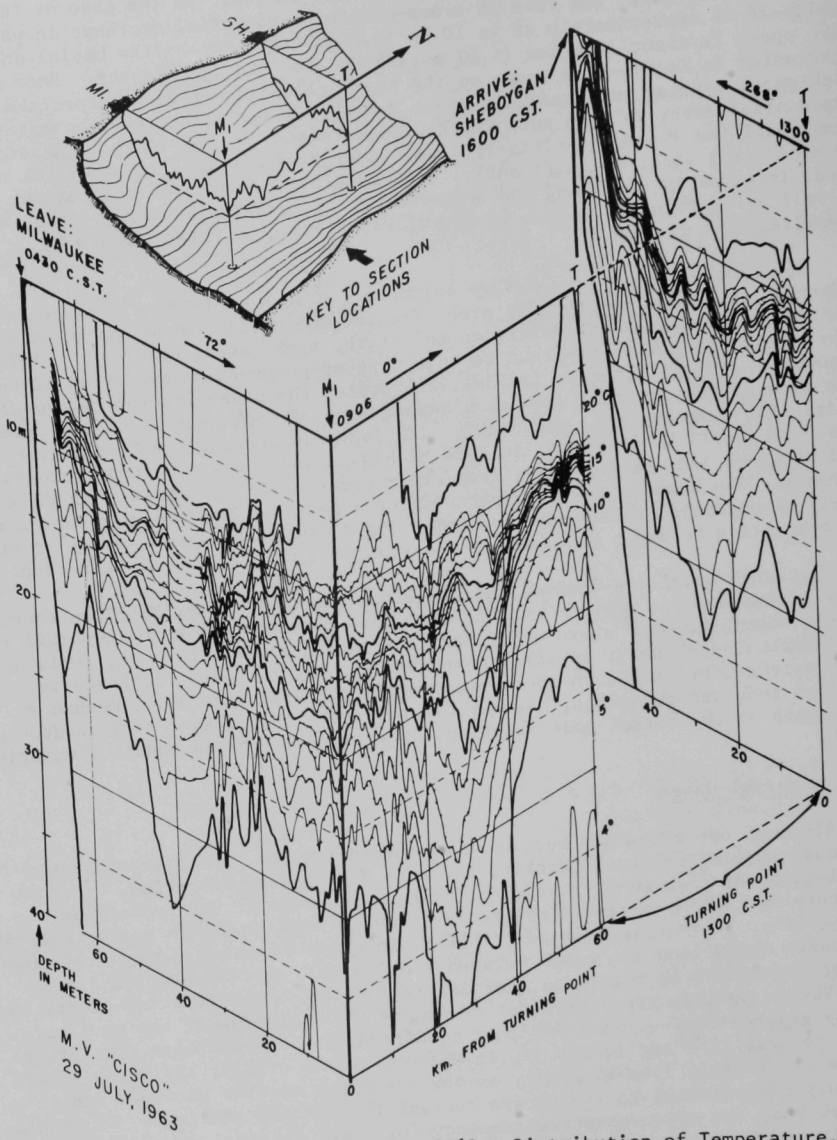

Fig. 55. Lake Michigan, July 29, 1963. Distribution of Temperature, °C, Observed from *R/V Cisco* on a Cruise from Milwaukee to Mid-Lake, Then North for 60 km, Then West to Sheboygan. Isometric projection; directions °(true). Modified from Mortimer (1968).

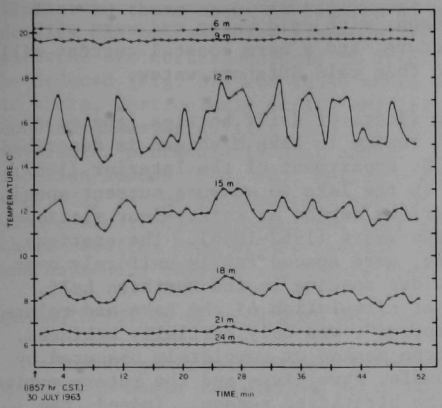

Fig. 56.

Short Internal Waves in Lake Michigan, July 30, 1963. Temperature, °C, at several depths ranging from 6 to 24 m at anchor station M_2 (43°14'N, 87°08'W) during a 54-min interval (slightly modified from Mortimer, McNaught, and Stewart, 1968) (with permission, see credits).

These little-studied internal waves are not confined to large basins. Their generating mechanisms are still unclear, but these waves probably arise as a consequence of the type of shear instability (Richardson Number < 0.25) illustrated in Figure 20. The relation of such waves to those of longer period and to non-wave currents awaits investigation, but it seems reasonable to assume that they will increase turbulent diffusion.

NONPERIODIC RESPONSES AND THEIR INTERACTIONS WITH PERIODIC CURRENTS

CHARACTERISTICS OF WHOLE-BASIN CURRENT PATTERNS

The extent and nature of steady or quasi-steady currents in Lake Michigan are not well known. The rationale for this is found, first, in the lack of systematic, long-term, direct current measurements (as opposed to inferences from changes in the temperature structure) and second, in the dominance of the Poincaré-type rotational motion during the stratified season. Apart from thermally driven circulations, such as the thermal bar, which are particularly active during the seasons of cooling and heating (Huang, 1971; Bennett, 1971), circulation in Lake Michigan is wind-driven.

In general, we may distinguish between the primary, wind-driven currents set in motion by the application of the wind stress combined with stresses associated with breaking waves and the secondary, quasi-geostrophic currents generated by tilting of the lake surface or of the internal density surfaces. Gradient currents strike a balance between the horizontal pressure forces thus generated and Coriolis force, and usually persist longer than the primary wind-driven currents after the wind has died down.

Another general conclusion is that effectiveness of the airflow in driving water depends strongly on whether the air is cooler or warmer than the water. In the latter case, a stable density stratification develops in the lowest air layers. These then exert less frictional drag than when water warmer than air creates convectional instability and greater frictional force is applied to the water. Therefore, the stress will be much less for a given

wind speed during the spring warming season, with cold water and warm air, than during the fall when the reverse occurs, and a warm coastal current will experience more stress from a given wind than cold offshore water.

Since Harrington's 1894 study using fleets of drift bottles, the most ambitious attempt to explore the current regime in Lake Michigan is described in the "Lake Currents" report of the U. S. Department of the Interior (1967). Oceanographic instruments were deployed in the lake to measure current speed, current direction, and temperature at various depths at thirty-four stations, occupied in some cases for a period of two years (1962-1964). The stations, none nearer than 5 km (3.1 mi) from shore, were spaced fairly uniformly over the southern half of the basin, with a wider spacing in the northern half. The major objective, to "determine the net circulation of the Lake and relate this to wind movement for prediction purposes", was only partially achieved, because net circulation patterns were often masked or completely obscured by large, short-term perturbations, for example, upwellings and the rotary motions of internal Poincaré-type waves during the stratified season. Indeed, the U. S. Department of the Interior findings provided abundant confirmation of the strong influence of upwelling and near-inertial internal waves forecast by Mortimer (1963), some examples of which are described here (Figs. 49 and 61). The general conclusions for offshore waters were as follows (U. S. Department of the Interior, 1967, p. 118):

> *"During stratified conditions the short-term analysis of data does not indicate a wind-driven current system. The hour-to-hour currents are dominated by the internal wave regime which receives its principal energy from the wind. The internal wave regime is also affected by the Earth's rotation which tends to obscure the direct relationship between winds as the driving force and currents produced by internal waves. The internal wave rotation, with a period close to the inertial frequency, is often altered by sudden wind inputs. This regime lasts from late spring (April) into November or early December. The rotating influence is normally not found in the inshore waters.*
>
> *By contrast, the winter circulation is less complex and almost entirely wind-driven. The major exception appears when an ice cover occurs or a reverse (winter type) thermocline develops in the central basin.*
>
> *A straight prediction model, based on wind, is not valid for summer (stratified) conditions in mid-lake."*

The above conclusions were based on direct measurements of currents. Others, for example, Ayers *et al.* (1958), attempted to deduce circulation patterns from the distribution of density in Lake Michigan, making the assumption that the flow is everywhere in geostrophic equilibrium. That assumption, employed by physical oceanographers in the computation of ocean currents, is equivalent to the statement that the horizontal pressure gradients associated with tilted (isopycnal) surfaces of equal density exactly balance Coriolis force. The geostrophic assumption would be also valid for Lake Michigan if an averaged density field could be used which removed the effects of short-term perturbations such as diurnal heating, local wind-induced changes, and internal waves. Because the density data are collected from vessels traversing sections

similar to those shown in Figures 45 and 46, an averaging of fluctuations in density may not adequately remove irregularities. The computed circulation patterns are correspondingly in error; nevertheless, some general patterns can be deduced (Fig. 57) and these often show the strongest currents running close to shore, particularly during upwelling-downwelling episodes. They also show considerable variability from day to day, with frequent current direction reversals, particularly near shore. In another example, later in the stratification season (Fig. 58), Bellaire and Ayers (1967) described a large clockwise eddy in the southeastern part of the Lake. They considered it to be wind-controlled, and concluded that strong northward currents along the western shore resulted from strong thermal (upwelling) gradients there. The pattern was obviously complex and intermittently modified by changes in the wind.

CHARACTERISTICS OF NEARSHORE CURRENT PATTERNS

Investigations mentioned in the foregoing paragraphs were mainly concerned with whole-basin circulation patterns. Recently more emphasis has been placed on circulation near shore, because this zone is the scene of maximum man/lake interaction and is the recipient of inflowing waste materials and heat. Some conclusions concerning nearshore current patterns were drawn from the U. S. Department of the Interior Study (1967, pp. 118-119):

> *"Inshore current patterns in the upper 5 m appear to have a wind-driven circulation throughout the year. The response to this system appears in about 1 hour under moderate wind conditions.*
>
> *The inshore zone varies in width and probably extends as much as 10 miles from the shore during the most favorable conditions and as little as 2 miles during periods of upwelling. Mid-lake circulation patterns in winter are not under the influence of internal waves except under very special conditions. Spectral analysis of current meter data, for the winter period, gives no evidence of a dominant frequency which could control current patterns. Winter patterns in mid-lake are, similar to the inshore areas during summer, wind-driven. The response time of the mid-lake portion is probably the same as the inshore waters."*

In fact the nearest station to shore during the above survey was 4 km (2.5 mi) off Waukegan, Illinois. Records from that station were compared with records from a station 34 km (21 mi) offshore by Davidson and Birchfield (1967). Current at the latter station showed very low correlations with the wind, while current at the nearshore station was highly correlated with the wind. Measurements closer to shore have been few, although more effort has recently been devoted to filling this gap: Monahan (1973) in Grand Traverse Bay, Michigan; Terrell and Green (1972) using aerial photography of floating poster boards off Point Beach, Wisconsin; and Sato and Mortimer (1975) with current meters moored near Oak Creek, Wisconsin.

The general conclusion from these few nearshore current measurements in Lake Michigan, and from the more comprehensive measurements in Lake Ontario made during the International Field Year for the Great Lakes and reviewed by Boyce (1974), is that a nearshore strip about 10 km (6.2 mi) wide is the scene of the main transfer of energy from wind to total basin motion and contains the greater part of the Lake's kinetic energy. As we have seen, it is within

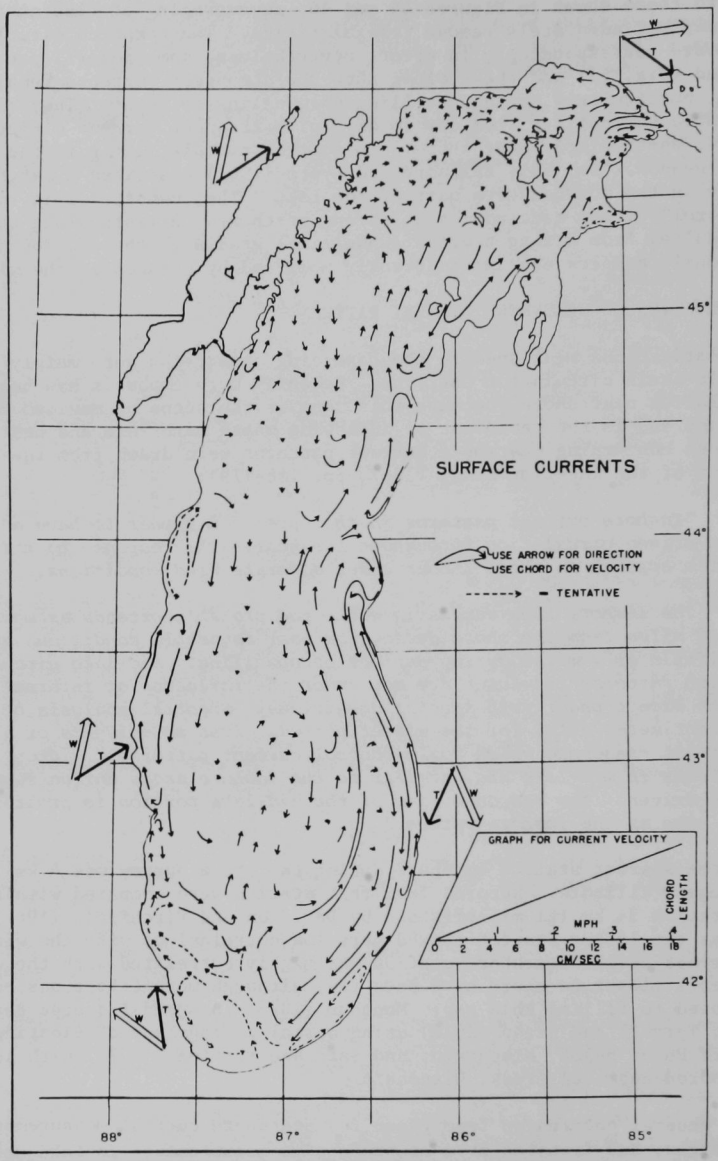

Fig. 57. Surface Currents in Lake Michigan, June 29, 1955. Slightly modified from Ayers *et al.* (1958) (with permission, see credits).

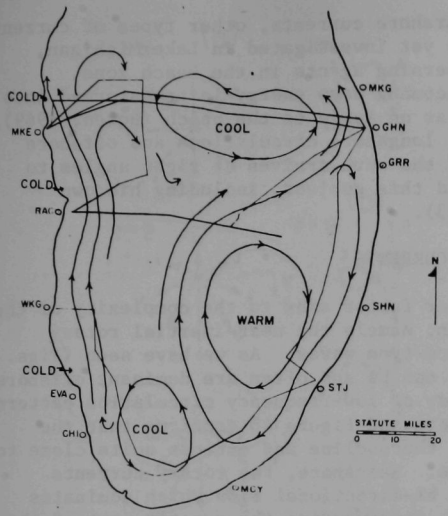

Fig. 58.

Current Pattern Derived from Surface Temperature Pattern and Dynamic Height Calculations, October 23-26, 1963 (Bellaire and Ayers, 1967) (with permission, see credits).

a strip of similar width that extensive upwellings and downwellings occur, generating long internal waves. That strip also contains a complex combination of (*i*) shore-trapped boundary waves of long period, often indistinguishable from steady baroclinic geostrophic currents, and (*ii*) direct wind-driven flows, which show lagging correlations with changes in direction and magnitude of the wind stress.

Because the momentum flux from air to water takes place at the lake surface, the average wind-derived stress per unit volume of fluid in a fully mixed layer is inversely proportional to the depth of that layer. Therefore, shallow nearshore water masses respond more quickly to changes in wind force than deeper layers further offshore. At the same time, the momentum of the deeper currents confers a degree of relative persistence, and large horizontal shears are therefore expected in the transition zone between coastal and offshore waters during the periods of changing wind.

We may expect that currents in coastal waters of Lake Michigan will be predominantly shore-parallel and will respond most strongly to winds blowing along the long axis of the basin and with maximum fetch length over the water. This is confirmed by the recent findings of Sato and Mortimer (1975) which disclose the episodic character of current response to individual storms, characterized by a relatively rapid rise in current speed followed by a slower decay in speed after the storm passes. Each major storm, involving large changes in stress or stress direction, will be reflected in large adjustments in the coastal current regime after some lag period, the length of which will depend on the strength of the previous current, on water depth, and on the time history of the changing wind stress. Also, during summer stratification, frequent upwelling-downwelling changeovers will cause the surface layers to move onshore or offshore and will generate quasi-geostrophic along-shore currents. Superimposed on these complex and little understood processes are the effects of variability in bottom topography and wind stress.

Before we leave the subject of nearshore currents, other types of current should be mentioned, which although not yet investigated in Lake Michigan, probably play an important role as dispersing agents in the beach zone. Within the breaker zone, part of the incoming wave energy is transformed into longshore currents if the wave arrives at an angle to the beach (Bowen, 1969), or into a cellular pattern of alternate longshore circulations and offshore rip currents (Bowen and Inman, 1969) if the wave arrives at right angles to the shore. Longuet-Higgins has surveyed this subject, including his own recent work, in a chapter in Meyer (1973).

INTERACTIONS BETWEEN STEADY AND ROTARY CURRENTS

During summer stratification another factor adds to the complexity of the nearshore current field in Lake Michigan, namely the near-inertial rotary motions associated with internal Poincaré-type waves. As we have seen (Figs. 49 and 50), the wave-driven rotary motions can be and often are dominant offshore, making it difficult to observe any steady or low-frequency circulation pattern. The Poincaré wave model (Fig. 47) predicts and Figure 48 confirms that the rotary pattern affects the whole of the thermocline and extends quite close to shore, although on a reduced scale there. Nearshore, the rotary currents combine with the mainly shore-parallel, bi-directional flow which dominates that zone. The combined nearshore flow, representing the greater part of the lake's kinetic energy, is itself a complex combination of currents which are wind-driven or gradient-driven by upwelling-downwelling events as well as by surface seiches and long-period internal Kelvin-type waves.

To aid interpretation of currents observed in the Lake, it is instructive to examine Figure 59. This displays two methods of modeling the combination between a rotary current and varying proportions of a unidirectional current. The first method, in the left-hand column (a), takes the form of a set of current roses, in which the current vectors are shown for every 2 hr of a 16-hr Poincaré wave cycle. These rotating vectors, of constant speed u and emanating from a common point, are combined with unidirectional current components of speeds: $v = o$; $v = u/2$; $v = u$; $v = 2\,u$, corresponding respectively to the (u/v) speed ratios, r, shown in the figure. The second form of presentation is a set of progressive vector diagrams corresponding to the set of current roses just described, but with the successive, 2-hr, combined vectors joined in series tail to head. For the pure rotary motion ($r = \infty$) the progressive vector diagram is an inertial circle. With the addition of increasing proportions of unidirectional component, v, the current track may be respectively described as: (b) looping; (c) cusping; and (d) meandering.

Examples of all these current types are frequently seen when progressive vector diagrams are prepared from actual Lake Michigan current meter records. Examples from Verber (1966), matched to (b), (c), and (d), are shown in the right-hand column (e) of Figure 59. It should be noted that progressive vector diagrams, prepared from records at a fixed recorder, will not be an exact representation of the actual current track unless the flow field is uniform, although changing with time, over the whole region covered by the diagram. This is likely to be true only in the neighborhood of the fixed recorder. The true extended track can only be measured by instruments drifting with the current.

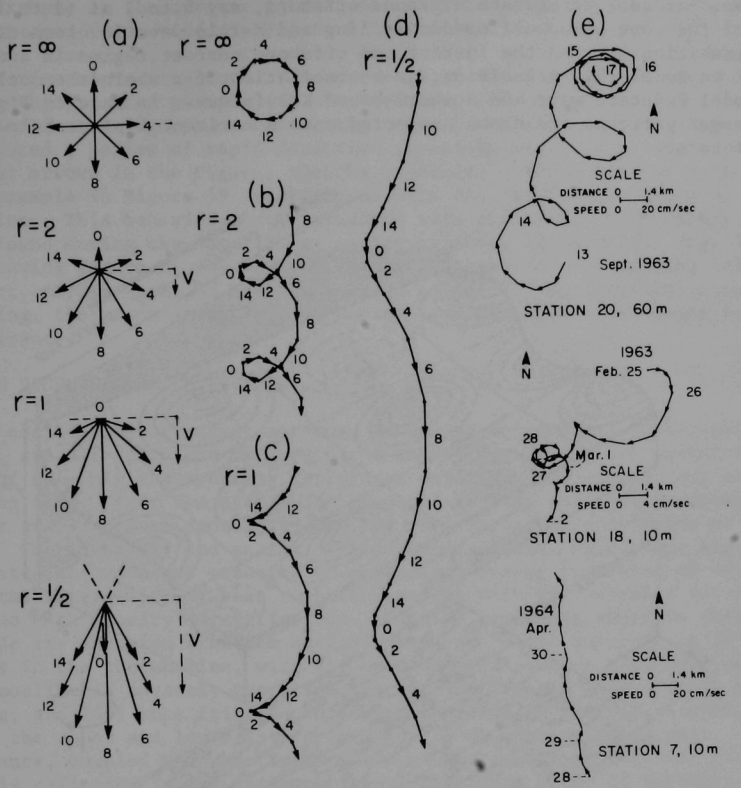

Fig. 59. (a) Current Roses in Which a Rotating (Poincaré wave) Current Component of Constant Speed, u, is Combined with Unidirectional Current Components of Speeds V = 0, $u/2$, u, and $2u$. The respective rotating/unidirectional speed ratios, $r = \infty$, 2, 1, 1/2; (b), (c) and (d) are the combined current trajectories corresponding to r = 2, 1, and 1/2, respectively; (e) observed current trajectories in Lake Michigan (Verber, 1966) (with permission, see credits).

Very near shore, within 3 mi (5 km), very little rotary current component is found, i.e. the currents are mainly shore-parallel, sometimes meandering [see Fig. 59, Station 7, 4 km (2.5 mi) from shore], and subject to frequent direction reversal following disturbances by wind. More than 10 mi (16 km) offshore, rotary near-inertial currents are conspicuous, producing circling, looping or cusping current tracts [see Fig. 59, Station 20, 20 km (12.4 mi) offshore; see also results for that station in Fig. 49] depending on the relative magnitude of unidirectional current components which may be present at

the time. At an intermediate distance offshore, say 5 to 7 mi (8 to 11 km) width of the zone of upwelling-downwelling and Kelvin wave involvement, there is a transition between the inshore and offshore current regime in summer. An attempt to model this transition, as a combination of a whole-thermocline, multinodal Poincaré wave and a shore-bound Kelvin wave, is made in Figure 60. The current patterns are shown projected onto a horizontal plane below the wave picture.

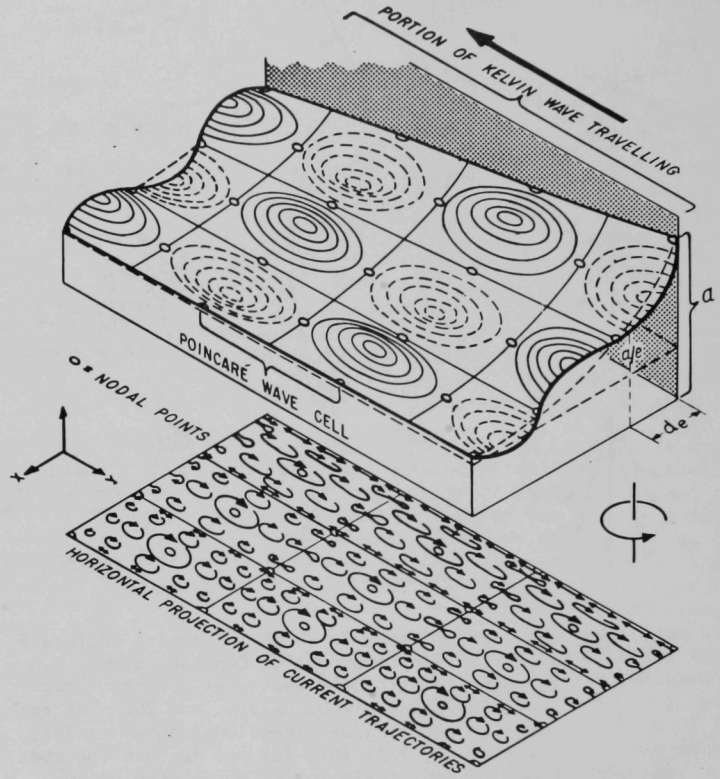

Fig. 60. Combination of a Multinodal Standing Poincaré Wave in a Simi-infinite Ocean Model (or in a very wide rotating channel, of uniform depth, of which only one side is shown) and a Portion of a Kelvin Wave Traveling along the Side. The elevation and current amplitudes associated with the Kelvin wave are at a maximum at the channel side and decrease exponentially away from the side of the x-direction. The figure illustrates the transition, in current trajectories, from a nearshore pattern dominated by the Poincaré wave offshore. Modified from Mortimer (1968).

An example of the current pattern commonly found in the nearshore-offshore transition zone is provided in Figure 61 for a station 6 km (3.7 mi) off Port Washington, Wisconsin, where the water depth is 22 m (72 ft) and the shoreline runs approximately north-south. The currents at the 15-m (49-ft) depth were either southgoing (for example, at the beginning and end of the interval illustrated in the figure) or northgoing. The northgoing current, August 4-9, also executed a series of rapid direction reversals every 17 hr or so, shown by smaller arrows in the figure, thereby producing a track similar to the looping example in Figure 59 synchronized with the temperature waves on the thermocline. This behavior may be compared with the almost pure rotary current pattern found during the same 12-day period offshore (Station 20, Fig. 49). Before leaving Figure 61, we may note a clear example of downwelling induced by a short, strong burst of N to NE wind on August 9. As a result of the downwelling, the north-going looping current was replaced by a steady south-going current.

A NOTE ON DISPERSAL AND DIFFUSION

The oscillatory or steady motions, described and modeled in foregoing sections, are all turbulent to greater or lesser degree and are therefore capable of not only transporting introduced materials and wastes, but also of dispersing them. From the standpoint of water quality and quality management, transport and dispersal capability are the most important attributes of lake motions. The intensity and scales of turbulence depend, of course, strongly on the rates and modes of transfer of mechanical energy from wind to water, as well as the interaction of that turbulent energy with the buoyancy forces associated with density stratification. Density gradients suppress turbulence and impede its invasion from the surface downward. That suppression is strongest in the thermocline, with the consequence (*i*) that transport across the thermocline is severely curtailed, except for dynamic "leaks" such as upwelling, and (*ii*) that friction on the thermocline is greatly reduced, allowing the upper and lower layers to slide about with relative ease. This circumstance, coupled with the large ratio of horizontal to vertical basin scales, is reflected in the large horizontal/vertical ratio of turbulence scales. In practice it is the horizontal or lateral turbulence which is primarily responsible for dispersal of materials and heat introduced into Lake Michigan, and to which the concept of the "eddy spectrum," outlined in a previous section, applies. These practically important but theoretically difficult matters will be treated by Dr. G. T. Csanady in the following essay. The present essay concludes with a brief description of recent modeling developments as they apply to present and future perceptions of Lake Michigan's dynamic behavior.

MODELING OF CIRCULATION PATTERNS

In assembling a coherent picture of the principal motions in Lake Michigan, I have examined clues that the lake has provided to various investigators and have interpreted those clues in terms of simple, descriptive or analytical, constant-depth models. This approach has the merit of staying close to nature, and exploitation of the simple models has brought some components of a general circulation model into reasonably sharp focus.

Another approach, taken in recent years, is the following. It (*i*) starts with the basic equations of motion and conservation as influenced by the

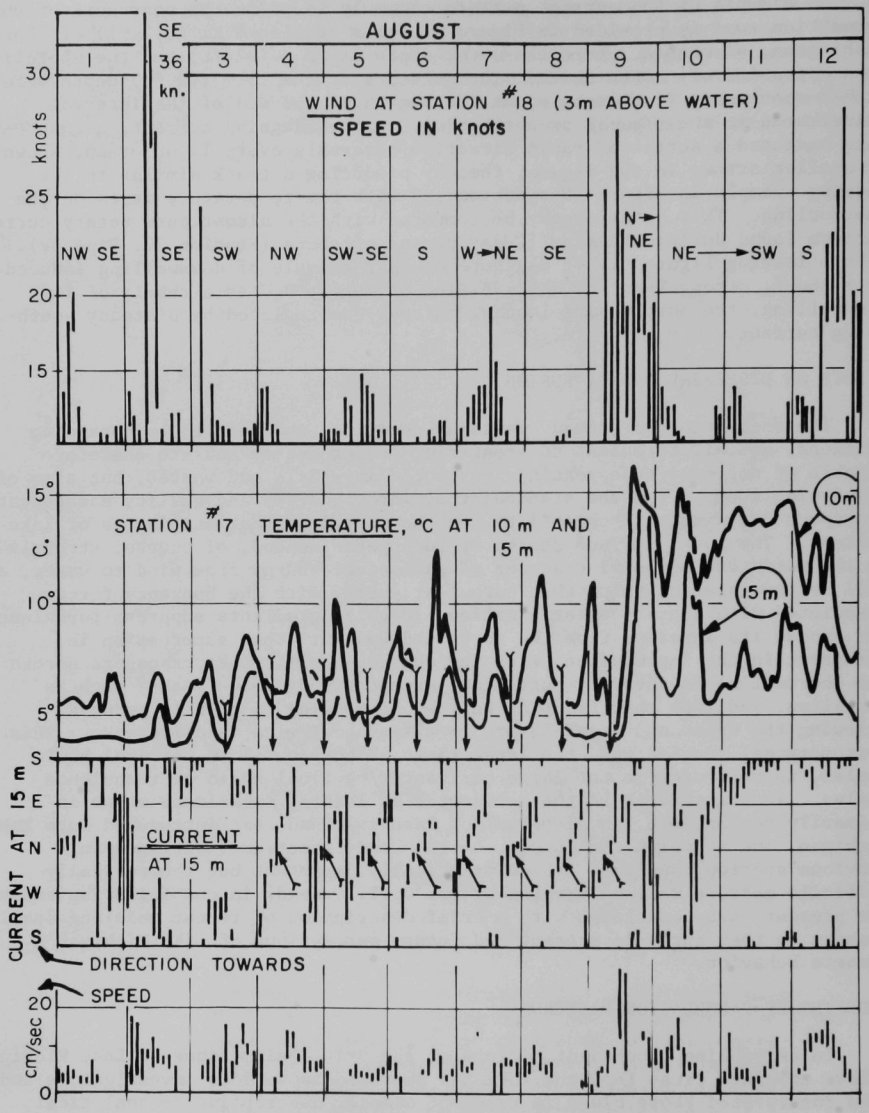

Fig. 61. Lake Michigan, Station 17 (43°08'N, 87°51'W) August 1-12, 1963: Temperature (Hourly) at 10 m and 15 m; Current Speed and Direction (2-hr ranges) at 22 m; Wind Speed and Direction at Station 18 (43°09'N, 87°28'W). U. S. Department of the Interior (1967) as presented in Mortimer (1971).

earth's rotation; (*ii*) transforms the equations into versions convenient for numerical processing; (*iii*) defines appropriate boundary conditions; (*iv*) incorporates realistic assumptions required to treat wind stress, turbulence, and friction; and (*v*) finally combines all components into a computerized model of circulation in basins of shape and density distribution approximating the actual lakes. The objectives of a good modeling procedure, which is verified stage by stage against observed lake motions, are: accuracy and stability of the computations, economy in computer use, and versatility. These objectives permit relatively inexpensive testing of many different combinations of surface and bottom stresses, turbulent coefficients, density distributions, and bottom topography. Even though the degree of approximation to reality is severely limited by the present size of computers and research budgets, numerical modeling has already scored some notable successes (e.g. Simons, 1973, 1974).

Because it can take actual basin topography into account, numerical modeling has been able to free itself from the restrictive and unrealistic assumption of constant depth and from the emphasis which constant-depth models have placed on the set-up (wind-induced slopes) and seiching aspects of basin responses. Models of variable-depth channels or basins disclose additional patterns of flow, clearly related to the distribution of water depth (Murty and Rao, 1970; Simons, 1973, 1974; Bennett, 1973b). In the Murty and Rao example, a steady-state model of a wind-driven unstratified Lake Michigan (Fig. 62), uniform wind stress directed along the axis of the basin produces a forward flow with the wind in the shallower water, along both sides, and a return flow against the wind in the central, deeper water mass. This produces circulation cells, which Csanady (1975) has called "topographic gyres." With northgoing wind (Fig. 62, top left) two pairs of elongated gyres are formed. The western and eastern members of each pair rotate clockwise and counterclockwise, respectively. Circulation is more rapid in the northern pair. A uniform cross-lake wind stress, on the other hand, produces only weak counterclockwise circulations in the southern and northern ends of the basin. The corresponding set-ups (water surface deviations from equilibrium) are shown in the lower part of Figure 62.

While steady-state circulation patterns of the type illustrated in Figure 62 throw light on the nonoscillatory part of a large lake's response to wind stress, it appears likely that truly steady-state patterns will rarely be found in Lake Michigan. We must note, for example, that the only observations of whole-basin gyres to date (Harrington, 1894, and the findings of Ayers *et al.*, 1958, and of Bellaire and Ayers, 1967, respectively, illustrated in Figures 57 and 58) bear little resemblance to the patterns shown in Figure 62. The following conclusions are developed by the U. S. Department of the Interior (1967):

> *"Although the winds are the primary driving force in winter, other forces exist which complicate the pattern. When a wind reversal occurs in one sector of the Lake, the remainder of the Lake is at or attempting to maintain equilibrium under the prevailing wind regime. No steady-state system can exist while external conditions are constantly changing. For this reason, Lake Michigan probably never achieves a steady-state or equilibrium condition everywhere at one time. However, large sectors, such as the southern basin, do achieve a near-equilibrium condition. Under these conditions, during the nonstratified period, a prediction model is applicable."*

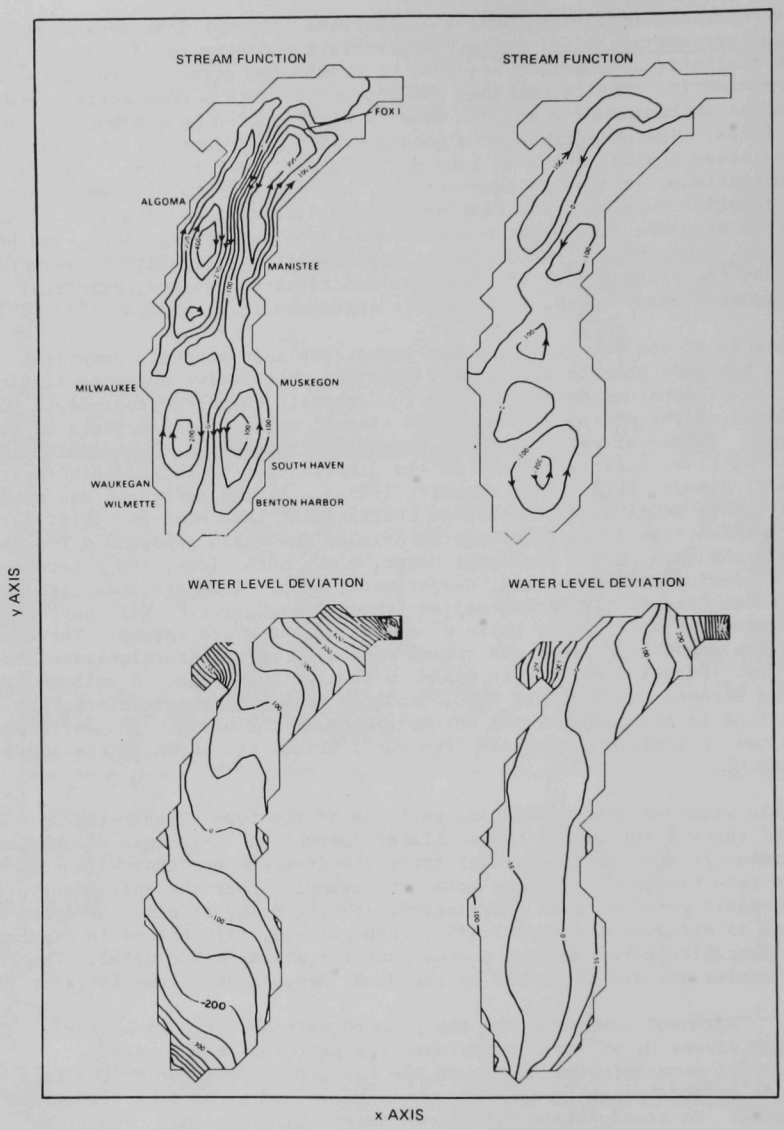

Fig. 62. Upper Portion: Circulation Patterns for Lake Michigan for Uniform Wind Stress in y Direction Only (left) and Uniform Wind Stress in x Direction Only (right).
Lower Portion: Water Level Deviations for Lake Michigan for Uniform Wind Stress in y Direction Only (left) and Uniform Wind Stress in x Direction Only (right). Modified from Murty and Rao, 1970.

Fortunately, however, modeling is not restricted to steady-state or unstratified winter cases. Models have been developed with realistic simulations of time-dependent wind stresses and non-uniform density distributions. A Lake Michigan example is the two-layered, wind-driven model of Kizlauskas and Katz (1974). At present, verification by field measurements generally lags behind hydrodynamic modeling capability, but the International Field Year for the Great Lakes (IFYGL) program on Lake Ontario provided the stimulus for notable advances in modeling (Simons, 1973; Wu, 1975). In some cases the observations have fitted the model results closely (e.g. Simons, 1974), providing a much better understanding of the coupling and the inherent differences between nearshore and offshore motions (reviewed by Boyce, 1974). A well-founded hope is emerging that careful, systematic, step-by-step alternation between model improvements and experimental verification will promote progress toward deeper understanding and better predictive capability.

CREDITS

The authors and the Argonne National Laboratory gratefully acknowledge the courtesy of the individuals and organizations who granted permission to use illustrations or, where appropriate, other material in the ANL/ES-40 series. Sources of illustrations used in Volume 2, Part 1, are listed below.

Figure

1 Lake Michigan Bathymetric Chart compiled and drawn by Ratko J. Ristic, copyright 1968. Reprinted by permission of R. J. Ristic.

7 Sverdrup, H. U., M. W. Johnson, and R. H. Fleming. 1942. *The oceans, their physics, chemistry, and general biology.* Prentice-Hall, Inc. Copyright 1942, renewed 1970. Figure 7 reprinted by permission of Prentice-Hall, Inc., Englewood Cliffs, N. J. pp. 105, 106 *(Figs. 21, 22).*

19 Platzman, G. W. 1958. *A numerical computation of the surge of 26 June 1954 on Lake Michigan.* Geophysica Vol. 6. Figure 19 reprinted by permission of Geophysical Society of Finland, Helsinki-Porthania, Finland. p. 430 *(Fig. 11).*

Church, P. E. 1942. *The annual temperature cycle of Lake Michigan. I. Cooling from late autumn to the terminal point, 1941-42.* Univ. Chicago, Inst. Meteorol. Misc. Rep. 4. Figures 21, 22, 24, and 25 reprinted by permission of University of Chicago Press, Chicago, Ill.

21 p. 17 *(Fig. 4)*

22 p. 21 *(Fig. 6)*

24 p. 25 *(Fig. 8)*

25 p. 35 *(Fig. 13)*

Church, P. E. 1945. *The annual temperature cycle of Lake Michigan. II. Spring warming and summer stationary periods, 1942.* Univ. Chicago, Inst. Meteorol. Misc. Rep. 18. Copyright 1945 by the University of Chicago. All rights reserved. Figures 27, 30-35, 37, 39a, 39b, 40, and 41 reprinted by permission of University of Chicago Press, Chicago, Ill.

27 p. 9 *(Fig. 3)*

30 p. 15 *(Fig. 7)*

31 p. 21 *(Fig. 10)*

Figure

(Continued from Church, P. E. 1945.)

32 p. 19 *(Fig. 9)*

33 p. 41 *(Fig. 23)*

34 p. 67 *(Fig. 40)*

35 p. 73 *(Fig. 45)*

37 p. 87 *(Fig. 54)*

39a p. 45 *(Fig. 25)*

39b p. 47 *(Fig. 26)*

40 p. 25 *(Fig. 13)*

41 p. 53 *(Fig. 31)*

38 Unpublished figure sent to C. H. Mortimer by P. E. Church.

56 Mortimer, C. H., D. C. McNaught, and K. M. Stewart. 1968. *Short internal waves near their high-frequency limit in central Lake Michigan.* Proc. 11th Conf. Great Lakes Res., Int. Assoc. Great Lakes Res. Figure 56 reprinted by permission of International Association for Great Lakes Research. p. 460 *(Fig. 5)*.

57 Ayers, J. C., D. C. Chandler, G. H. Lauff, C. F. Power, and E. B. Henson. 1958. *Currents and water masses of Lake Michigan.* Univ. Michigan, Great Lakes Res. Div. Publ. No. 3. Figure 57 reprinted by permission of Great Lakes Research Division. p. 53 *(Fig. 24)*.

58 Bellaire, F. R., and J. C. Ayers. 1967. *Current patterns and lake slope.* Proc. 10th Conf. Great Lakes Res., Int. Assoc. Great Lakes Res. Figure 58 reprinted by permission of International Association for Great Lakes Research. p. 257 *(Fig. 5)*.

59e Verber, J. L. 1966. *Inertial currents in the Great Lakes.* Proc. 9th Conf. Great Lakes Res., Great Lakes Res. Div. Publ. No. 13, Univ. Michigan. Figure 59e reprinted by permission of Great Lakes Research Division. p. 378 *(Fig. 4)*.

REFERENCES CITED

Those marked with an asterisk (*) may be consulted for futher general discussions or bibliographies.

*Asbury, J. G. 1970. *Effects of thermal discharges on the mass/energy balance of Lake Michigan.* ANL/ES-1, Argonne National Laboratory, July 1970. 24 pp.

Ayers, J. C. 1963. *Water-volume transports across the midlake sill, and current structure over the sill; Studies in water movements and sediments in southern Lake Michigan.* Part I of the Final Report of H.E.W., Contract PH-86-63-30, Great Lakes Res. Div., Univ. Michigan.

_____. 1967. *The surficial bottom sediments of Lake Michigan.* In: J. C. Ayers, and D. C. Chandler (eds.), *Studies on the environment and eutrophication of Lake Michigan.* Univ. Michigan, Great Lakes Res. Div. Spec. Rep. 30. pp. 247-253.

*_____, D. C. Chandler, G. H. Lauff, C. F. Power, and E. B. Henson. 1958. *Currents and water masses of Lake Michigan.* Univ. Michigan, Great Lakes Res. Div. Publ. No. 3. 169 pp.

Beeton, A. M. 1962. *Light penetration in the Great Lakes.* Proc. 5th Conf. Great Lakes Res., Great Lakes Res. Div. Publ. No. 9, Univ. Michigan. pp. 68-76.

Bellaire, F. R., and J. C. Ayers. 1967. *Current patterns and lake slope.* Proc. 10th Conf. Great Lakes Res., Int. Assoc. Great Lakes Res. pp. 251-263.

Bennett, J. R. 1971. *Thermally driven lake currents during the spring and fall transition periods.* Proc. 14th Conf. Great Lakes Res., Int. Assoc. Great Lakes Res. pp. 535-544.

_____. 1973a. *A theory of large amplitude Kelvin waves.* J. Phys. Oceanogr. 3:57-60.

_____. 1973b. *On the dynamics of wind-driven lake currents.* Contr. No. 15, Marine Studies Center, Univ. Wisconsin--Madison. 85 pp.

Beutikofer, L. B., and D. D. Meredith. 1972. *Annotated bibliography on Great Lakes hydrology.* Univ. Illinois, Water Resources Center Res. Rep. 56. 62 pp.

Birge, E. A. 1897. *Plankton studies on Lake Mendota: II, The crustacean of the plankton from July, 1894, to December, 1896.* Trans. Wis. Acad. Sci. Arts Lett. 10:274-448.

Birge, E. A. 1904. *The thermocline and its biological significance.* Trans. Am. Microsc. Soc. 25:5-33. 2 pl.

_____. 1910. *An unregarded factor in lake temperatures.* Trans. Wis. Acad. Sci. Arts Lett. 16:889-1002. 2 pl.

_____, and C. Juday. 1929. *Transmission of solar radiation by the waters of inland lakes.* Trans. Wis. Acad. Sci. Arts Lett. 24:509-580.

*Bowen, A. J. 1969. *The generation of longshore currents on a plane beach.* J. Mar. Res. 27:206-215.

_____, and D. I. Inman. 1969. *Rip currents. 2. Laboratory and field observations.* J. Geophys. Res. 74:5479-5490.

*Boyce, F. M. 1974. *Some aspects of Great Lakes physics of importance to biological and chemical processes.* J. Fish. Res. Board Can. 31:689-730.

Brunk, I. W. 1963. *Additional evidence of lowering of Lake Michigan-Huron levels.* Proc. 6th Conf. Great Lakes Res., Great Lakes Res. Div. Publ. No. 10, Univ. Michigan. pp. 191-203.

Church, P. E. 1942. *The annual temperature cycle of Lake Michigan. I. Cooling from late autumn to the terminal point, 1941-42.* Univ. Chicago, Inst. Meteorol. Misc. Rep. 4. 51 pp.

*_____. 1945. *The annual temperature cycle of Lake Michigan. II. Spring warming and summer stationary periods, 1942.* Univ. Chicago, Inst. Meteorol. Misc. Rep. 18. 100 pp.

_____. 1947. *Convection in the annual temperature cycle of Lake Michigan.* Ann. N. Y. Acad. Sci. 48:789-800.

Csanady, G. T. 1973. *Wind-induced barotropic motions in long lakes.* J. Phys. Oceanogr. 3:429-438.

*_____. 1975. *Hydrodynamics of large lakes.* Annu. Rev. Fluid Mech. 7 (in press).

Davidson, D. R., and G. E. Birchfield. 1967. *A case study of coastal currents in Lake Michigan.* Northwestern Univ., Tech. Inst., Dept. Eng. Sci. Tech. Rep. 14 pp., figs. and tables.

Davis, R. A., and W. T. Fox. 1971. *Beach and nearshore dynamics in eastern Lake Michigan.* Western Michigan Univ., Office of Naval Research Tech. Rep. 4, Task No. 388-092/10-18-68(414). 145 pp.

_____, and D. F. R. McGeary. 1965. *Stability in neashore bottom topography and sediment distribution, southeastern Lake Michigan.* Proc. 8th Conf. Great Lakes Res., Great Lakes Res. Div. Publ. No. 13, Univ. Michigan. pp. 222-231.

Defant, F. 1953. *Theorie der Seiches des Michigansees und ihre Abwandlung durch Wirkung der Coriolskraft.* Arch. Meteorol. Geophys. Bioklimatol. Wien. (Vienna) Ser. A 6:218-241.

*Edinger, J. E., and J. C. Geyer. 1965. *Heat exchange in the environment.* The Johns Hopkins Univ., Dept. Sanitary Eng. and Water Resources. EEI Publ. No. 65-902. 259 pp.

*Great Lakes Basin Commission. 1972. *Great Lakes Basin Framework Study. App. 4, Limnology of Lakes and Embayments.* Draft No. 2, Vol. 1. 657 pp.

Harrington, M. W. 1894. *Currents of the Great Lakes.* U. S. Dept. Agric., Weather Bureau Bull. B.

Holland, R. E., and A. M. Beeton. 1972. *Significance to eutrophication of spatial differences in nutrients and diatoms in Lake Michigan.* Limnol. Oceanogr. 17(1):88-96.

Hough, J. L. 1935. *The bottom deposits of southern Lake Michigan.* J. Sediment. Petrol. 5(2):57-80.

*_____. 1958. *Geology of the Great Lakes.* University of Illinois Press, Urbana, Illinois. 313 pp.

Huang, J. C. K. 1971. *The thermal current in Lake Michigan.* J. Phys. Oceanogr. 1:105-122.

Jerlov, N. G. 1968. *Optical oceanography.* Elsevier Publ. Co., New York. 199 pp.

Kizlauskas, A. G., and P. L. Katz. 1974. *A numerical model for summer flows in Lake Michigan.* Arch. Meteorol. Geophys. Bioklimatol. Wien (Vienna) Ser. A 23:181-197.

Lauwerier, H. A. 1960. *The North Sea problem. Free motions of a rotating rectangular bay.* Proc. K. Ned. Akad. Wet. Ser. A 63:423-438.

*Lineback, J. A., N. J. Ayer, and D. L. Gross. 1970. *Stratigraphy of unconsolidated sediments in the southern part of Lake Michigan.* Illinois State Geological Survey, Environmental Geology Notes No. 35. 35 pp.

*Meyer, R. E. (ed.). 1973. *Waves on beaches.* Academic Press, New York. (Symposium Volume, Math. Res. Ctr., Univ. Wisconsin, Madison).

Monahan, C. 1973. *Drogue measurements of the circulation in Grand Traverse Bay, Lake Michigan.* Univ. Michigan, Dept. of Atmos. and Oceanic Sci. Tech. Rept. No. 35, Sea Grant Prog.

Mortimer, C. H. 1963. *Frontiers in physical limnology with particular reference to long waves in rotating basins.* Proc. 6th Conf. Great Lakes Res., Great Lakes Res. Div. Publ. No. 10, Univ. Michigan. pp. 9-42.

_____. 1965. *Spectra of long surface waves and tides in Lake Michigan and at Green Bay, Wisconsin.* Proc. 8th Conf. Great Lakes Res., Great Lakes Res. Div. Publ. No. 13, Univ. Michigan. pp. 304-325.

_____. 1968. *Internal waves and associated currents observed in Lake Michigan during the summer of 1963.* Univ. Wisconsin--Milwaukee, Center for Great Lakes Studies Spec. Rep. 1, mimeo. 24 pp., 120 figs.

*_____. 1971. *Large-scale oscillatory motions and seasonal temperature changes in Lake Michigan and Lake Ontario.* Univ. Wisconsin--Milwaukee, Center for Great Lakes Studies Spec. Rep. 12. Part I text, 111 pp; Part II illustrations, 106 pp.

_____, D. C. McNaught, and K. M. Stewart. 1968. *Short internal waves near their high-frequency limit in central Lake Michigan.* Proc. 11th Conf. Great Lakes Res., Int. Assoc. Great Lakes Res. pp. 454-469.

*_____, and E. J. Fee. 1973. *The free surface oscillations and tides of Lake Michigan and Superior.* Philos. Trans. R. Soc. Lond. (in press).

Murty, T. S., and D. B. Rao. 1970. *Wind-generated circulations in Lakes Erie, Huron, Michigan and Superior.* Proc. 13th Conf. Great Lakes Res., Int. Assoc. Great Lakes Res. pp. 927-941.

*Noble, V. E. 1966. *Observations on the fall overturn of Lake Michigan.* Limnol. Oceanogr. 11:413-415.

_____, and A. Michaelis. 1968. *Winter temperature data from Federal Water Pollution Control Administration buoy stations, Lake Michigan, winters of 1962-63 and 1963-64; Lake Huron, winter of 1965-66.* Univ. Michigan, Great Lakes Res. Div. Spec. Rep. 39. 387 pp.

*Phillips, D. W., and J. A. W. McCulloch. 1972. *The climate of the Great Lakes Basin.* Dept. Environment, Ottawa, Canada, Climatol. Ser. No. 20. 40 pp., 57 charts.

*Platzman, G. W. 1958. *A numerical computation of the surge of 26 June 1954 on Lake Michigan.* Geophysica 6:407-438.

Rainey, R. H. 1967. *Natural displacement of pollution from the Great Lakes.* Science 155:1242-1243.

Richardson, L. F. 1920. *The supply of energy from and to atmospheric eddies.* Proc. R. Soc. Lond. Ser. A 97:354-373.

Rodgers, G. K. 1966. *The thermal bar in Lake Ontario, spring 1965 and winter 1965-66.* Proc. 9th Conf. Great Lakes Res., Great Lakes Res. Div. Publ. No. 15, Univ. Michigan. pp. 369-374.

*Sato, G. K., and C. H. Mortimer. 1975. *Lake currents and temperatures near the western shore of Lake Michigan.* Univ. Wisconsin--Milwaukee, Center for Great Lakes Studies Spec. Rept. No. 22 (in press).

Saville, T. 1953. *Wave and lake level statistics for Lake Michigan.* U. S. Army Corps of Engineers, Beach Erosion Board, Tech. Memo. No. 36.

Simons, T. J. 1973. *Development of three-dimensional numerical models of the Great Lakes.* Canada Centre for Inland Waters, Sci. Ser. No. 12. 26 pp.

*_____. 1974. *Verification of numerical models of Lake Ontario: Part I, Circulation in spring and early summer.* J. Phys. Oceanogr. 4:507-523.

Sommers, L. H., and P. D. Josephson. 1968. *Bottom sediments of southwestern Lake Michigan.* Proc. 11th Conf. Great Lakes Res., Int. Assoc. Great Lakes Res. pp. 245-252.

*Sverdrup, H. U., M. W. Johnson, and R. H. Fleming. 1942. *The oceans, their physics, chemistry, and general biology.* Prentice-Hall Inc., New York. 1087 pp.

Terrell, R. E., and T. Green. 1972. *Investigations of the surface velocity structure of lake currents.* Limnol. Oceanogr. 17:158-160.

Thorpe, S. A. 1969. *Experiments on the stability of stratified shear flows.* Radio Sci. (Amer. Geophys. Un.) 4:1327-1331.

Tikhomirov, A. I. 1963. *The thermal bar in Lake Ladoga.* Bull. (Izvestiya), All Union Geogr. Soc. 95:134-142. (Amer. Geophys. Un. Transl. Soviet Hydrol., Collected Papers No. 2).

U. S. Department of Commerce. 1973. *Monthly Bulletin of Lake Levels.* NOAA, Lake Survey Center, 630 Federal Building, Detroit, Michigan 48226.

*U. S. Department of the Interior. 1967. *Water quality investigation, Lake Michigan basin: Lake currents.* Fed. Water Poll. Contr. Admin., Great Lakes Region, Chicago, mimeo. 364 pp.

_____. 1968. *Water quality investigations, Lake Michigan basin: Physical and chemical quality conditions.* Fed. Water Qual. Contr. Admin. Tech. Rep., Great Lakes Region, Chicago. 81 pp.

Verber, J. L. 1966. *Inertial currents in the Great Lakes.* Proc. 9th Conf. Great Lakes Res., Great Lakes Res. Div. Publ. No. 13, Univ. Michigan. pp. 375-379.

*Witherspoon, D. F. 1971. *General hydrology of the Great Lakes and reliability of component phases*. Dept. Environment, Ottawa, Canada. Inland Waters Board, Tech. Bull. No. 50. 14 pp.

Wu, P. K. 1975. *Numerical simulation of wind-driven motions in a two-layered lake*. Univ. Wisconsin--Milwaukee, Center for Great Lakes Studies Spec. Rep. No. 21 (in press).

ADDITIONAL REFERENCES

*Beeton, A. M. 1971. *Chemical characteristics of the Laurentian Great Lakes*. Proc. Conf. on "Changes in the Chemistry of Lakes Erie and Ontario". Bull. Buffalo Soc. Nat. Sci. 25:1-20.

*Csanady, G. T. 1970. *Dispersal of effluents in the Great Lakes*. Water Res., 4:79-116.

_____. 1971. *Turbulent diffusion in the Great Lakes: some fundamental aspects*. Int. Symp. on Stochastic Hydraulics (Pittsburgh, May 31-June 2, 1971) pp. 169-191.

_____. 1972. *Response of large stratified lakes to wind*. J. Phys. Oceanogr. 2:3-13.

*_____. 1973. *Turbulent diffusion in the environment*. Riedel Publ. Co., Boston. 248 pp.

Malone, F. D. 1968. *An analysis of current measurements in Lake Michigan*. J. Geophys. Res. 73:7065-7081.

*Mortimer, C. H. 1974. *Lake hydrodynamics*. Mitt. Int. Ver. Theor. Angew. Limnol. 20:124-197.

Noble, V. E., and K. J. Ehwing. 1968. *Winter temperature structure of Lake Michigan*. Univ. Michigan, Great Lakes Res. Div. Spec. Rep. 40. 63 pp.

_____, and J. C. Wilkerson. 1970. *Airborne temperature surveys of Lake Michigan, October 1966 and 1967*. Limnol. Oceanogr. 15:289-296.

VOL. 2. PHYSICAL LIMNOLOGY OF LAKE MICHIGAN

PART 2. DIFFUSION AND DISPERSION

by

Gabriel T. Csanady

Abstract

The local concentration of a conservative pollutant in Lake Michigan depends on the rate at which some discharged batch mixes with ambient waters and thereby expands in size. The physical mechanism of such growth of pollutant-batches is discussed in terms of several theoretical models which have appeared in the literature over the years, in order to throw light on the important processes involved in pollutant disposal. Simple means of estimating pollutant concentration are then briefly described, to allow the assessment of nuisance or hazard associated with the release of pollutants in the lake.

INTRODUCTION

When an impurity of some kind is introduced into the waters of Lake Michigan, it becomes subject to two physical effects broadly attributable to fluid motion: transport and diffusion. The former is bulk bodily motion of a given mass of impurity with the waters of the lake, the latter a distribution of the impurity throughout a continuously growing body of water to the point where the identification of the impurity no longer remains possible. While both these processes are quite irregular, effective diffusion or mixing essentially depends on the irregular random motions, known as turbulence, which are naturally present in lake currents. In the present section we shall confine ourselves to a discussion of turbulent diffusion* in Lake Michigan. The

---

**In the literature, a distinction is sometimes made between "diffusion" and "dispersion". The former is meant to denote the mixing effects of turbulence, the latter the similar effects of nonuniform bulk fluid motion. Such a distinction has not proven to be useful in practice, because the two processes are inextricably coupled, and we shall include both in our usage of the term "turbulent diffusion".*

practical focus of the discussion is, of course, how fast or how thoroughly an artificially introduced impurity may be expected to mix with the vast total mass of Lake Michigan. Bulk bodily movements of clouds of impurity are clearly important in the total picture, but to limit the scope of our discussion we shall take these for granted.

The process of turbulent diffusion in Lake Michigan does not differ in its fundamentals from diffusion in the ocean, and it is even in its details much the same as the diffusion process in the other Great Lakes. Therefore, much of our discussion below is fairly general while the specific quantitative information to be presented applies more or less unchanged to other Great Lakes.

CONCENTRATION AND ITS VARIABILITY

With the exception of a few stable layers, within which the density varies rapidly with depth, water movements in Lake Michigan, as in other Great Lakes, are generally turbulent. As a result, when any dissolved or suspended impurities are introduced into the lake in a specific location, at a source region, the amount of impurity per unit mass or volume of the host water substance, its concentration, varies irregularly in space and time. As many another quantitative characteristic of turbulent flow, concentration of an impurity at a given instant and location is a random variable. Although this is more or less what one would expect, the inherent randomness of observations concerning the distribution of a given pollutant or intentionally introduced tracer is often disregarded or incorrectly ascribed to imperfections of the measurements.

When a given quantity of tracer is released, it forms a cloud or "patch" which may be mapped, for example by isoconcentration contours. For an individual cloud such isopleths usually have irregular shapes, and cover areas which grow in a highly complex manner. An example of an isoconcentration map (obtained in Lake Ontario by Kullenberg *et al.*, 1973) is shown in Figure 1. In a continuously maintained pollutant or tracer plume, flowing along with a steady lake current, cross-sections of tracer concentration are similarly irregular curves, as Figure 2 illustrates.

As in dealing with other turbulent (random) signals, it is customary to remove the randomness from the observed concentration distributions by suitable averaging. For example, in the case of the tracer-plume cross sections shown in Figure 2, one may overlap the abscissae so the centers of gravity of the individual distributions coincide, then average the ordinates, the observed concentration readings, at given values of the normalized abscissa, at fixed distances from the center of gravity. One obtains a much smoother looking curve, mean concentration versus distance from a cloud's or plume's center (Fig. 3). Not to be forgotten is that, in an individual realization of the experiment, departures from the mean curve are the rule rather than the exception. The magnitudes of such departures are on the order of the root mean square (rms) fluctuation (Fig. 4, for the specific experiments shown in Figs. 2 and 3). Experimental work in the Great Lakes has consistently shown that average fluctuating magnitudes are not much smaller than the peak concentration level of the smoothed mean concentration curve (the center value in Fig. 3, for that particular experiment). In other words, the randomness of concentration readings is relatively large and individual concentration profiles across a plume can look very different from the smoothed average. Not all properties of

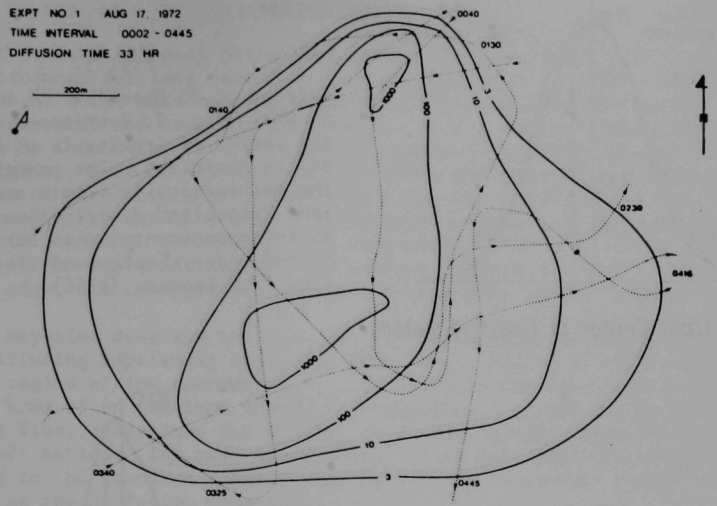

Fig. 1. Contours of Constant Concentration in a Batch of Rhodamine B Dye, 33 hr after Release at a Constant Depth of 20 m. Observations of Kullenberg *et al.* (1973) in Lake Ontario (with permission, see credits).

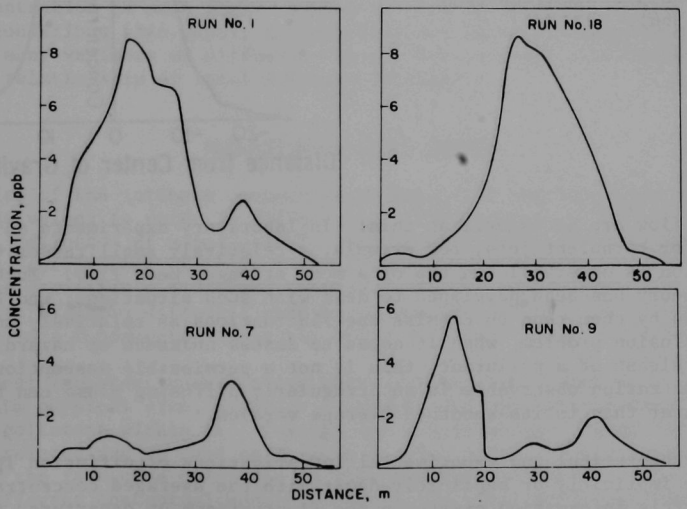

Fig. 2. Concentration Distribution at a Constant Depth of 1 m in a Cross Section of a Continuous Dye Plume in Lake Huron. A continuous source often generates a long, narrow ribbon of dye (plume) but the distribution within the ribbon is as irregular as a batch. This figure shows observations at the same cross section (1 km from the source) carried out at 15-min intervals. Modified from Csanady (1966).

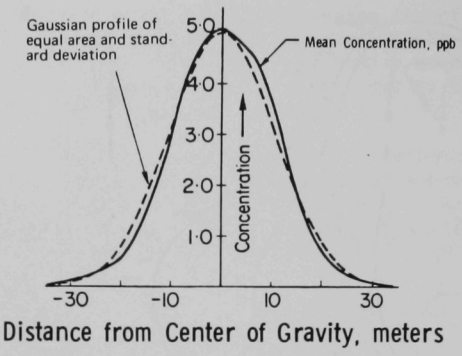

Fig. 3.

Average of 25 Observations of the Kind Shown in Fig. 2, Overlapped so that the Center of Gravity is at the Origin of the Absicissa. The smooth curve is the mathematically simple and convenient "Gaussian" distribution, approximating experimental mean curves obtained under simple conditions. Modified from Csanady (1966).

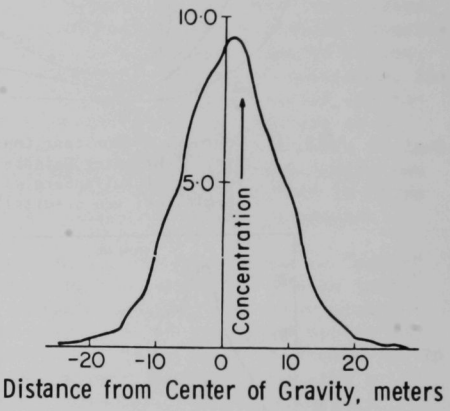

Fig. 4.

Mean Square Fluctuation of Concentration in the Plume Cross Section (Figs. 2 and 3). Modified from Csanady (1966).

turbulent flow are as chaotic as this: In laboratory experiments on turbulent pipe flow or turbulent jets, for example, a relatively small random velocity perturbation is observable on top of a much stronger mean flow. Much of turbulence theory has been developed to deal with such situations, and scientists conditioned by them tend to dismiss the fluctuations as relatively unimportant. In the diffusion problem, when it comes to assess nuisance or hazard associated with the release of a pollutant, this is not a permissible assumption: the peak concentration observable in an irregularly diffusing plume can be several times greater than in its smoothed average version.

Most theoretical and experimental investigations of diffusion in the Great Lakes have implicitly or explicitly dealt with the averaged concentration field. Little information exists on the fluctuations or departures from the mean and we shall not further discuss this topic, referring the reader to a paper by Murthy and Csanady (1971) and a recent text (Csanady, 1973).

CONSERVATION OF MASS

Most tracers and many pollutants retain their chemical identity in the lake environment for long periods: such substances are called conservative, because their total mass remains conserved, whatever its distribution over the lake's horizontal and vertical dimensions. When a quantity of conservative substance is introduced into the lake, it gradually spreads over a larger and larger region. Because its mass is conserved, the substance's concentration at the center of the cloud must decrease in time; the cloud must become more and more diluted. For example, 1 kg of conservative pollutant divided over a cube of water 10 m on edge gives rise to a concentration of one part in one million (10^{-6}). As the pollutant spreads and becomes distributed over a cube of water 100 m on edge, its concentration reduces to one part in one billion (10^{-9}).

One may also describe this process in terms of the movement of particles of the diffusing substance; they move away from a region of high concentration, toward a region of low concentration. The rate of the substance's transport per unit area of an envelope imagined surrounding a source region and per unit time, its flux, determines the rate at which the concentration decreases in the region left behind. The mass balance expressing this process, written down according to the standard rules of the physics of continuous media, yields what is known as the diffusion equation.

A mass balance of course holds for an individual, irregular diffusing patch or plume of conservative substance. In a theoretical approach, however, one usually deals with the averaged form of the diffusion equation, relating mean concentration to mean flux. Solutions of this equation for appropriate boundary conditions then supply mathematical models of diffusion phenomena. There are many variants of diffusion theory, but they all essentially express the above relationship of local dilution to flux.

MECHANISM OF CLOUD GROWTH

In view of the intimate connection between flux and dilution, it is more or less equivalent to refer to diffusion as "cloud growth", "spreading out of a tracer", "dilution of a pollutant", "mixing of a substance with ambient fluid", or "entrainment of ambient fluid into a tracer cloud". Each of these expressions describes a different aspect of the diffusion process, and they also suggest slightly different conceptual models of diffusion, which are equivalent in a fundamental sense but offer different practical advantages.

The most important quantitative characteristic of a diffusing patch or plume is its physical size, diameter or width, and the maximum concentration of tracer or pollutant within it. Through the conservation of mass the two are inversely related and we need only focus on size alone. The key question in describing the fate of a pollutant is then the rate at which a patch or plume grows. Different conceptual models of diffusion yield different quantitative answers to this question, and also provide physical insight from different points of view. In the next few sections we shall discuss these different models.

For the subsequent discussions it is necessary to adopt a specific definition of size for a cloud, patch, or plume. Under homogeneous conditions the

distribution of mean concentration in a patch or plume is Gaussian, or expressed by a bell-shaped curve of simple mathematical properties, which was already indicated in Figure 3. A Gaussian distribution is described mathematically by

$$\chi = \chi_0 \, e^{-r^2/2\sigma^2} \quad , \tag{1}$$

where χ is mean concentration at distance r from the center,
χ_0 is center mean concentration, and
σ is the "standard deviation".

The standard deviation σ of a Gaussian distribution is a convenient measure of size. The observable cloud width is about four times this quantity.

RANDOM WALK MODEL

In a turbulent fluid, an individual element of pollutant or tracer executes a succession of random movements. This is similar to the classical problem of a "drunkard's walk" or "random walk" in which a forward step is equally probable with a backward one. The result of many particles executing random walks is dispersion, characterized by a growth rate which is given by the equation

$$\frac{1}{2}\frac{d\sigma^2}{dt} = K = \text{constant } u\ell \quad , \tag{2}$$

where t is time and K is diffusivity, equal to a constant times step velocity u times step length ℓ.

Turbulent fluid motion may be thought to consist of many eddies of different sizes, or more or less closed flow structures qualitatively similar to vortices of different diameters. When a diffusing batch of tracer comes under the influence of an eddy much larger than the size of the patch, it simply travels along the streamlines of the eddy. This clearly does not lead to an increase of the patch's size; velocities relative to the center of the patch produced by such an eddy are small. Most effective in producing relative motion, and hence dispersion, are eddies which are about of the same diameter as the patch. (Fig. 5 illustrates the effect of a hypothetical, very simple field of eddies on diffusing patches of different size.)

The effective step length, in the random walk conceptual model, is therefore proportional to cloud size, as long as there are eddies of the required size present. In a certain range of eddy sizes the step velocity also increases slowly with eddy size, actually as the third root of size in homogeneous conditions, so that in this range the diffusivity is

$$K = \text{constant } \sigma^{4/3} \quad , \tag{3}$$

a relationship known as the "4/3 power law". Equations 2 and 3 now imply that

$$\sigma = \text{constant } t^{3/2} \quad , \tag{4}$$

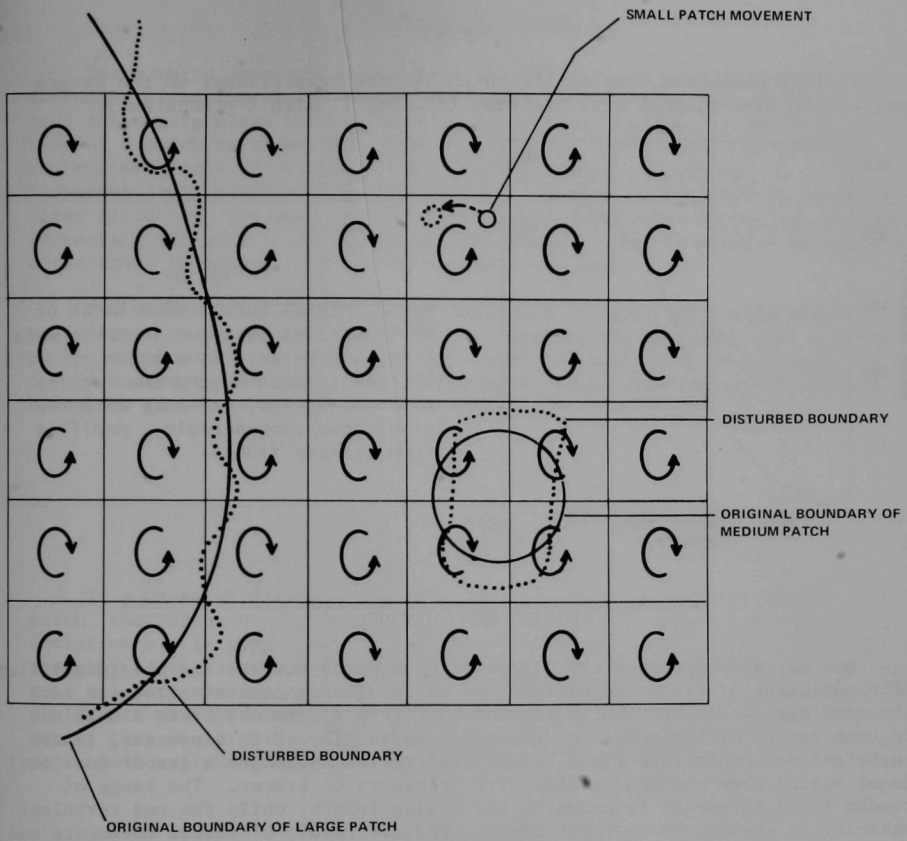

Fig. 5. Effect of a Hypothetical, Simple Field of Uniform Eddies on Diffusing Patches Which Are Small, Large, and Comparable in Size to the Eddies. The small patch undergoes bulk displacement and its rate of growth is not affected. Eddies distort the boundaries and cause modest mixing at the fringes of the large patch. The patch comparable in size to the eddies is most affected; ambient fluid moving close to its center moves fluid away from the patch at a fast rate, resulting in rapid mixing.

or that the cloud grows faster than in direct proportion to the time elapsed. These conditions apply only to a relatively narrow range of eddy sizes; any given cloud very quickly outgrows the range of validity of the 4/3 power law. Figure 6 shows such a phase of rapid growth, which terminates when the patch or plume becomes comparable in size to the largest eddies present. After this the diffusivity becomes constant and equal to the product of rms turbulent velocity u' times eddy size L:

$$K = u'L \ . \tag{5}$$

In this phase the size of the patch becomes proportional to the square root of the time elapsed since release (cf. Eq. 2, with K = constant).

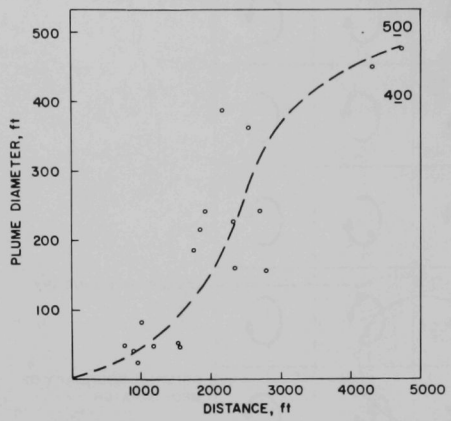

Fig. 6.

Rapid Initial Spread of a Batch of Drift Bottles is Shown in these Data from Lake Huron. As a batch of drift bottles spreads beyond the locally dominant eddies, its rate of spread slows down considerably. Modified from Csanady (1963).

MIXING LENGTH MODEL

One may also approach the diffusion problem by attributing the (mean) flux of a pollutant or tracer to differences in the (mean) concentration, in much the same way as one attributes flow of heat from a warm object to a cold one to temperature differences. On the microscopic view of this process, random turbulent movements take fluid from a tracer-rich region to a tracer-poor one; local mixing then ensures an effective transport of tracer. The range of random fluid movements is known as the mixing length, while the rms turbulent velocity is assumed to be their speed. The net result of random movements and local mixing is a flux F along a direction n perpendicular to concentration isopleths, and of a magnitude

$$F = - K \frac{\partial \chi}{\partial n} \ , \tag{6}$$

where K is again diffusivity (given by mixing length times rms turbulent velocity) and $\partial\chi/\partial n$ is the gradient of concentration, the negative sign signifying flux down the gradient. Through an application of mass balance one finds now that the growth rate implied by this model is precisely as before, expressed by Equation 2. The diffusivity K is also clearly subject to the remarks already made, notably that it increases when the mixing length does. It is remarkable that the random walk and the mixing length models, although based on quite different hypotheses, lead to essentially the same physical picture of diffusion.

ENTRAINMENT MODEL

Yet a third approach is based on the observation that at the edges of a diffusing cloud the concentration drops off rapidly and, moving outward, one soon encounters clean ambient fluid. It is thus possible to identify boundaries of a patch or plume and speak of fluid "within", which has a certain content of tracer or pollutant, and fluid "without", which has no tracer. Turbulent fluid movements at the boundary may then be regarded as bringing clean fluid into the patch or plume, diluting the fluid within, and of course increasing the size of the cloud in the process. Such a process is known as entrainment of ambient fluid into a patch or plume.

The rate of entrainment may be expressed in terms of a mass transfer coefficient or entrainment velocity w. Suppose, for example, that a patch is of the shape of circular cylinder in a vertical position, of radius R. The inflow across the boundary per unit depth is $2\pi Rw$, which requires by mass balance a growth in the area of the patch, πR^2

$$\frac{d\ (\pi R^2)}{dt} = 2\pi Rw$$

or

$$\frac{1}{2}\frac{dR^2}{dt} = wR \ . \qquad (7)$$

If a Gaussian distribution is fitted to the concentration within the patch, the radius R turns out to be a constant factor times the standard deviation σ. In other words, the content of Equation 7 is very similar to that of Equation 2, with the diffusivity in this case being given by entrainment velocity times patch size (times a numerical factor). In a homogeneous field, one would reasonably expect the entrainment velocity to remain constant; this would give a diffusivity proportional to patch radius R, and a patch radius growing in direct proportion to time elapsed.

SHEAR FLOW DISPERSION

The final diffusion model of importance takes into consideration the differences in mean velocity, shear, which affect diffusing clouds. This mechanism is of especial importance in the ocean and in large lakes, where diffusing clouds of pollutant or tracer often become large enough for their mean, non-turbulent, velocity to be significantly different from one end of the cloud to the other. Clearly such velocity differences distort the shape of a cloud, so that instead of resembling a circle, it looks more as an elongated crescent or some other complex shape. The immediate effect of such distortion is a sharpening of the concentration differences existing in the fluid. Turbulent mixing across these sharpened concentration gradients increases the flux, as we have seen in the mixing length model above, and produces a cloud growth rate which can be much in excess of what it would be without the distortions. The increased flux may under simple conditions still be described by Equation 6 (i.e. the cloud growth by Equation 2), but we now have to interpret diffusivity as being a product of shear and turbulent mixing.

It is now easy to see that such an effective diffusivity is again likely to increase with cloud growth, much as in random walk diffusion with increasing

step length. For a practically important range of cloud sizes one would expect the mean velocity differences between two points in a cloud to become greater and greater as the cloud grows larger. Quantitative models of similar processes yield effective diffusivities which may be characterized as increasing a little faster than cloud size:

$$K = \text{constant } \sigma^{\alpha} , \tag{8}$$

where α = 1.0 to 1.3 or so, depending on the precise mean velocity distribution adopted. The corresponding cloud growth rate in time is, using Equation 2,

$$\sigma = \text{constant } t^{1/(2-\alpha)} . \tag{9}$$

We observe that the predictions of this model stretch from those of the entrainment model (α = 1.0) to random walk in homogeneous turbulence with increasing step length (α = 4/3).

BOUNDARIES

In the above discussion we have tacitly ignored the effect of such boundaries as the coastline, the free surface, or the bottom of the lake. When a diffusing patch or a tracer or pollutant encounters such a boundary, its further growth is clearly prevented. Conservation of mass then implies that the rate of dilution slows down when growth ceases in one spatial dimension (e.g. the vertical, as a diffusing cloud hits bottom).

An important complication is that stable sheets within the body of the fluid may act as false bottoms for diffusion. Within a stable sheet, the vertical change of density is fast enough for the force of gravity to suppress turbulence completely. Without turbulence, diffusion is so slow as to be negligible from the point of view of pollutant dispersion, and the patch or plume behaves as if it had encountered bottom at the depth of the stable layer. During the summer in the Great Lakes diffusion floors may be frequently observed, on hot, calm days sometimes quite close to the surface, at a depth on the order of a meter or two. Tracer introduced above such a shallow floor soon distributes itself evenly between two boundary surfaces, free surface and diffusion floor, or two diffusion floors, and its further diffusion is then confined to the two horizontal dimensions.

The physical reason why such changes of density occur in the vertical is that heating or cooling of the water causes thermal expansion and contraction. In the spring and summer, the sun heats the top layer of a lake and causes its density to decrease, a process which results in the formation of the thermocline. This process is of central importance in physical limnology, its effects not being confined to influences on vertical diffusion, and it is extensively treated in an earlier section by Dr. Mortimer.

PRACTICAL ESTIMATES OF MAXIMUM CONCENTRATION

While it is possible to solve the diffusion equation for various complex boundary conditions by analytical or numerical means, many approximations have

to be made in the mathematical definition of such problems, and almost equally good results may be obtained by much simpler approximations. The basic principle is that the concentration within a patch or plume of tracer or pollutant is determined by the conservation of mass and can be calculated, once the size of the patch or plume is known.

Thus if a patch containing a total amount Q of tracer is diffusing in an unrestricted three-dimensional domain, the patch size being σ_x, σ_y, σ_z along the three coordinate axes, the center concentration is

$$\chi_c = C \frac{Q}{\sigma_x \sigma_y \sigma_z} , \tag{10}$$

where C is a constant, equal to $(2\pi)^{-3/2} = 0.0635$, if the concentration distribution is Gaussian in all three directions. In a patch released at the free surface, the top half of the cloud is missing and if Q is still the material actually present, the constant C becomes double the above value. (Fig. 7 illustrates this point.)

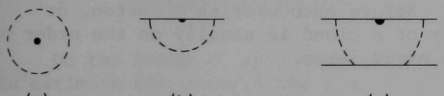

Fig. 7.

Effect of Boundaries on Diffusion. In an unrestricted medium (a) the pollutant spreads out in all directions. When one boundary is present (b) it cuts off half the space available for spreading and roughly doubles concentrations. Two boundaries (c) confine diffusion to a sandwich of fixed vertical extent.

In the presence of a diffusion floor at depth h, σ_z in Equation 10 has to be replaced by h, and the constant C then becomes $(2\pi)^{-1} = 0.159$, if the horizontal distributions are Gaussian. In a continuous plume, if the release rate now is q, a quantity qdt diffuses in two dimensions in each cross section of the plume, while along the plume axis the material is distributed over a slice of depth Udt, where U is the speed of the current within which the plume is embedded. Thus in a plume far from any boundaries the center concentration is

$$\chi_p = C \frac{q}{U \sigma_y \sigma_z} , \tag{11}$$

where C is again 0.159 for a Gaussian plume. If σ_z is replaced by h in a layer of this depth, C becomes $(2\pi)^{-1/2} = 0.399$, should the lateral concentration distribution still be Gaussian. If the shape of the distribution changes, so does the precise value of C, but this is of little practical consequence, because concentrations cannot be predicted with very great accuracy. We should also remember, of course, that what we are predicting by such calculations are mean values, and that in individual clouds the actually realized maximum concentration may be a factor of two or three higher.

EMPIRICAL DATA ON CLOUD GROWTH

Thus the problem of predicting concentrations of pollutants resolves itself to the estimation of cloud size. Our earlier discussion has shown that this may be approached using Equation 2, but we require empirical information on the growth rate, either in the form of an entrainment velocity, data on σ_x, σ_y and σ_z as a function of time, or on diffusivity in the three coordinate directions. At present it appears to be most convenient to quote data on diffusivities.

A considerable amount of data have been accumulated during the past decade or so on diffusion in various Great Lakes. The work of Huang (1971) and Zivi *et al.* (1974) has demonstrated that diffusion constants in Lake Michigan are indistinguishable from those in other Great Lakes, as one would expect. This is true within the accuracy of the present evidence, which, however, is still relatively crude.

Vertical diffusion is in general of subordinate importance, because a diffusing patch or plume usually reaches bottom or a stable sheet, diffusion floor, soon after release. Thus, as far as vertical cloud growth is concerned, the most important problem is to determine the mixing depth relevant for any particular release: the surface mixed layer in some instances, but often an intermediate or near-bottom mixed layer. Before encountering a bottom, or diffusion floor, the vertical diffusivity of a cloud is usually on the order of K_z = 10 cm^2/sec, at least in the surface mixed layer.

Horizontal diffusivities K_x and K_Y are larger, but between themselves usually on the same order of magnitude, although a patch is usually longer along the mean current than across it. An important influence on the value of the horizontal diffusivity is the size of the cloud, diameter of a patch or width of a plume. In small-scale nearshore plumes, a few hundred meters in width, the horizontal diffusivity K_Y is generally on the order of 10^3 cm^2/sec. By the time a patch is 10 km in diameter, its effective diffusivity becomes of order 10^5 cm^2/sec.

A similar result applies to oceanic diffusion. Okubo (1971) has summarized available oceanic observations in a diagram showing horizontal diffusivity, effectively $K_h = \sqrt{K_x K_y}$, against patch diameter, ℓ. A clear-cut trend emerges, quantitatively described by K_h = constant $\ell^{1.1}$, or Equation 8 with a = 1.1 . In the light of our earlier discussion, this result may be interpreted as being presumably due to the influence of a nonuniform velocity field.

It is possible to summarize Great Lakes diffusion data in a diagram similar to Okubo's. Murthy (1970) has constructed such a diagram with some Lake Ontario data. Zivi *et al.* (1974) have constructed a diagram with Lake Michigan data; adding Murthy's data, they increased the range covered. Zivi *et al.*'s data are replotted here in Figure 8, also showing Okubo's oceanic diffusion line, and a straight line (in this log-log plot) of the same slope fitted to the Great Lakes data. The trend is seen to be very similar in the Great Lakes as in the ocean, but the numerical values of diffusivities in the Great Lakes appear to be somewhat higher.

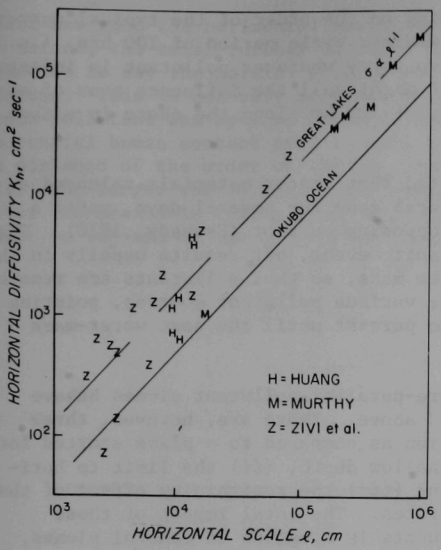

Fig. 8.

Horizontal Diffusivity Versus Cloud Size in the Great Lakes and in the Ocean. Data from Zivi *et al.* (1974) and Okubo (1972).

On the basis of data such as that contained in Figure 8, it is possible to estimate for example the size of a sewage field at a given distance from an outfall. Knowing the rate of release, the formulae of the previous section then enable one to estimate the concentration of a given undesirable constituent at a given location. There are various complications which may be handled (e.g. that the bacteria in the sewage die off at a specific rate) and problems with complex geometry simulated using a more complete formulation of the diffusion equation. The philosophy of this approach is that one can assess nuisance or hazard due to a given pollutant by calculating a mean concentration; one must remember in this context that considerable random fluctuation may also be expected. Whether this philosophy itself is correct or not is outside the scope of diffusion theory, but is a question which should at least be asked, as one has learned in connection with the effects of DDT.

SPECIAL PROBLEMS OF THE COASTAL ZONE

Most pollutants are discharged into Lake Michigan at or very close to the shore, usually through an outfall pipe ending a few hundred meters from the shoreline, in water a few meters deep. Although the principles of diffusion summarized above apply to this situation as well as to dumping of refuse much further offshore, some special practical problems arise near shore which are worth extra emphasis.

In the section of this report dealing with lake currents, Dr. Mortimer points out that within the coastal zone, of about 10 km width, currents are generally shore-parallel and persist in one direction or the other for a period on the order of weather cycles, typically 100 hours. On the rise of a stronger wind opposing an established current, the latter reverses direction within a few hours. As a result, parcels of water travel up and down along a

coast, their total excursion one way being on the order of the typical current velocity, 30 cm/sec, times the typical weather cycle period of 100 hrs, i.e. up to 100 km. Because water parcels also carry whatever pollutant is injected into them by a nearshore source, what we might call the influence zone of such a source extends a distance of the order of 100 km along the shore in either direction.

Direct observations have demonstrated that tracer materials released at the shore in fact travel within the coastal zone for several days, until a major opposing wind event generates an opposing current (Csanady, 1970). The current reversal is in its details a chaotic event, but results usually in the mixing of coastal waters with the midlake mass, so that pollutants are removed en block. New plumes then form from the various pollutant sources, pointing in the opposite alongshore direction, to persist until the next water-mass exchange episode.

While within the coastal zone, shore-parallel pollutant plumes behave according to the principles we discussed above. There are, however, three influences reducing their rate of dilution as compared to a plume started far offshore. These influences are: (*i*) shallow depth, (*ii*) the limit to horizontal mixing presented by the shore, and (*iii*) the restraining effect of the shore on eddy size and hence on mixing rates. The total impact of these influences is that the dilution of effluents is sluggish in coastal plumes, especially in plumes of large size.

To make these points quantitative, we observe that a diffusing plume in the coastal zone soon exhausts all the vertical space available and hits bottom, so that in Equation 11, σ_z has to be replaced by total depth h. Also, because the shore cuts away half of the horizontal space available (according to the principle illustrated in Fig. 5) the constant C doubles, and the maximum concentration becomes approximately

$$\chi_p = 0.8 \frac{q}{Uh\,\sigma_y} . \qquad (11a)$$

The restraining effect of the shore on eddy size makes itself felt in the magnitude of the eddy diffusivity K_Y. Somewhat contrary to Figure 8, K_Y close to shore does not become much larger than $10^3 - 10^4$ cm^2/sec, so that we have, using Equation 2,

$$\frac{d\sigma^2_y}{dt} = 2 \cdot 10^3 - 2 \cdot 10^4 \text{ cm}^2/\text{sec} . \qquad (2a)$$

Because the square of the plume size σ_Y is involved in this expression, further growth of large plumes is relatively slow. Physically the reason is that, in the case of large plumes, as already illustrated in Figure 5, eddies merely nibble at the fringes and only cause slow expansion.

To take a quantitative example, consider a plume extending initially from shore to 1000 m, which has a standard deviation σ_y of roughly 500 m. The maximum diffusion time available before the next mass exchange episode is on the order of 100 hours ($3.6 \cdot 10^6$ sec). Within this period a plume grows from σ_Y = 500 m, according to Equation 2a above, to σ_Y = 1000 - 2500 m, depending on

just how good the horizontal mixing is locally. Because its depth remains constant, the total further dilution of plume water is only by a factor of 2-5, that is to say the initial plume mixes with ambient water 1-4 times its own volume. This is not very much further relief, if the initial concentration of some pollutant was by some standard too high, noting especially that a vast potential human contact area is open to such a plume, which hugs the shore for a distance of the order of 100 km. The general principle in such situations is: the larger the initial plume size, the less important further dilution over the available time period, and the more stringent the standards are that must be imposed on the quality of water within the plume.

CREDITS

The authors and the Argonne National Laboratory gratefully acknowledge the courtesy of the individuals and organizations who granted permission to use illustrations or, where appropriate, other material in the ANL/ES-40 series. Sources of illustrations used in Volume 2, Part 2, are listed below.

Figure

1 Kullenberg, G., C. R. Murthy, and H. Westerberg. 1973. *An experimental study of diffusion characteristics in the thermocline and hypolimnion regions of Lake Ontario.* Proc. 16th Conf. Great Lakes Res., Int. Assoc. Great Lakes Res. Reprinted by permission of International Association for Great Lakes Research. p. 784 *(Fig. 5b)*

REFERENCES CITED

Csanady, G. T. 1963. *Turbulent diffusion in Lake Huron.* J. Fluid Mech. 17:360-384.

_____. 1966. *Dispersal of foreign matter by the currents and eddies of the Great Lakes.* Univ. Michigan, Great Lakes Res. Div. Pub. No. 15. pp. 283-294.

_____. 1970. *Dispersal of effluents in the Great Lakes.* Water Res. 4:79-114.

_____. 1973. *Turbulent diffusion in the environment.* D. Reidel Publishing Co., Dordrecht, Boston. 248 pp.

Huang, J. C. K. 1971. *Eddy diffusivity in Lake Michigan.* J. Geophys. Res. 76:8147-8152.

Kullenberg, G., C. R. Murthy, and H. Westerberg. 1973. *An experimental study of diffusion characteristics in the thermocline and hypolimnion regions of Lake Ontario.* Proc. 16th Conf. Great Lakes Res., Intern. Assoc. Great Lakes Res. pp. 774-790.

Murthy, C. R. 1970. *An experimental study of horizontal diffusion in Lake Ontario.* Proc. 13th Conf. Great Lakes Res., Int. Assoc. Great Lakes Res. pp. 477-489.

_____. and G. T. Csanady. 1971. *Experimental studies of relative diffusion in Lake Huron.* J. Phys. Oceanogr. 1:17-24.

Okubo, A. 1972. *Oceanic diffusion diagrams.* Deep-Sea Res. Oceanogr. Abstr. 18:789-802.

Zivi, S. M., D. E. Frye, R. E. Buell, and S. Van Loon. 1975. *Measurements of eddy diffusivities in nearshore regions of Lake Michigan.* In: J. V. Tokar, S. M. Zivi, A. A. Frigo, L. S. Van Loon, D. E. Frye, and C. Tome, *Measurements of physical phenomena related to power plant waste heat discharges: Lake Michigan, 1973 and 1974.* ANL/WR-75-1, Argonne National Laboratory. pp. 164-210.